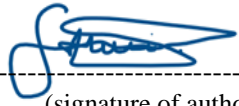# FACULTY OF SCIENCE AND TECHNOLOGY

MASTER'S THESIS

Study programme/specialisation: Engineering Structures and Materials Science - **Mechanical Systems**	**Spring** semester, 2019 **Open**
Author: Fithawi Ghebretinsae	------------------------------------ (signature of author)

Programme coordinator: Supervisor(s): Ove Mikkelsen

Title of master's thesis: **Mechanical Testing And Finite Element Analysis Of 3D Printed Continuous Carbon Fiber Reinforced Onyx® Thermoplastic**

Credits: 30

Keywords: - *Composite Materials* - *3D Print* - *FEA of composite materials in Ansys* - *Mechanical testing of composite materials* - *Continuous fiber reinforced Onyx® thermoplastic*	Number of pages: ……61…… + supplemental material/other: …16… Stavanger, 14/05/2019…. date/year

Abstract

While Additive manufacturing (AM) has been limited in prototyping and research areas, this technology has several advantages and significant potential to revolutionize nowadays conventional manufacturing processes. In recent years, several materials, including metals has been studied and tested in AM. However, polymers are the dominating currently available commercial materials. Polymers have low strength and stiffness, and their implementation in engineering applications that require high strength and stiffness is limited. However, by introducing a strengthening fiber, the polymer based material can turn into a stronger and stiffer material, namely, composite materials.

Currently, it is commercially possible to fabricate small size components from two or more filament materials using desktop 3D printers. However, there is limited understanding, on the material properties of the composites, produced by the 3D Print technology. To overcome this, there is a demand of several research both on the 3D printing processes and the material properties. This study was meant to provide more understanding on the parts fabricated from composite materials using 3D printer. Therefore, mechanical properties of 3D fabricated composite samples using Markforged® Mark-Two 3D printer were investigated. Tensile and flexural test had been carried out and the results were validated with Finite Element Analysis (FEA) results carried in ANSYS Mechanical Parametric Design Language (APDL) 17.0. Furthermore, carbon fiber (CF) as reinforcing, and "Onyx" as matrix materials were used in the fabrication of the test samples.

The tensile and flexural samples was fabricated with a fiber volume fraction of about 62% and 42%, respectively. Furthermore, the tensile samples provided 559.90 MPa and 25.04 GPa in maximum tensile strength and tensile modulus, respectively. Whereas 270.70 MPa in maximum flexural strength and 16.42 GPa in flexural modulus were achieved by the flexural samples. The obtained tensile strength and modulus results had a standard deviation of 17 MPa and 2.65 GPa, respectively. While the flexural strength and modulus results had a corresponding standard deviation of 28.30 MPa and 1.35 GPa. For comparison reasons, the ultimate tensile strength of 6061-T6 Aluminum, commonly used for bike frames, is 310 MPa[1]. The tensile strength of composite samples in this study was about 80% higher than the strength of Al6061-T6. However, the tested samples contain high fiber volume fraction.

---

[1] http://www2.glemco.com/pdf/NEW_MARTERIAL_LIST/Alumina%206061-T6.pdf

Author: Fithawi Ghebretinsae

ACKNOWLEDGMENT

Table of Contents

Table of Figures

List of Tables

List of Abbreviations

3D	3 Dimensional
AM	Additive Manufacturing
AFP	Automated Fiber Placement
APDL	Ansys Parametric Design Language
BC	Boundary condition
CF	Carbon Fiber
CFF	Continuous Filament Fabrication
CFRP	Continuous Fiber Reinforced Polymer
CMC	Ceramic Matrix Composites
DDM	Direct Digital Manufacturing
DED	Direct Energy Deposition
DOF	Degree Of Freedom
EPELX	Elastic strain x-direction
FDM	Fused Deposition Modeling
FEA	Finite Element Analysis
FEM	Finite Element Model
FFF	Fused Filament Fabrication
FG	Fiber Glass
HSHT	High Strength High Temperature
LOM	Laminated Object Manufacturing
LSS	Laminate Stacking Sequence
MMC	Metal Matrix Composites
PBF	Powder Bed Fusion
PMC	Polymer Matrix Composites
PMC	Polymer Matrix Composites
ROM	Rule Of Mixture
RP	Rapid Prototyping
SLS	Selective Laser Sintering
STL	Stereolithography
SX	Stress in x-direction
SZ	Stress in z-direction
UD	Unidirectional
UTS	Ultimate Tensile Strength
UX	Displacement in x-direction
YTS	Yield Tensile Strength

1 INTRODUCTION

Additive manufacturing (AM) is one of the currently developing method of manufacturing processes [1]. AM is defined as the manufacturing of a component by laying a material layer upon a layer [2]. AM builds a component as per the design requirements and there is a significant possibility of design optimization. As a result, avoiding structurally unnecessary material, reduces the mass of a component and material waste. Product development time can be reduced by the fast fabrication of prototypes models using Fused Filament Fabrication (FFF). Prototypes make communication easier by "touch and feel" kind of visualization between different departments   and several prototypes can be manufactured during product development time with low cost [1]. Specially 3D printing has a great advantage due to 3D models can be fabricated without geometrical complexity limitations, almost without material waste and no additional machines are required, thus the manufacturing cost can be reduced significantly [1]. However, products fabricated with 3D printing have product size limitation due to the capability of the 3D printer, products have isotropic mechanical properties, are more porous than traditionally manufactured products [3, 4]. Throughout this study the terms such as '3D printer' referrers specifically to the three-dimensional additive manufacturing machine and '3D printing' to the additive manufacturing processes by 3D printers .

Additively manufactured components have been studied in several research and it has been detected to experience an anisotropic property [4, 5]. The directional difference in mechanical property is due to the weak bonding between consecutive layers [5, 6]. Even though, metal matrix, ceramic matrix, and polymer matrix are used in AM, the most commonly used materials are polymers. Pure polymers have been used in many applications, but their application in engineering structural application is limited due to low engineering property. Reinforcing polymers with strong fibers improves the structural applicability of these materials [1]. This method of forming a composite material is well known and have been applied in many aerospace and automobile industries [7].

As mentioned earlier polymer-based plastics are commonly used FFF materials, introducing strong fiber within a polymer matrix make components stiffer and stronger [3-5, 8, 9]. Laying continuous reinforcing fiber within a resin has been commonly practiced in traditional manufacturing of parts from composite materials [10]. However, it occurs to be relatively new to the additive manufacturing world. Laying continuous fiber reinforcement in a polymer base matrix using 3D printer increase the benefits of AM. The introduction of composite materials to additive manufacturing is relatively new technique and it takes the AM technology from prototyping stage further to the fabrication of strong functional parts [11]. Fiber Reinforced composites have shown properties that are comparable with aluminum

Introducing short fiber reinforcements into polymer based matrix, increases the strength of additively manufactured parts, and it has been practiced by "mixing and extruding" , Fused Deposition Manufacturing (FDM) techniques [12]. Furthermore, it is important to mention that the mechanical properties of parts produced by 3D printing do not agree with the "Rule of Mixture" (ROM) known in composite material's books [9], this is due to the nature of various parameters of 3D printing method, and the mechanical properties of the filament material manufactured for use in 3D printers is different from those used in the traditional manufacturing methods.

Composite materials can be defined as a combination of two or materials in a macroscopic level, resulting new material with a better property than the individual elements [7, 13-16]. Basically, a composite material consists of a continuous matrix phase and a reinforcing phase [2, 7]. AM and composite materials are reviewed in the literature section.

In this study, earlier studies about composite materials manufactured by AM particularly by 3D printers had been revised. Moreover, literature of composite materials, 3D printing processes; particularly Mark-Two 3D printer from Markforged® and important points of Finite Element Analysis (FEA) of composite materials using Ansys was discussed in the literature section.

 The methods used to perform the experimental tests and the FEA in Ansys were explained in section 3. Following the methodology, the obtained results were provided. Furthermore, the results and other important issues were discussed on section 5. Conclusions and recommendations were provided on section 6. At last references and some additional diagrams/images were included on section 7 and 8, respectively.

2   LITERATURE REVIEW

This literature covered the background of composite materials properties, application, manufacturing methods and simulation of composite. Furthermore, the rule of mixture (ROM) for predicting the properties of parts from composite materials was discussed.

2.1   Composite materials

"Composite materials are engineering materials made of two or more materials combined on a macroscopic scale to form a third material with different material properties" [7, 17]. Composites consist two phases, a reinforcement phase which provides most of the strength and a continuous matrix phase that provides the shear and compression resistance [2, 4, 15, 18, 19].

Composite materials have been used for decades starting in the ancient Mesopotamia and Egyptians, where wood strips were used to make a plywood and straw to reinforce mud bricks [18, 20]. Nowadays, composite materials are commonly used in several field of engineering, specially in the aerospace and automotive industries [13]. Comparing to metals, composite materials have high strength to weight ratio [7]. In addition, composites have high corrosion and wear resistance, good fatigue life and thermal conductivity [12]. These mechanical properties make composite materials attractive in engineering applications that require high strength and stiffness while maintaining low weight. Aerospace industry have been using composite materials in several component designs, such as engine nozzle, aircraft wings, rocket fuel tanks and helicopter blades [2, 7, 12, 16, 18]. To mention, Boeing 787 Dreamliner is one of public airplanes recently built 50% by weight of its parts from composite materials [7, 18]. Due to the introduction of composite materials in the aerospace, production cost, maintenance time due corrosion, fuel consumption and aerodynamic drag have been reduced [15, 16].

Basically, one of the materials required to produce a composite part must be a reinforcing material. The reinforcing material is made of thousands of fiber threads combined together into a small single strand and they are available in different forms such as woven rolls [2]. Composites have an anisotropic material properties, meaning they have different material properties in different directions [4, 13]. They are stronger and stiffer along the reinforcing element (0-degree) and weaker perpendicular to the reinforcement (90-degree). The fiber provides strength to the composite part when loaded in the direction of the fiber, whereas the loads applied not in the direction of the fiber are mostly depend on the weak matrix phase [16].

Some design techniques such as laying fibers in different orientation at each layer can reduce the an anisotropic properties of composites [15]. The strength and stiffness of the composite materials is mainly dependent on the type reinforcing phase [3, 8, 12, 21]. Basically, fibers give a significant strength improvement to a composite material [2, 3, 6, 8]. The reinforcing fiber can be continuous (long) or discontinuous (short) fibers. Continuous fibers have large aspect

ratio compared to discontinuous fibers. Reinforcing fibers are more effective if their length is not shorter than the critical length [18, 19]. Moreover, the strength of a single fiber filament is dependent on its production diameter. The strength of the filament is inversely proportional with the diameter [13]. Furthermore, the term "fiber" was meant to be the reinforcing material or strengthening material throughout this thesis. In general, fibers used for strengthening polymers-plastics can be categorized into three groups; namely, glass fibers, aramid fibers and carbon/Graphite fibers [18]. The mechanical property of some commonly used fibers is listed on Table 1. The applications of the different fibers vary depending on the required functionality of a designed component.

Table 1. Mechanical properties of some common fibers[2].

Type of Fiber		Tensile strength GPa	E-Modulus GPa
Glass Fibers	E-glass	2.00	76
	C-glass	3.30	69
	S-glass	4.60	85.50
Aramid Fibers	Kevlar 29	2.90	83
	Kevlar 49	3.00	130
	Kevlar 149	3.45	185
Carbon Fiber	Low strength HS	3.45 - 5.00	230 - 240
	Intermediate	4.13 - 6.37	250 - 300
	Ultra-high HM	1.89 - 4.90	300 - 350

Carbon fibers are commonly used in high performance composite applications. Carbon fiber composites have great heat, corrosion, wear and creep resistance and high strength to weight ratio [2, 7, 22]. This make carbon fiber reinforced composite materials attractive in the aerospace, automotive, marine and sport industry [7]. Parts such as helicopter blades, engine nozzle, radar applications, racing car brakes and wind turbine blades are some of components made from CF composite materials [7].

The stiffness of a composite materials are highly dependent on the type of fiber, angle orientation and fabrication methods [2, 4, 8]. For instance, the elastic modulus along the 0-degree of a traditionally manufactured carbon fiber can reach up to 1000 GPa, while the transverse modulus is about 35 GPa [2]. The directional stiffness variation of the reinforcing fiber makes composite materials to have an anisotropic property. Moreover, high modulus fibers have low strain to failure, compared to low modulus fibers [2].

In addition to the mentioned factors, the volume fraction of reinforcing and matrix phase determine the final properties of the composite material[8]. Basically, high volume fraction fiber provides higher strength and stiffness. However, to obtain adequate matrix support to the fiber, the volume percentage of the reinforcement should be less than 70% of the total volume of a component [13]. Furthermore, the length of the reinforcing fiber affects the effectiveness of the fiber. To obtain an effective strength and stiffness the length of the fiber must be longer than the critical fiber length. This critical length depends on the diameter of the fiber filament,

its tensile strength, and the fiber-matrix bonding strength (shear yield strength of the matrix) [18].

Critical length (l_c):

$$l_c = \frac{\sigma_f d}{\tau_c}$$

(1)

Where d is fiber diameter , τ_c is shear and σ_f is max. strength of the fiber.

The continuous phase within the composite material, known also as the "matrix phase" has low mechanical properties compared to fiber material [8]. The matrix phase material can be plastic polymer, metal or ceramics. The role of the matrix phase is to keep the reinforcing fiber in desired orientation and location, as well as protect them from abrasion and environmental damages[13]. Furthermore, the matrix phase transfers load to the adjacent fibers and provides the geometry to the structure.

There are various matrix composites, such as Metal Matrix Composites (MMC), Polymer Matrix Composites (PMC) and Ceramic Matrix Composites (CMC). PMC are widely used matrix materials and they are categorized as thermosets and thermoplastic polymers [13]. Epoxy is one of the commonly used polymer matrix in the aerospace applications. Epoxies have low shrink rate, great insulation, produces less residual stress at bond with the reinforcement and have high strength and stiffness [13]. one disadvantage of epoxy matrix is its high viscosity and weaker properties when exposed to UV-light. Moreover, thermoplastics tend to exhibit good chemical resistance and thermal stability [2].

2.2   Characteristics of Fiber Reinforced Composite Materials

Parts fabricated from composite materials have anisotropic material properties and their mechanical properties differ directionally. They have high stiffness and strength along the strengthening material and they are much weaker along their transverse direction [13, 15, 17, 18]. Often, the composite materials have orthotropic properties. This means they have three different mechanical properties for each of the principal axis.

$$E_{11} \neq E_{22} \neq E_{33}$$

(2.0)

Where E_{11}, E_{22} and E_{33} are elastic modulus in x-,y- and z-direction, respectively.

Mechanical properties of composites depend on length of fiber[8], fiber orientation [4], fiber shape, type of fiber, volume fractions of phases [8] and the fiber-matrix bonding [5, 6]. Furthermore, the method of fiber production and later manufacturing method of the composite material have significant effects on the final mechanical properties of a composite component [18]. As the mechanical properties of a part fabricated from composites differ from the individual constituents, such method is required to estimate the final mechanical property. An estimation method called "Rule of Mixture" (ROM) can be applicable.

For a continuous and aligned fiber reinforced composite, modulus of elasticity in the longitudinal direction is described by the 'Rule of Mixtures' (ROM). The rule shows that "the

stiffness of the composite material is a weight- mean of the modulus of the two phases and simply depends on the volume fraction of fibers"[2].

Modulus (parallel to the fibers) [2]:

$$E_1 = E_m V_m + E_f\, V_f \tag{2.1}$$

Assuming the fiber and matrix have equal strain, and if no voids are present, the entire area of the composite part (A) is then the sum of the area occupied by the fiber (A_f) and the matrix (A_m).

$$E_1 = E_m \frac{A_m}{A} + E_f\, \frac{A_f}{A} \tag{2.2}$$

 Where E_1 is the Young's modulus of the composite material. E_f and V_f are Young's modulus and volume fraction of the fiber respectively, while the E_m and V_m represents for the matrix.

The stress in the composite material can be expressed: Stress (parallel to the fibers):

$$\sigma_C = \sigma_m V_m + \sigma_f V_f \tag{2.3}$$

A similar equation to Eq. 2.2 and 2.3 can be used to predict the density, Poisson's ratio, shear of the composite part.

To summarize, maximum strength is achieved when long fibers are oriented parallel to the applied load [4]. Combination of different degrees of orientation can be used to obtain properties closer to isotropic property, also known as "quasi-isotropic "property [10] . Generally, better overall composite properties are obtained when the fiber distribution is uniform. Various types of voids can present in composite materials depending on the fabrication processes and matrix type. Small voids form usually adjacent to fibers [2, 4]. These are some of many challenges on achieving the desired   mechanical properties in composites.

2.3   Manufacturing methods of components from composite materials:

There are several manufacturing methods of parts using composite materials , among others wet layup and prepreg manufacturing methods. Parts are made by lying a pre-impregnated fibers and resins layer-by -layer by hand or an automated production method until the desired thickness is reached. Often, the successive layers have an alternating fiber direction to minimize the isotropic mechanical property of the finished part [23].

Composite parts can be manufactured by using prepreg fiber cut in desired size and direction and then lay-up in successive layers. "layup" simply refers here to the processes of staking several layers together to produce a laminate. The prepreg is commonly used term for the intermediate product where several individual fiber tows are embedded within a polymer matrix, ready for layup when delivered [14]. The part is then cured in autoclave which controls the temperature and amount of applied pressure to the part. After the curing in the autoclave and post-processing is completed, the part is ready for use. This process produces very strong and stiff engineering parts, proportional   to commonly used engineering   metals while maintaining light weight. However, the process requires long manufacturing time, high

manufacturing skills and involves high material waste. Additionally, there is a design limitation due to the manufacturing difficulties of parts with complex geometry [10].

Moreover, large parts in the aerospace and automotive industry are fabricated by the manufacturing method known as Automated Fiber Placement (AFP) [14]. In AFP the fiber tapes are laid next to each other in specific orientation, and heated to melt the thermoplastic matrix by a movable robot head [14]. This method has similarities with continuous fiber fabrication method used by some 3D printers where fiber and plastic filaments are heated and extruded through a nozzle fitted in a movable head [10]. Parts manufactured using composite materials by AFP and FFF have their similarities since both methods build parts layer-by-layer. However, the FFF method has more design freedom, lower material waste and production cost [16, 24].

2.4   Additive manufacturing and 3D print technology

Additive manufacturing (AM) is a manufacturing process of components by adding material layer upon a layer [2, 15, 16]. The term AM represents various technologies, such as Rapid Prototyping (RP), Direct Digital Manufacturing (DDM), Fused Deposition Modeling (FDM) or Fused Filament Fabrication (FFF), Selective Laser Sintering (SLS) , Stereolithography (STL) and Laminated Object Manufacturing (LOM) [24]. Today, different materials, such as plastics, polymers, metals and composite materials are used in additive manufacturing. However, structural materials with high melting temperature face many challenges and are currently expensive and less commercially used.

The history of AM starts back in 1980s [25], when Charles Hull invented stereolithography (SLA); a form of 3D printing system, STL- file format and slicing technique [24, 26]. The STL-file format and slicing technique is commonly used by the AM machines. On the late years, several technologies among them FDM developed by Stratasys are commercialized. Furthermore, several AM technologies have been developed and commercialized. Nowadays, conventional AM is widely used manufacturing process of prototypes and specific functional parts.

AM have several advantages comparing to the traditional manufacturing methods. The design freedom, reduction of material waste and manufacturing cost are among others that make AM an attractive technology to the manufacturing industry and research community. AM allow engineers to design more complex geometries without restricted by manufacturing complexity. Fabricating such complex geometries in conventional manufacturing method is difficult and time-consuming process. In AM process the designing and manufacturing processes takes place at same place [27]. This eliminates delivery time, part storage, transport cost and manufacturing expenses [24]. Despite all the advantages of AM, there are some drawbacks that must be solved; Parts are built layer-by-layer in AM, this means the strength of the part is weaker perpendicular to the working plane [6, 28]. This is due to the interfacial bonding between layers [6]. This kind of problem is more problematic in additive manufacturing of composite materials, where the fiber-matrix bonding is weak in addition to the AM parameters [4]. Unlike conventional manufacturing processes of composite materials, no pressure/vacuum is applied during fabrication of parts by AM process. Therefore, composites produced by AM

experience an increase in porosity and this largely weaken their property in the building direction (z-direction) [1, 4, 21].

All AM techniques operate in the similar principle. The processes of 3D printing (AM) starts with designing a geometry of a component in 3D CAD (computer-aided design) software. The file is then converted into a stereolithography file format (STL), commonly used by all AM machines. The design is then sliced into thin layers by a slicing software. The required information of the part such as layer thickness, tool path, part orientation, type of material and others are prepared in the slicing software and included in the STL-file. This STL-file is then sent to the AM machine and used as a command when fabricating the designed part.

 During fabricating using 3D print, a filament is extruded through a hot nozzle at a constant rate laying thin layers of material upon each other until the designed component is completed. The filament is pushed into the nozzle by a stepper motor pushing the melted filament out of the nozzle. The filament is heated inside the nozzle until it reaches its glass transition temperature (T_g). The 3D printer head moves only in XY-plane, printing the outer edges of the part first and then proceeds to the infill patterns. Once one layer is successfully printed, the working bed moves one step down leaving one-layer thickness for the next print. This process repeats until the entire component is printed.

Surface finish of additively manufactured parts depend on the fabrication layer thickness. When printing curved geometries in the z-direction, the process produces a stair-steps. The raster-effect is appearing as successive layer must lay at an offset from the previous layer. This raster effect creates poor overall surface finish and strength. Typically, design orientation play an important role in additively manufacturing of components. Understanding the loading conditions of the component is required when making decision on the printing orientation, this is due to bearing capacity of parts in z-direction is often weak. The highest strength is obtained when the load bearing part lays in the xy-plane. Sometimes it can be essential to split parts into multiple printed pieces to achieve optimal strength. Identifying critical dimensions of your part is another case which require consideration, because 3D printers have higher precision in plane parallel to the working plane.

Complex inner geometries or overhangs require a support. Supports can be reduced by selecting the maximum bed contact. However, this is not always possible due to the several parameters to prioritize. One option to solve this is to used angled overhangs to reduce and improve support . Supports are printed in a pattern that is relatively easy to remove wither in solution or break out. Some AM machines have a separate material only used to print   the support. However, Mark-Two has not a separate support material, instead the plastic matrix material is used to build the support and the matrix phase of the part. The support is printed in some way it is easily to remove.

AM have great advantages over conventional manufacturing process and previously tedious complex geometries can be manufactured easily using AM. AM requires less raw material for manufacturing of same component compared to subtractive manufacturing processes. Since components can be additively manufactured at sites, time of delivery, undesired mass and storage of excess parts can significantly reduced. AM reduces additional machine requirements

since from start-to- finish manufacturing is provided by the 3D printer. However, AM fabricated parts have anisotropic [29] material property due to the weaker bonding strength between adjacent printed layers both in Y- and Z-direction[6, 28], and are used for fabricating parts with known loading conditions .

Thermoplastic materials ABS, PLA and Nylon are commonly used filaments in 3D print [29], but these materials have limited stiffness/strength and cannot applied to conventional engineering applications. However, strengthening these polymers with continuous fiber reinforcement (CFR) has provided significant increase in stiffness/strength of the components[4, 5]. Dickson et al, in study reported a tensile strength comparable with engineering materials such as aluminum 6061-T6[21]. Additively manufacturing of Continuous Fiber Reinforced Polymers (CFRP) using 3D machines is relatively new method and it is at its early stage. Moreover, understanding mechanical properties of additive manufactured materials is still limited [5].

Table 2. Few Advantages of Additive manufacturing.

Advantages of AM	Explanation
Design freedom	Complex geometries can be manufactured with minimum limitation
Material efficiency	Reduced material waste
Weight reduction of parts	Giving a part strength only at required functionality and reducing unwanted mass
Reduce storage	No need to have spare parts at store
Low manufacturing cost	No need for additional machines and operators and low product development cost

The mechanical properties of components produced by AM is dependent on several factors [8], such as the building direction [5], thickness of layer [3, 6], bonding strength between layers [6], formation of voids [21] and type of filament material [6]. The effect of printing parameters such as infill-speed, nozzle temperature and layer thickness has studied by Ning et al, [3]. Results indicated infill-speed of 25 mm/s, nozzle temperature of 220°C and thicker layers led to largest average stiffness/strength [3]. Ning et al. also concluded high nozzle temperature increases porosity of composites and reduce their strength [21].

Generally, in composite materials both the AM parameters and fiber orientation influence the anisotropic property [30]. A unique advantage of AM when used for composite materials is that the orientation and alignment of continuous fiber can be accurately located in complex geometries, which is very difficult in traditional molding fabrication [3].

Finally, FFF method can be used to additively manufacture parts from several materials, such as metal parts. AM of material with high melting temperature requires special printing parts and is expensive compared to thermoplastic filament. Moreover, Powder Bed Fusion (PBF), Direct Energy Deposition (DED) are commonly used AM methods for metals.

2.5   Markforged® Mark-Two 3D Printer

Mark-Two 3D printer produced by the Markforged® is the second generation of their desktop Mark-one continuous fiber fabrication 3D printers introduced in 2016[31]. This 3D printer is referred as Mark-Two in this thesis. Mark-Two is a compact and small desktop AM machine. The machine is capable of laying two filament materials with its two nozzles. The matrix phase can be Nylon or Onyx, whereas the reinforcing material can be carbon fiber (CF), fiberglass (FG), Kevlar and high-strength high-temperature fiberglass (HSHT)[32].

Nylon and Onyx are the two plastic materials which can be used in Mark-Two. Onyx is made of nylon strengthened with a carbon micro-fiber and has a mechanical property better than nylon. Onyx can be used alone, or it can be reinforced with continuous fibers. The plastic materials can absorb moisture easily [10] and parts built from wet plastics have poor surface finish and strength. Therefore, it must be stored in a tight enclosed box. The plastic material is supplied through small tube to the extruder which pushes the filament further to the hot nozzle. The 3D printer has two storing places for reinforcing fiber spools inside the machine.

Figure 2-1. Markforged® Mark-Two 3D printer for composites and airtight box

The maximum size that can be built by mark Two is 320 mm x 132 mm x 154 mm (x-y-z respectively). Mark-Two has two nozzles, one nozzle extrudes the matrix material of either Nylon or Onyx, while the second nozzle is for the reinforcing fibers. The filament material is heated to its glass transition at the nozzle and extrudes at constant rate while the printing head move in the XY-plane. Only one nozzle can extrude material at a time and the continuous fiber is cut at every layer. After one layer is deposited the working bed moves a one-layer thickness along the z-direction as specified in the slicing software, which is 0.125 mm if carbon fiber is used and 0.1 mm for the other fibers. This thickness is pre-defined when printing parts with

reinforcing fibers, while it is possible to define a layer thickness for parts without reinforcement.

The Onyx is heated to 272 °C before it deposits. Unlike other AM machines, no heat is required to the bed and parts can be removed out right after fabrication is finished. Mark Two starts printing first the walls and then infill pattern inside the walls starting by the floor layers if no support or elevation is selected. The first layer of the floor prints with an orientation of positive 45-degrees following by negative 45-degrees . The orientation of the matrix material at ±45-degrees is pre-defined and user has limitations printing in other orientations. Moreover, there are more pattern options such as rectangular, triangular, hexagonal and solid infill patterns which are not discussed in in this study.

Markforged® has developed their own cloud based slicing software to upload the STL-file and make desired print settings. It is there the material and reinforcement settings such as layer thickness, fiber orientation, type of pattern, pattern density and number of fiber layers decided. Moreover, internal layer-by-layer fiber lay-out modification can be specified manually under the internal view settings. More information about the 3D printer and Eiger software is provided on section 3.1.

Continuous fiber reinforcing of polymers in 3D print

Nowadays, it is possible to use several types of materials in AM. However, materials for matrix phase that are available for AM using FFF/3D printing method are limited to polymer filaments. These polymer filaments can be combined with strengthening materials such as fiber stands to obtain stronger and stiffer product[17]. Laying continuous fiber reinforcement in a polymer base matrix using 3D printer allow to combine the advantages of AM and composite materials at the same time. This combination is relatively new technique and it takes the FFF/3D printing technology further from prototype fabrication stage to fabrication of stronger functional parts.

Companies such as CF3D® and Markforged® develop composite 3D printers for industrial purpose. However, currently available commercial desktop composite 3D printers are developed only by Markforged®. The latest announced printer by Markforged® , named "Mark-two" 3D printer combines the Continuous Filament Fabrication (CFF) and FFF technology to manufacture composite parts [33]. This printer was used for fabrication of the testing samples for this study. Mark-Two printer lays layers of matrix phase and continuous fibers following the input setting obtained by the user in "Eiger", an online slicing software. The fiber is heated to the glass transitional temperature (T_g) and extrudes through a hot nozzle moveable in XY-plane. There is a possibility of building layers of fibers oriented in various angles. The part can be reinforced only in 2D plane, namely XY-plane (Figure 3-1). Therefore, the component is weak when loaded on out-of-plane (z-direction). This is one of downsides of the manufacturing technology due to parts in real world are exposed for several directional loading. Thus, the possibility of reinforcing a part in the out of plane direction becomes a constrain limit for design freedom. Due to layer by layer adding of materials the bonding between the successive layers is weak and reinforcing this direction by fibers is limited. As a

result, printed components greatly exposed to more orthotropic mechanical behavior. Detailed description of the 3D printer and the printing process are presented in section 3.1.

2.6   Finite Element Modeling using Ansys software

Composite materials are specially used in aircraft structures, automobiles, and sport goods. Composite material models can be modelled with layer elements . After creating a model using layered elements, structural analysis including large deflation and stress stiffening can be performed [34].

Composites materials are more challenging to model than isotropic materials due to each layer may have different orthotropic material property, orientation angle and layer thickness. Depending upon the application and   type of results required,   SHELL181, SHELL281, SOLSH190, SOLID185 and SOLID186 (Layered Solid) are types of element available for modeling composite materials [35]. Shell elements allow to define layered composite of thin-walled structures which are common in aircraft structure, boat hulls and racing cars analysis [38].

There are several ways of modelling composite materials in Ansys software. It can be modelled in Workbench or in Mechanical Parametric Design Language (APDL) Ansys software [35]. The FE models in this study were modeled and analyzed in ANSYS Mechanical APDL 17.0 . Finite Element Analysis (FEA) of composite materials can be performed in micromechanical, lamina, and laminate level of approach [34]. One method to achieve a lamina or mesoscale level analysis is using shell element, which were used in this study [35]. To analyses a composite laminate, input parameters including number of layers, orthotropic material properties and orientation angle of the reinforcing material must be provided [36, 37]. An isotropic material requires minimum two material properties ; Youngs modulus and Poisson's ratio in x-direction. Whereas an orthotropic material requires nine elastic constants, three Young's modulus, three Poisson's ratio and three shear modulus values [37]. The nine elastic constants are used in the strain-stress relation matrix of Hook's law. The properties of the materials are stored in the material stiffness matrix $[D]^{-1}$ as in equation 2.4.

From orthotropic form of Hook's law:

$$\{\varepsilon\} = [D^{-1}]\{\sigma\} = \begin{bmatrix} \dfrac{1}{E_x} & \dfrac{-v_{xy}}{E_y} & \dfrac{-v_{zx}}{E_z} & 0 & 0 & 0 \\[2mm] \dfrac{-v_{xy}}{E_y} & \dfrac{1}{E_y} & \dfrac{-v_{yz}}{E_y} & 0 & 0 & 0 \\[2mm] \dfrac{-v_{zx}}{E_z} & \dfrac{-v_{yz}}{E_y} & \dfrac{1}{E_z} & 0 & 0 & 0 \\[2mm] 0 & 0 & 0 & \dfrac{1}{G_{yz}} & 0 & 0 \\[2mm] 0 & 0 & 0 & 0 & \dfrac{1}{G_{zx}} & 0 \\[2mm] 0 & 0 & 0 & 0 & 0 & \dfrac{1}{G_{xy}} \end{bmatrix} \begin{Bmatrix} \sigma_x \\ \sigma_y \\ \sigma_z \\ \tau_{xy} \\ \tau_{yz} \\ \tau_{zx} \end{Bmatrix} \qquad (2.4)$$

Laminate beam theory can be used to construct finite element for analyzing of composite structures [36]. In static analysis of a simple loaded composite beam, the deflection and stress at the beam can be derived by differentiation. The thin beam theory considers that normal-to-the- beam- mid-surface remain straight and normal after deformation. Furthermore, if rotation and shear are ignored then the strain and curvature equations can be expressed as follows [38].

$$\varepsilon_0 = \frac{\partial u}{\partial x} \quad , \quad k = -\frac{\partial^2 w}{\partial x^2} \tag{2.5}$$

Where ε, κ, represents   strain and curvature, while u and w are displacements in x and z-directions, respectively. Normal strain at any point can be then expressed as $\varepsilon = \varepsilon_0 + zk$. The stress in the axial direction is determined by

$$\sigma_x = Q_{11}(\varepsilon_0 + zk) \tag{2.6}$$

For simply supported beam zero displacement in the z-direction and zero moment are defined at the supports. Furthermore, the equation for the Hook's law can be stated as in equation 2.7.

$$\begin{bmatrix} N \\ M \end{bmatrix} = \begin{bmatrix} A & B \\ B & D \end{bmatrix} \begin{bmatrix} \varepsilon^\circ \\ \kappa \end{bmatrix} \tag{2.7}$$

Where A ,B and D are 3x3 matrix. A matrix represents the in-plane stiffness properties [36], B matrix is coupling that arise between the bending and the membrane action and B is zero   in case of symmetric laminate. D-matrix is the bending stiffness properties. The mid-plane strain, curvature, in-plane loads and moment are represented by ε, κ, N and M, respectively.

In equation 2.7 the stiffness matrix relates the stress results to strains. In case of non-symmetric laminate of composite materials, an out-of-plane bending can be occurred [36]. The non-symmetric lay-up of fiber give non-zero value to the B-matrix of the laminate stiffness and that coupled the in-plane and bending response. Therefore, the material lay-up in this study were modeled symmetry to avoid the out of plane movements [10] . Furthermore, it is important to remember the FE results are an approximate result and their occupancy depends among others on the choice of element type and mesh density [35].

Rule of Mixture

For a continuous and aligned fiber reinforced composite, modulus of elasticity in the longitudinal direction is described by the 'Rule of Mixtures' [10, 11]. The rule shows that the stiffness of the composite material is the sum of the individual volume fraction and their corresponding material property . The ROM simply depends on the volume fraction of fibers [2, 10].

If we assume there is no interfacial gliding between the layers of the matrix and reinforcement during loading along the fiber axis, then there will be equal strain for both plies [2, 10].

$$\varepsilon_{11} = \varepsilon_{11f} = \frac{\sigma_{11f}}{E_f} = \varepsilon_{11m} = \frac{\sigma_{11m}}{E_m} \tag{2.8}$$

Where f refers for fiber and m is for matrix and the numbers represents the direction with respect to the fiber axis, σ_{11f} and σ_{11m} are strength of the fiber and matrix parallel to the fiber, respectively.

Since the reinforcing fiber is much stiffer than the matrix phase and the fiber will be subjected to higher stress. The overall stress is then the sum of the stresses from both materials with the factor of their strength[2, 13].

$$\sigma_{11} = (1 - V_f)\sigma_{11m} + V_f\sigma_{11f} \tag{2.9}$$

The V_f represents volume percent of fiber and $(1-V_f)$ is matrix volume fraction and σ_{11} is the tensile strength of composite parallel to the fiber . Furthermore, the elastic modulus of the composite along the fiber axis will be formulated as [10]:

$$E_{11} = (1 - V_f)E_m + V_fE_f \tag{2.10}$$

Where E_{11} is the Young's modulus of the composite material along the fiber. E_f and V_f are elastic modulus and volume fraction of the fiber respectively, while the E_m and V_m represents the elastic modulus of the matrix and its volume fraction.

If parts have uniform cross-sectional area, the volume fraction of the fiber can be estimated by the area ratio:

$$V_f = \frac{A_f}{A_{total}}, \quad V_m = \frac{A_m}{A_{total}} = (1 - V_f) \tag{2.11}$$

If no void presents and the material is assumed to have transversely isotropic mechanical property, then $E_{22} = E_{33}$, $v_{12}=v_{13}$, and $G_{12}=G_{13}$.

$$E_{22} = \frac{E_fE_m}{E_f - V_f(E_f - E_m)} \tag{2.12}$$

The in-plane shear modulus, G_{12}, can be estimated from:

$$G_{12} = \frac{G_fG_m}{G_f - V_f(G_f - V_m)} \tag{2.13}$$

$$G_{23} = \frac{E_3}{2(1 + v_{23})}$$

The Poisson's ratio coefficient can be obtained from:

$$v_c = v_mV_m + v_fV_f \tag{2.14}$$

Based on the knowledge of the fiber elastic modulus E_f , matrix modulus E_m , and fiber volume fraction V_f , the rule-of-matrix approach allows prediction of E_{11}, $E_{22}=E_{33}$, $v_{12}=v_{13}$, and $G_{12}=G_{13}$ of a composite [2, 15, 34].

The ROM (equations 1.2-1.6) predicts the mechanical properties of a part fabricated from composite materials based on the mechanical properties of the individual.

3 METHODOLOGY

To characterize the mechanical properties of 3D printed composite materials, tensile and flexural experimental tests was performed. Furthermore, a Finite Element Model (FEM) was developed.

The 3D printer used in this thesis was Markforged® Mark-Two, continuous fiber 3D printer[32]. Test samples were fabricated from carbon fiber filament imbedded in a thermoset plastic matrix named "Onyx" by its producer Markforged®. Both materials were delivered by the 3D printer manufacturer Markforged®. "Onyx" is the matrix phase material and it is used in synonym to the matrix material or matrix phase in this report[39].

First, a 3D model of the specimen was modeled in Autodesk inventor 2018 and the file was converted into STL-file. STL-file is type of file commonly used by additive manufacturing machines. The STL-file contains a triangular mesh patterns of the 3D CAD model. This 3D model was then sliced into thin layers in parallel to the working plane by a slicing software called "Eiger". The working plane lays in XY-plane as illustrated in Figure 3-1. "Eiger" is an online freely available cloud-based software, developed by Markforged® 3D printer manufacturer. In this study, this slicing software was used to cut the 3D model provided as STL-file into several thin layers.

During slicing, the slicing software generate information about the tool path, layer thickness, fiber orientation angle, number of fiber layers, infill density, type of pattern, number of total layers and type of material in each layer according to the settings provided. This information is used as a command by the 3D printer during printing.

3.1   Additive Manufacturing of CFRP using Mark-Two® 3D Printer

Among several additive manufacturing technology, Fused Deposition Modeling (FDM), Fused Filament Fabrication (FFF), Stereolithography (SLA) and Selective Laser Sintering (SLS) are commonly used in 3D printing technology. The 3D printer used in this study uses the FFF technology.

Testing samples were fabricated by FFF technology using Markforged® Mark-two 3D printer. Mark-two is a compact 3D printer for composite materials which benefits from the combination of FFF and Continuous Filament Fabrication (CFF) technology. It has the capability of laying continuous fiber such as Carbon Fiber (CF), Fiber Glass (FG), Kevlar and High Strength High Temperature fiberglass (HSHT) within nylon or Onyx matrix. Mark-Two 3D printer has two nozzles, one nozzle for each type of material. The fiber nozzle is 0.9 mm wide, while the thermoset matrix phase nozzle is 0.4 mm wide[32]. For fabricating the samples, a continuous carbon fibers are imbedded inside a chopped carbon-fiber-reinforced nylon polymer called "Onyx®" [40]. Mark-Two 3D printer heats the filaments to the glass transition temperature (T_g), which is about 272℃ for the carbon fiber, and extrudes it through the hot nozzles,

building a component layer-by-layer on XY-plane[40]. Both materials were provided by the Markforged®, and measurements provided by the manufacturer shows, the carbon fiber- and Onyx -filament was 0.38 mm and 1.75 mm in diameter, respectively. The mechanical properties of Onyx provided by Markforged® was 1.4 GPa and 2.9 GPa in tensile and flexural stiffness, respectively [39].

Onyx is a nylon polymer reinforced with micro- chopped carbon fiber. It is moisture sensitive material and it must be stored dry [39]. The polymer matrix material feeds from a dry box into the stepper motor into the nozzle through small tubes in Mark-Two. However, there is a possibility of observing moisture within the stepper motor if it has not been used for some time. It is then important to perform a purge printing to remove any wet plastic filament. The 3D printer usually takes a purge printing before it starts printing new parts if it has been not used for a while. In addition, it removes material s that have been inside the nozzle when changing material during printing. But it important to perform the purge test manually from the setting before giving order to print a new part.
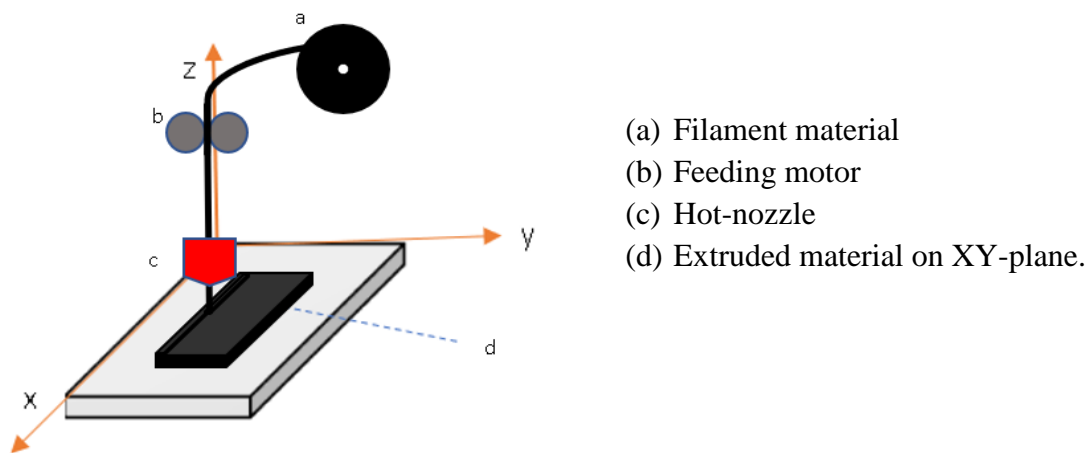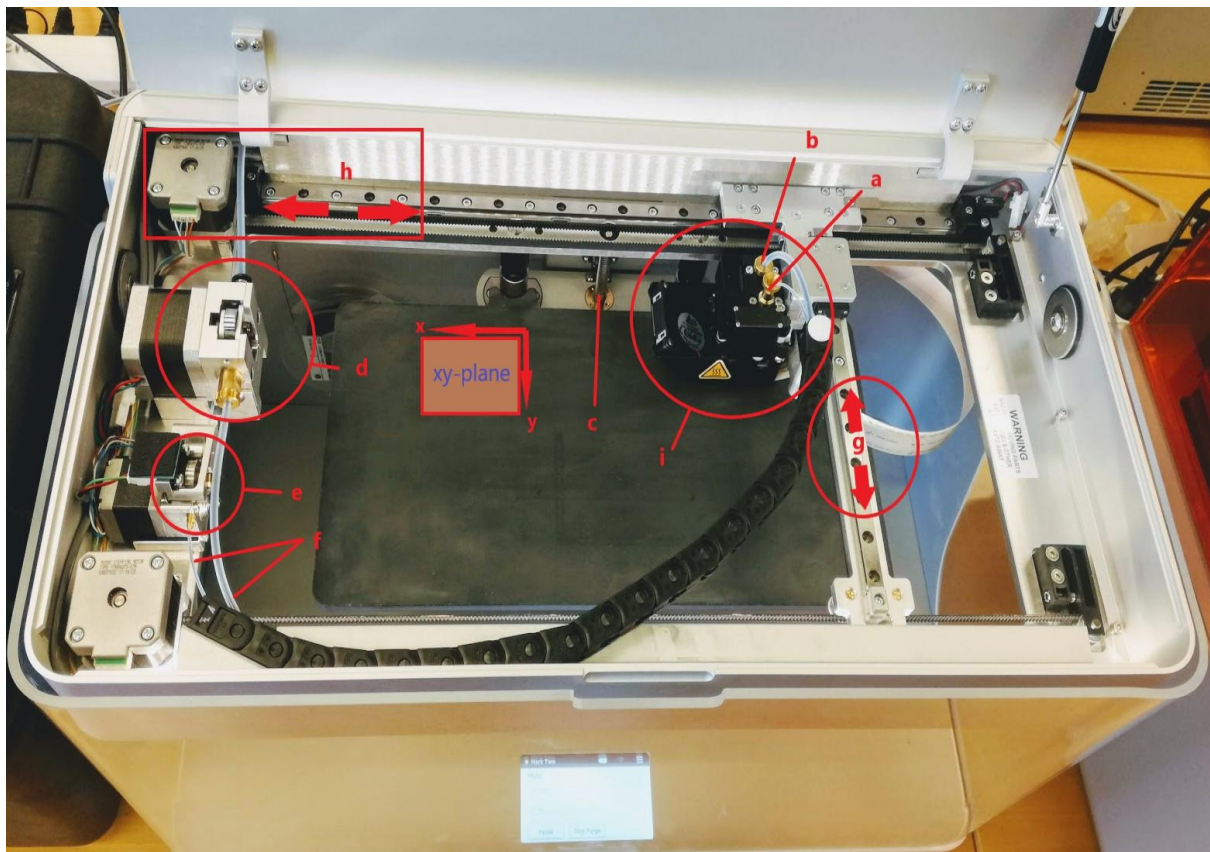
(a) Filament material
(b) Feeding motor
(c) Hot-nozzle
(d) Extruded material on XY-plane.

Figure 3-1. 3D printing illustration

|					
a)	Nozzle for Fiber from top	d)	Plastic feed motor	g)	Movement in y-direction
b)	Nozzle for plastic	e)	Fiber feed motor	h)	Movement in x-direction
c)	Stepper z-direction	f)	Transport tubes	i)	Printer head

Figure 3-2 . Inside Markforged® Mark-Two 3D Printer

The printer head moves in horizontal xy-plane at a given rate by belt and push systems in both
x- and y-direction as shown in Figure 3-2. A stepper motor moves the working bed in z-
direction at a rate of one-layer-thickness. The thickness of the layer was as specified 0.125 mm
in the Eiger software. During fabrication, Mark-Two uses one nozzle at a time for extruding
material and the extruding rate is dependent on the type of the filament and its melting rate.
These settings are pre-defined by the manufacturer in Mark-Two 3D printer and the user has
no possibility to change them.

The direction and orientation of the working plane were illustrated in Figure 3-1. The printer
builds layer upon a layer in the z-direction providing 100-200-micron layer resolution. The
best resolution that can be obtained is 125-micron if carbon fibers is used as reinforcing
material. Moreover, the printer has a tolerance of $\pm$ 0.05 mm in x- and y- direction[32]. 3D
printed components are stronger along the working plane than in-plane (z-axis). The 3D printer
can lay continuous fiber only on the XY-plane. Hence, systematic design orientation during
designing and printing is required. This consideration is crucial due to the strength and stiffness
of component depends on the fiber material significantly [28]. 'Fiber' was used to refer the
reinforcing material or the carbon fiber in this study.

In 3D fabrication of parts from composite materials, the setting of the printer has significant effects, in addition to the weak bonding between successive layers due to AM as discussed in the literature. At the end of each fiber layer, the fiber must be clipped. The starting and ending point of the fiber for each layer introduces a fiber discontinuity to the component. Lozada, J.N. et al. investigated tensile properties and failure behaviors of chopped and continuous carbon fiber 3D printed composites. The failure in some of the test samples occurred at the discontinuity locations[8]. To avoid such discontinuity of reinforcing fiber, a special attention was then given in setting-up the printer in Eiger. In this study, the start and end location of a fiber was specified to be at the end part of the sample for each fiber layer (Figure 3-3). The location where the fiber starts and ends was far from the gauge section. Hence, the probability of failure due to fiber discontinuity was reduced.

The terms "isotropic" and "concentric" used in the Eiger software for the fiber pattern and ring are confusing. Particularly the term "isotropic" in Eiger has nothing to say about material property. Hence, it should not be exchanged with the well-known term "isotropic" in materials science which explains the material property. The concentric fiber ring and the isotropic fiber patterns start, and end location are shown in Figure 3-3 marked with "d". Concentric fiber rings lay around a boundary of a wall and it can be used to strengthen an outer walls of a part or inner walls such as bolt holes[28]. The isotropic fiber patterns are located within the concentric fiber rings. It is possible to set an angle for the isotropic-fiber-patterns as required in Eiger software.
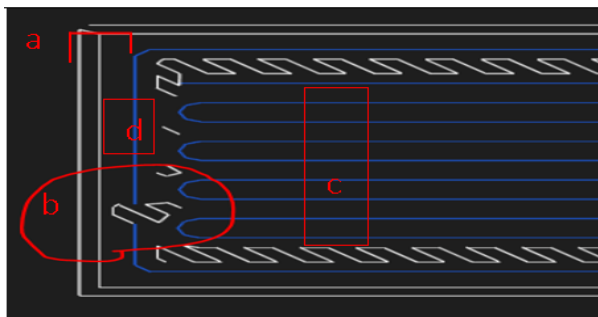
(a) Unreinforced part of specimen at both longitudinal   ends,   (b)   Carbon   fiber discontinuity, (c) An isotropic 0-degree carbon fiber infill pattern, (d) Concentric carbon fiber layer shown in XY-plan.
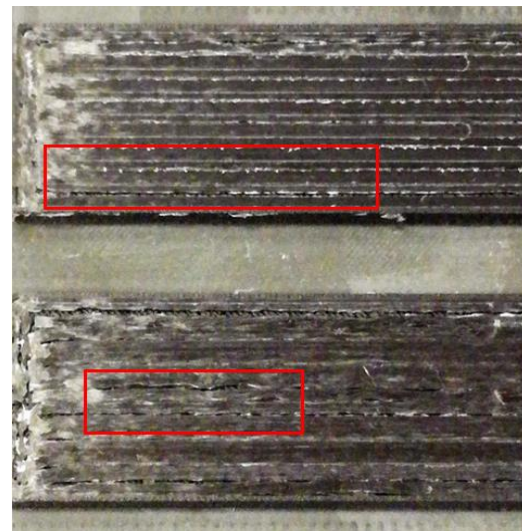

Figure 3-3. Locations and type fiber patterns   *Figure 3-4. Voids between consecutive layers*

Unlike Mark-One ® 3D printer, Mark- Two® can print continuous carbon fibers in isotropic pattern. Isotropic pattern at 0° angle orientation, as shown on Figure 3-3 "c", was used in this study. Infill density and pattern can affect the properties of 3D printed parts. Generally, parts that require higher strength and stiffness must use solid infill pattern with 100% infill density of the matrix material. The 100% infill density setting, which was also applied in this study, increases the weight of a component, and reduces the number of voids inside the part.

Lozada, J.N. et al. studied effect of density and type of infill patterns on the stiffness and strength of Nylon and Onyx. The E-modulus and strength of both materials increased with increasing density[8]. However, among all types of patterns the triangular pattern provided best results when comparing the strength per weight results[8].

(a) carbon fiber "isotropic pattern" and one "concentric fiber ring"

(b) Matrix material (Onyx) first layer at +45°

 (c) Matrix material (Onyx) second layer at -45°

Figure 3-5. (a) an isotropic 0-degree (UD) oriented fiber infill. (b) + 45-degree matrix. (c) – 45-degree matrix

Eiger has several options (Table 3) where type of pattern, infill density, number of fiber layers and their angle can be determined as required. These options have significant effects on the strength of the fabricated. The nozzle temperature and infill speed were predetermined by the 3D printer manufacturer and cannot be changed. All the settings used in this study are summarized in Table 3. The matrix phase was predetermined to be printed in orientation of $\pm45°$ shown in Figure 3-5 (b & c), while the fiber can be utilized in any required angle (Figure 3-5 a). The printer starts printing the matrix material always at positive 45° with respect to the reference x-axis, followed by an angle of negative 45°. This was predefined by the manufacturer and the user has no possibility to deal with. The predefined settings limit the design freedom of the user and those were some of the drawbacks of this 3D printer. The axis coordinates in the cartesian coordinate system and positive angle direction are predefined in reverse order in Markforged® mark-Two 3D printer (Figure 3-1). The x-axis was predefined as positive when moving from right to left and angles were measured positive in counter clockwise from the x-axis.
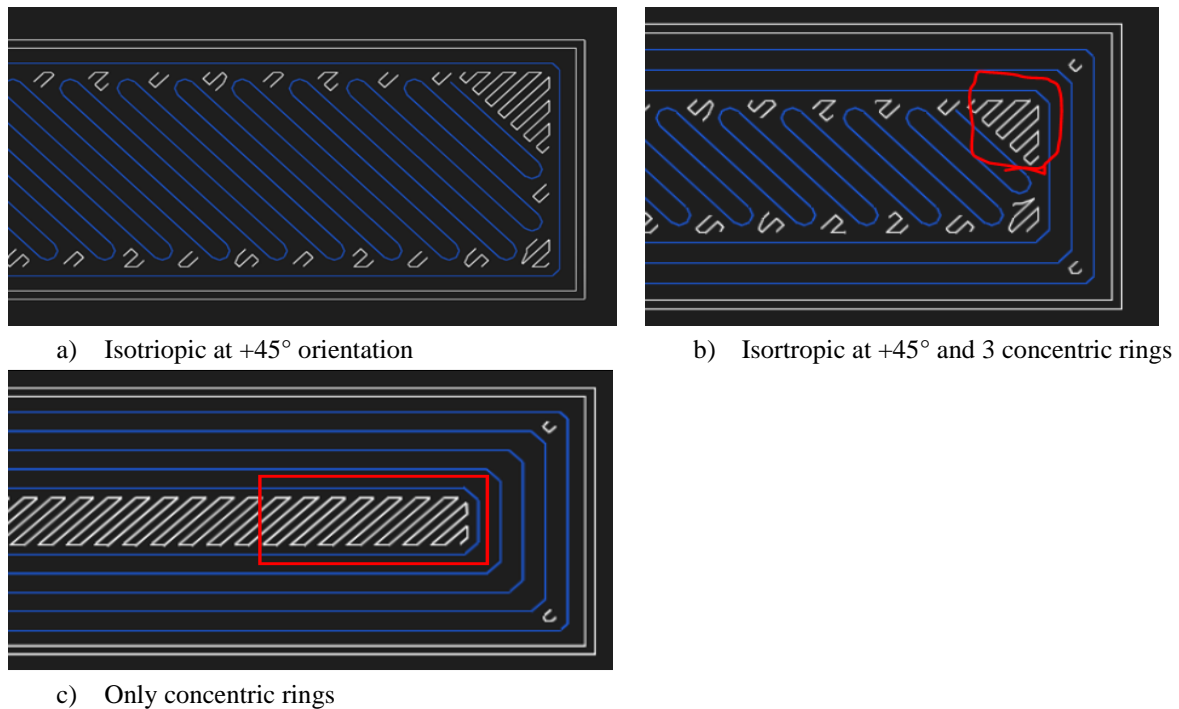
a)   Isotriopic at +45° orientation

b)   Isortropic at +45° and 3 concentric rings

c)   Only concentric rings

Figure 3-6. Isotropic and combination of concentric and isotropic fiber orientation.

When the isotropic fibers are laid at positive 45° as in Figure 3-6(a), it is clearly observed that a single continuous carbon fiber runs whole around the layer. Since the strength of the matrix is much less than the fiber, a pullout failure is likely to occur when loading in tension before the fiber is fully stressed. In such case, the composite material could absorb more energy due to the possibility of longer extension. Applying enough number of concentric fibers may reduce such problems. Furthermore, the corners of the fiber layers located at both ends of the sample, which are reinforced with concentric fibers oriented at non-zero angle, are filled only with the matrix material as marked on Figure 3-6(b). If only concentric fiber rings are used to construct a fiber layer, a region at the middle of the section has not enough space for more fibers and it will be filled only with matrix material, forming a sand-wish section.

The slicing software, Eiger, provides an estimation of used material volume for each material type, total mass, total material cost and printing time required. However, Eiger estimates the total material extruded from the nozzle and do not distinguish whether material was used for building supports or for building the real part. Therefore, it can only be used for estimating material consumption and cannot be used to calculate the volume fiber fractions.

Table 3. Eiger setting used when 3D printing test samples.

		Tensile Onyx/CF	Flexural Onyx/CF
Printer (Markforged®)		Mark-Two	Mark-Two
Extruder temperature	CF	272 °C	272 °C
	Onyx	272°C	272°C
Heat bed temperature		No heat	No heat
Fill pattern		Solid	Solid
Fill density		100%	100%
Sample dimension		250x15x1.75 mm	154x13x4 mm
Floor layers		2	4
Roof layers		2	4
Layer thickness		0.125 mm	0.125 mm
Wall layers		1	2
Total fiber layers		10	20
Total matrix layers		4	12
Fiber fill type		Isotropic	Isotropic
Concentric fiber rings		1	1
Fiber angle (degrees)		0	0
Print time per pcs		2h 05min	1h 44min

From the point of design view, It is important to remember that the minimum width and height of a part that can be reinforced by a carbon fiber is 2.8 mm and 1.125 mm, respectively [28]. This is due to the carbon fiber filament forms a rectangular shaped continuous carbon fiber layer when extruded from the hot nozzle. As the thicknesses of a printed single carbon fiber layer and the diameter of unprinted carbon fiber filament were 0.125 mm and 0.38 mm, respectively. The average width path of a single fiber layer is then approximately 0.90 mm. If two layers of walls on both sides are provided, as recommended by the producer of the 3D machine, the minimum width of a component that can be reinforced by a single fiber becomes 2.8 mm wide [33]. While the minimum thickness that can be reinforced varies depending on how many floors and roofs are selected. If four layers, each 0.125 mm thick are selected above and below a single carbon fiber, then the minimum thickness of a part that can be reinforced with a carbon fiber becomes 1.125 mm [28]. A terms roof and floor are used to mean the first layer on the working bed and the above last layers of the part, respectively.

When an STL-file is imported to the Eiger, slicing software, it is important to check whether the dimensions are as in the designed model. Often, the imported part should be scaled to obtain the required dimensions . the samples in this study had been scaled by a factor of 10. Another thing to be noted with the Eiger software was the number of the fiber layers do not update after fiber layer modifications in the internal view.

First layer starts at the left far end, four layers of fiber (marked red rectangle) at the middle were removed in the "internal-view" manually, while the "floor and roof" were sett to only Onyx at the part settings in Eiger. The blue infill region represents the carbon fiber layers.

Figure 3-7. Fiber layers orientation details of bending sample.

 Generally, considering several parameters related to the 3D printing of a component, such as nozzle temperature, printing thickness, infill speed, loading conditions, printing patterns, critical dimensions, bed contact, support and overhangs etc. at early stage have significant effect on optimizing the strength and the layer-by-layer printing process[3] [1]. However, in Mark-Two some of these parameters were predefined by 3D manufacturer. Moreover, 3D printed parts are stronger parallel to the print bed along x-direction, and they have higher printing dimensional precision at on the XY-plane [28].

3.2   Tensile Test and sample preparation

The purpose of this tensile test was to determine the behavior of a 3D printed continuous carbon fiber in a chopped-carbon-fiber reinforced matrix called "Onyx". Tensile test is one of the commonly used experiments to understand the existing material properties and predict the response of parts made from these materials in the real world. Tensile test is performed by preparing a standard specimen often from large size fabricated part and stretching the test samples until failure using standard testing machines, which have the capability of measuring the deformation and the applied load at a given intervals. The interval is usually controlled by providing head speed or fixed strain rate. The strain rate control method is recommended to measure deformation and speed. The head speed control method is also used, but incase of gliding due to weak grip and shear deformation in presence of tabs, the measured deformation can lead to errors [19]. Furthermore, yield tensile strength (YTS), ultimate tensile strength (UTS), yield strain (%), Young's modulus (E) and the type of fracture can be obtained from tensile experimental test [19].

Hart, R.J., E.G. Patton, and O. Sapunkov performed tensile test on carbon fiber reinforced composite samples fabricated by 3D printer using a dog bone shape specimens, in which failure occurred at the grip section in all the samples. It was recommended rectangular specimen with bonded tabs of type ASTM D3039 standard, to avoid fiber damage and failure at the grips [5]. The tensile test in this study was performed following the recommendation and ASTM – D3039 standard for Tensile Test of composite Materials was used.

A rectangular carbon fiber reinforced specimen was loaded in tension by Instron-5000 testing machine at a constant strain rate of 0.008 mm/mm/min. The standard states that the strain rate should be selected so as to produce failure within 1 to 10 min and 0.01 mm/mm/min is

suggested [41]. However, during the initial trial test, the suggested strain rate was fast and fatigue failure occurred. To overcome this a reduced strain rate of 0.008 min^{-1} was used in this study. The sample was clamped to a fixed part at the bottom and to the movable head of the testing machine at the other end as shown in Figure 4-2(a). The Load was applied parallel to the unidirectional carbon fiber and the samples were loaded until failure. The extension of the specimen were measured by an extensometer at gauge length of 100 mm. The samples were tested at room temperature and normal humidity.

A rectangular specimen for unidirectional (UD) reinforced composite was adapted from the standard with 250 mm in length, 15 mm in width and 1.75 mm in depth. The thickness of the specimen in the standard requirements is left to be determined "as needed", while in the geometry recommendations, a thickness of 1 mm was recommended. For the convenience of achieving enough fiber-volume-fraction and adequate extensometer contact in the sample surface, a thickness of 1.75 mm was selected. The total thickness was then 14 times the thickness of printed layer (0.125 mm). It was important to consider the thickness of a single layer when deciding the thickness of the test sample because Mark-Two 3D printer cannot print layers that are less than the minimum layer thickness defined in the slicing software [41].

As mentioned in section 3.1 the samples were fabricated from CF and Onyx using Mark Two 3D printer. When fabricating the tensile samples, the sample was positioned in a way its length and width lay in x-and y-axis, respectively. This was decided, first due to the working bed is rectangular with its longest side in x-axis and secondly, to reinforce a part with fiber, its width should have to be at list 2.8 mm wide. Since the thickness of the samples was 1.75 mm the selected orientation was the only option. Moreover, 3D manufactured parts have weaker bonding between successive layers than layers laid side-by-side in the xy-plane. Such weakness can lead to delamination failure of parts.

The first two layers was only Onyx material laid above a support. The user has no possibility to decide number of layers for the support. In case of parts are thin and if supports at the bottom of the part ate too small to peel off, there is an option to provide a raiser support in Eiger®. However, the number of layers to the raiser support are predefined to 20 layers by the software. This limitation lead to more material wastage and was only used in one extra sample which was not part of the five samples. Due to the tabs, there was a space of 1.5 mm which had to be filled with a support material as shown in Figure 3-10. The support and the matrix part were of the same material, and the support was printed parallel to x-axis, at a double layer thickness of the provided layer height. Because of one material was uses as a matrix and as support, it was difficult to remove the support with out damaging the floor-layers of the sample. Hence, the sample face that was on direct contact to the support infill had poor surface finish.

Following the floor layers, the ten layers of the carbon fiber was printed. In the same principle when printing the Onyx, the 3D printer starts printing with the concentric rings followed by the isotropic carbon fiber. Concentric rings are the outermost continuous carbon strands which were placed to strength the outer walls. The isotropic continuous carbon fibers were oriented parallel to the x-axis placed inside the concentric rings. The concentric rings and isotropic continuous carbon fibers are those marked with 'd' and 'c' ,respectively in Figure 3-3. When constructing new carbon fiber layer, the printer starts printing first with walls, then the

concentric fibers and it finishes with the isotropic fiber. The top and bottom two layer, also named "roofs and floors" in the 3D printer settings were constructed from pure Onyx material.
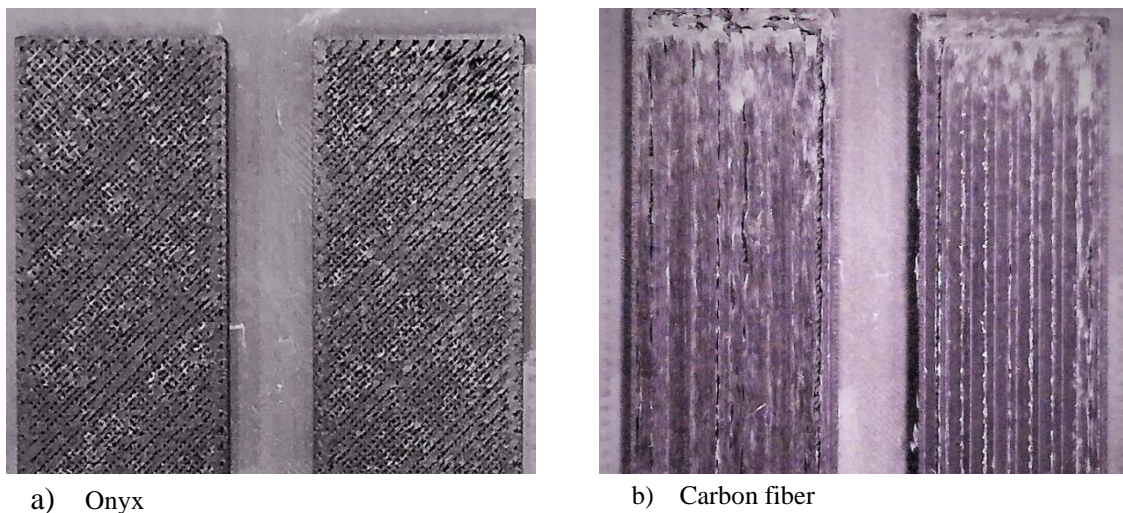

| a)   Onyx | b)   Carbon fiber |

Figure 3-8. Voids inside Onyx matrix and carbon fiber layers, visible with naked eyes.

To summarize, the tensile sample had total 14 printed layers at the gauge section, where ten of them was carbon-fiber layers and the rest was Onyx. About 62% fiber volume fraction was estimated at the gauge section following the procedure discussed on Section3.4. Each sample took approximately 2 hours printing time to complete. Furthermore, Eiger has a triangular infill default setting, but a solid infill with 100% density was used to reduce voids and achieve enough volume fraction ratio between matrix and fiber materials. Mark-Two 3D printer has triangular, hexagonal, rectangular and solid fill patterns to select from.

Lozada, J.N., et al., studied the effect of different parameters on the properties of parts fabricated with Markforged® Mark-Two 3D printer and triangular infill patterns show better strength to weight ratio[8]. However, solid infill of 100% density was selected in this study, due to the complexity of obtaining the fiber volume fraction from triangular patterns to be used in the ROM. In addition, one unreinforced extra test samples had been printed with triangular patterns and the patterns deformed at the clamping grips when tightening the grips.

The continuous carbon fiber was unidirectional, oriented at 0° (along the x-axis) inside Onyx matrix printed at $\pm$ 45- degree. To avoid stress concentration at the grip, the specimens were provided with 15 mm wide, 56 mm long and 1.5 mm thick tabs, beveled at 5° towards the gauge section from each end as shown in Figure 3-9(a). To prevent gliding, tabs were simply printed together with the rectangular samples only with the matrix material. Total five specimens were tested and results including the mean value and standard deviation are provided on Table 11. During fabrication of the tensile test specimens, it has been observed voids with the layers of Onyx. These voids have been neglected when estimating the volume fraction of the materials.

a) Dimensions of tensile specimen with tabs
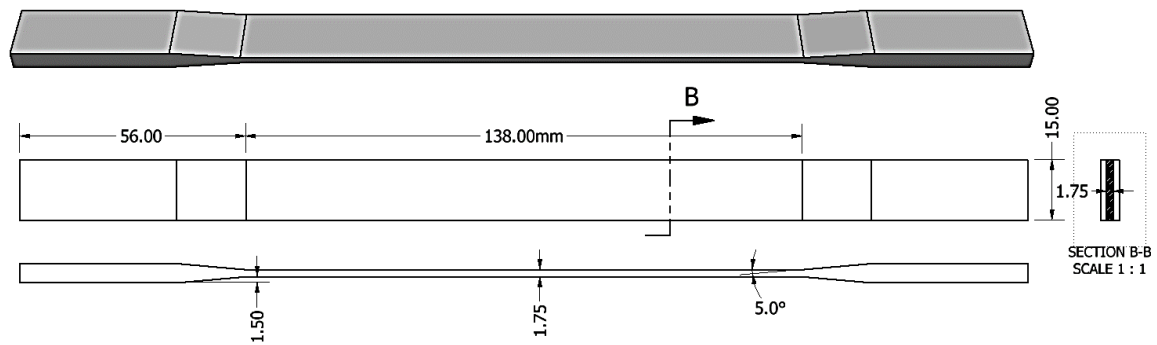
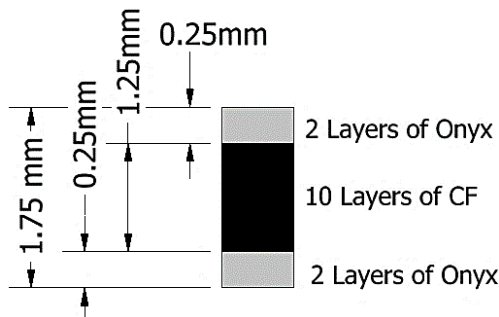b) Section view at midspan of the tensile sample illustrating location of CF.

Figure 3-9. Tabbed tensile test specimen

Figure 3-10. Location of support requirement for tensile sample at the gauge section.

3.3   Flexural Test and sample preparation

The three point flexural test was performed by Zwick/Z020 testing machine following the ASTM standards D7264/D 7264M – 07, procedure-A. Five specimens with 154 mm length, 13 mm width and 4 mm thick as shown in Figure 3-12, was fabricated by Markforged® Mark-two 3D printer with unidirectional(UD), continuous carbon fiber laid within an Onyx matrix. Following procedure-A from ASTM D7264-07   standard, the testing sample was simply supported at two end points, 124 mm apart and a concentrated load, uniformly distributed along the width of the beam was applied at the mid-span, as illustrated in Figure 3-13. The supporting and loading noises had a cylindrical contact with 3 mm in radius[42]. When selecting the dimensions of the specimen a span to thickness ratio of 32:1 was used from the standard. Five testing samples had been tested until failure at head speed of 1 mm/min. Moreover, the results from each sample, their average and standard deviation are provided in Table 13.

The distribution of the carbon fiber layers in the flexural test samples were decided by considering the loading conditions of a classical beam from the general beam theory, wherein the neutral axis of the beam is theoretically unstressed. Therefore, no reinforcing fiber was provided at the center of the beam as illustrated on Figure 3-12(b). The first four layers at the bottom and top of the beam were only Onyx. This was mean to protect the reinforcing fiber

from damage in direct contact with the supporting and loading parts of the testing machine. The 3D printer producer also recommended to provide 4 layers at both floor and roof, and 2 layers of wall for the remaining sides as illustrated on Figure 3-11(b). Therefore, for a single specimen of 4 mm in thickness a total of 32 layers, each 0.125 mm thick were required. Twenty of these layers were carbon fiber, whereas the rest was only Onyx. The number of fiber layers was determined to achieve an approximately 42% fiber volume fraction. As discussed in the literature, volume fraction of the fiber has a significant function in strengthening a part fabricated from composite materials.

The reason the total volume of the CF used was less than the total volume of Onyx, although the number of layers of the CF was more than the Onyx layers was, due to the carbon fiber layers had to be covered with 2 walls at each side, which reduces the length and width of the CF ply. This can be shown clearly when summing up all the Onyx volume used in the walls and layers as in Figure 3-11(b).
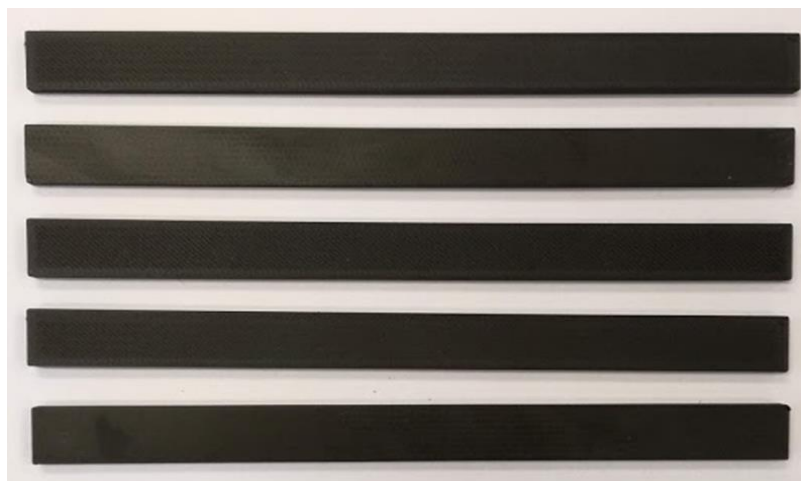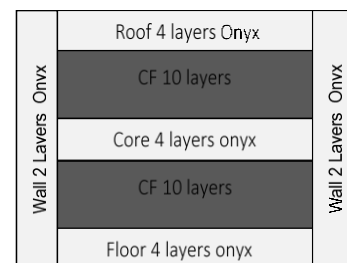
(b) cross-sectional illustration of material distribution

(a) 3D printed flexural test samples

Figure 3-11. schematic internal details of 3D printed flexural test specimen Detail material lay-out walls. roof, floor

The carbon fibers were symmetrically located with reference to neutral axis of the beam, providing 10 layers of carbon fiber at the compression and tension regions of the beam to prevent unbalanced strength. Hence, the first 4 layers from the top and bottom of the beam were Onyx, followed by 10 layers of carbon fiber from each direction and 4 layers of matrix at the middle of the beam as illustrated on Figure 3-12 (b).
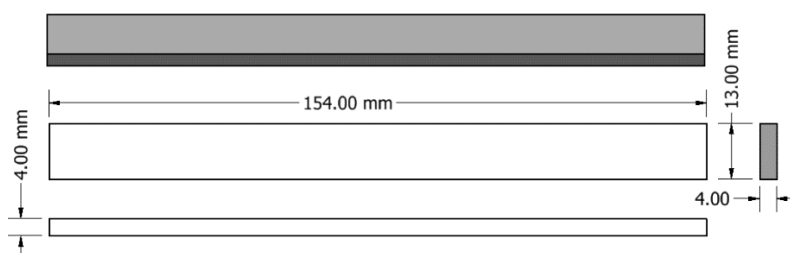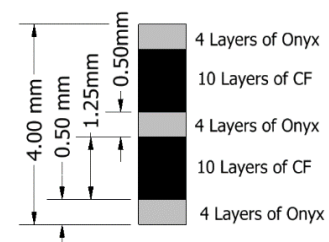
(a) Flexural specimen   (b) cross-sectional view

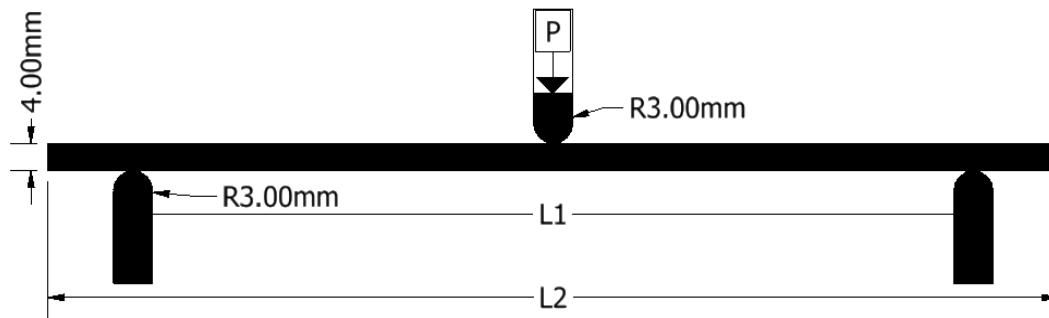*Figure 3-12. (a) Flexural specimen dimensions, (b) detail section view of layers and their assigned material*

Figure 3-13. Three-Point Loading and support illustration.

From the beam theory, beam of length L supported at its two ends with a roller support and a concentrated load applied at its midspan is used in three-point bending test as illustrated in Figure 3-13.

The deflection of the beam at the mid-span can be estimated using equations 3.0 [42].

$$\delta = \frac{PL^3}{48EI}$$
(3.0)

Where P is the concentrated load along a the width of the beam in newtons, L is span length of the beam measured from center to center of the support, E is Young's modulus and I is the second moment of area which is (wh^3)/12 for rectangular beam. Furthermore, the E-modulus can be estimated from the force-displacement curve using equation 3.1

$$\frac{dP}{d\delta} = \frac{48EI}{L^3}$$
(3.1)

3.4   Fiber Volume Fraction Estimation

The material volume provided by the Eiger slicing software was not the exact material used to build the component, this can be recognized if we calculate the theoretical volume of a sample and compare to the summation of the materials volume of both Onyx and carbon fiber. Eiger estimates total material used without considering whether the material was used to build the sample, purge or a support. Therefore, the estimated material volume cannot be used for estimating the volume fraction of fiber. To illustrate that, lets consider the one flexural sample with 154 mm in length, 13 mm in width and 4 mm in thickness.

Ideal volume:-

Ideal volume of specimen = Width x Length x thickness = 154 x 13 x 4 mm = 8008 mm^3 = 8.008 cm^3

Volume estimated by Eiger software:

Sum of carbon fiber and Onyx volume= V_{CF} + V_{Onyx} = 3.57 cm^3 + 5.11 cm^3 = 8.680 cm^3

Difference =volume from Eiger – ideal volume = 0.672 cm^3

From the above illustration, the volume estimated by Eiger software was larger by of 0.672 cm^3. A single layer which covers the whole length and width of the sample with a thickness of 0.125 mm requires a volume of 0.25 cm^3 material. Therefore, the extra volume of 0.672 cm^3 is enough to build about 2.7 layers. Due to this difference an assumption has been done to estimate the volume fraction of each material. The cross-sectional area of the rectangular test sample was divided in to small areas of walls, material layers, roofs and floors. An approximate width of an extruded filament was estimated since both materials were printed with same layer thickness of 0.125 mm. Since the circular filament was translated into tinny rectangular shape with 0.125 mm depth when extruded, a width of approximately 0.90 mm was estimated for the carbon fiber and 0.40 mm for the Onyx. The total area of each material was calculated by summing up the individual cross-sectional area of each material. The cross-sectional area was taken from a location within the gauge section. To find the fiber volume fraction the "rule of mixtures" were used. ROM as described in section 2.2 uses the material properties of the individual composite materials and their volume ratio to predict the property of the composite part. Considering the matrix and fiber layer cover same length and width of the part, the volume fraction can be represented by area fraction.

$$V_f = \frac{A_f}{A} \tag{3.2}$$

$$E_1 = E_m V_m + E_f V_f \tag{3.3a}$$

$$E_1 = E_m \frac{A_m}{A} + E_f \frac{A_f}{A} \tag{3.3b}$$

$$\sigma_1 = \sigma_m V_m + \sigma_f V_f \tag{3.4}$$

$$v_1 = v_m \frac{A_m}{A} + v_f \frac{A_f}{A} \tag{3.5}$$

Considering Figure 3-11(b), Figure 3-12 b, and the approximated width of a single printed carbon filament, the area covered by carbon fiber was approximated as in Table 4. The area calculated was assumed to be at the middle length of gauge section and the average dimension values of the printed sample were used on both tests. Moreover, the thickness of the layers was obtained by dividing the final thickness by the total number of layers in the sample. In similarity to the FE models, the presence of voids was ignored when estimating the fiber percent. From the 3D model and final printed sample dimensions the tensile and the flexural samples had a cross-sectional area increase of 7% and 1% , respectively. However, porosity and distribution of voids within the CF and Onyx was not studied.

Table 4. Fiber volume approximation of samples using ROM

	Tensile sample area 14.99 mm x 1.87 mm	Flexural sample area 12.98 mm x 4.03 mm
Number of single CF filament	15	10
Single CF filament width	0.87	0.87
Layer thickness as printed	0.134	0.126
Total number of layers with CF	10	20
CF Area as printed [mm^2]	17.40	21.90
Total sample cross-section area at gauge section [mm^2]	28.03	52.30
Fiber % by area	62%	42%
Note: All dimensions are taken from average printed samples		

Table 5. Flexural Composite Sample mechanical properties estimation by ROM

Flexural Composite Sample mechanical properties estimation by ROM				
	CF	Onyx	ROM	
E- modulus [MPa]	51000	2900	E_{11}	23102
Fiber volume fraction [%]	42%	58%	E_{22}	4802.30
Strength [MPa]	470	81	Flexural Strength	244.40

Table 6. Tensile Composite Sample mechanical properties estimation by ROM

Tensile Composite Sample mechanical properties estimation by ROM				
	CF	Onyx	ROM	
E- modulus [MPa]	54000	1400	E_{11}	34464.40
Volume fraction [%]	62%	38%	E_{22}	3611.10
Strength [MPa]	700	36	Flexural Strength	453.40

3.5   Modeling the tensile and flexural samples in Ansys

ANSYS Mechanical APDL 17.0 were used as a tool to analysis and simulate the specimens made from composite material. In this study element type SHELL181 4-node structural shell was used and the samples were considered as thin wall with length to thickness ratio greater than 10. Shell181 was selected due to shell elements allow to define layered composite of thin-walled structures which are common in aircraft structure, boat hulls and racing cars analysis [37]. Furthermore, the samples were flat and there was not necessity to consider a curvature between nodes.

The carbon fiber and Onyx composite specimens were modelled as a thin layered lamina. Since the layers fabricated in the 3D printer were made of either only the reinforcing or the matrix material, the model was also designed to contain only one type of material per lamina. This means one layer was made of either only carbon fiber or only Onyx. This was performed to

make the model as similar as possible with the fabricated test sample. During developing finite element model there have been made several assumptions.

The assumptions made in the formulation of the model were:

1. Constituents show linear elastic behavior
2. The matrix (Onyx) has isotropic material properties.
3. Fibers are transversely isotropic
4. Perfect fiber-matrix bonding
5. No voids or defects present in the test samples

In addition, the matrix material (Onyx) was considered as isotropic material with elastic modulus E=1.4 GPa and Poisson's ratio of v= 0.43. The Poisson's ratio of the Onyx, matrix material was estimated by tensile testing five 8 x 8 mm square cross-sectional pure Onyx samples, with 100% infill density. It is important to note that this Poisson's ratio do not represent the actual Poisson's ratio of Onyx. It is not robust to determine a Poisson's ratio of a new material by simply testing only five samples and it should not be used other than in this study.

Carbon fiber filament has orthotropic material properties with tensile elastic modulus E_1 and tensile yield strength of 54 GPa and 700 MPa, respectively. For the rest of the material properties, CF was assumed as transverse isotropic material as in Table 8. Furthermore, it is important to underline that the carbon fiber had different material properties for tensile and flexural analysis. Markforged® carbon fiber had flexural modulus and flexural strength of 51 GPa and 470 MPa, respectively. Similarly, the Onyx had flexural modulus of 2.9 GPa and strength of 81 MPa. Material properties presented on Table 8 were used for the simulation using Ansys.

The general beam theory was considered in the flexural model, and the reinforcing fibers were placed at the compression and tension regions only, in similar case with the experimental samples. Moreover, the fiber width was modeled taking the full width of the specimens, while in practice the width and length of the fiber was shorter due to the walls and CF rings provided by the 3D printer. Therefore, the fiber volume fraction in the FE models was higher than in the test samples. Moreover, a single layer was assumed as a lamina, whereas in practice the bonding strength between the adjacent material strand is weak.

Table 7 .Typical AS4 carbon fiber yarn properties adapted from Meddad, 2002 [43].

	Axial			Transverse		
	Elastic Modulus E_{11} [GPa]	Shear Modulus $G_{12}=G_{13}$, [GPa]	Poisson's Ratio, $v_{12}=v_{13}$	Elastic Modulus $E_{22}=E_{33}$, [GPa]	Shear Modulus G_{23}, [GPa]	Poisson's Ratio, v_{23}
AS4 Carbon Fiber yarn	231	22.1	0.3	22.4	8.3	0.35

F.van der Klift et al. estimated the amount of fiber volume fraction on a single bundle of Markforged® carbon fiber filament by evaporating the matrix according to JIK K7075 [1] and obtained a fiber volume fraction of 34.5% and the rest 65.5% was other coating and adhesive polymers. This estimation was used to calculate the assumed orthotropic material properties carbon fiber filament provided by Markforged® in this study.

Table 8. Assumed material properties of Markforged® carbon fiber and Onyx used for simulation in Ansys

	Markforged® CF filament		Data provided by
	Tensile	Flexural	
E-Modulus Onyx, [GPa]	1.4	2.9	Markforged®
Axial Elastic Modulus E_{11}, [GPa]	54	51	Markforged®
Transverse Elastic Modulus $E_{22}= E_{33}$, [GPa]	7.728*	7.728*	Assumed
Axial Shear Modulus $G_{12}= G_{13}$, [GPa]	7.625*	7.625*	Assumed
Transverse Shear Modulus G_{23}, [GPa]	2.864*	2.864*	Assumed
Axial Poisson's Ratio $v_{12}= v_{13}$	0.104*	0.104*	Assumed
Transverse Poisson's Ratio v_{23}	0.121*	0.121*	Assumed
*Note :- Values marked with * were obtained by considering only 34.5% of the AS4 carbon fiber values presented on Table 7.*			

Table 9. layer orientation and material for each lamina for the tensile specimens.

Layer number	Total number of layers	Material	Layer Thickness [mm]	Orientation Angle [°]	Illustration Cross-section
13, 14	2 layers	Onyx	0.125	(+45°,-45°)	2L Onyx
3, 4, 5, 6, 7, 8, 9, 10, 11, 12	10 layers	Carbon Fiber	0.125	$(0°)_{*10}$	10L CF
1, 2	2 layers	Onyx	0.125	(+45°,-45°)	2L Onyx

It is important to take special attention when modeling composite materials models for composite materials due to Finite Element analysis of composite materials require several material properties due to the material orthotropic property [34]. At list two materials are required for a composite material modeling. For isotropic material, only the material properties in x-direction are required, while material properties in x-, y-, and z-direction should have to be defined for orthotropic materials. The nine orthotropic material properties required for modeling are; Elastic moduli (E_1, E_2, E_3), shear moduli (G_{12}, G_{23}, G_{31}), and Poisson's ratios (v_{12}, v_{23}, v_{31}) each in three directions [34]. subscripts 1, 2, and 3 represents x-, y- and z-directions, respectively.

There were several challenges when defining the material properties used in 3D printers due to most materials used were patented and the producers do not have a willing to reveal detailed

engineering properties of the materials. This had been an issue in this study and assumptions in the material properties of carbon fiber and Onyx had been taken.

The matrix material (Onyx) contains chopped carbon fiber and were assumed to be an isotropic material. The carbon fiber used in the traditional manufacturing process and the carbon fiber strands produced for fused deposited manufacturing using 3D printing have different mechanical properties. For instance, the carbon fiber used in this study was produced by MarkForged® intended to use in their 3D printers, have an tensile and flexural elastic modulus of 54 GPa and 51 GPa, respectively [40], while a carbon fiber produced by PAN manufacturing processes has a tensile elastic modulus of 230 GPa. The finite element model developed were constructed in similar manner with the 3D fabrication processes the test samples. However, the model did not take consideration of the weak bonding between the layers due to the nature of 3D printing.

The descriptions of the laminate and properties of each lamina prerequired to obtain strain and stress results in mesoscale. The material properties of both materials should have to be provided to Ansys. A Laminate Stacking Sequence (LSS) was used to create the 0.125 mm thick laminas and material properties and its were entered. The lay-up was made in similar way as in the 3D printer settings. Hence, for the tensile model two layers of matrix at floor and at roof oriented at $\pm45°$ and 10 unidirectional reinforcing fiber layers between the floors and roofs were provided. Total 14 lamina with a thickness of 0.125 mm was combined to make 1.75 mm thick laminate. Whereas the bending model had 4 layers of floors with Onyx material, then 10 layers of carbon fiber, followed by 4 layers of Onyx as a core, and 10 layers of carbon fiber for strengthening the compression region of the beam. Finally, 4 layers of roofs to protect the carbon fiber from damage. Total 32 layers of 0,125 mm thickness lamina were used to make a 4 mm thick laminate. The first layer of matrix material starts +45-degree orientation followed by -45 degrees. This was performed due to the 3D printer starts its print of matrix at +45-degrees each time.

Table 10. Layer orientation and material of each layer lamina for the flexural specimens. [1 is bottom layer and 32 is top layer]

Layer number	Number of Layers	Material	Layer Thickness [mm]	Orientation Angle [°]	Illustration Cross-section
29, 30, 31, 32	4 layers	Onyx	0.125	$(+45°,-45°)_{*2}$	4L Onyx
19, 20, 21, 22, 23, 24, 25, 26, 27, 28	10 layers	Carbon Fiber	0.125	$(0°)_{*10}$	10 L CF
15, 16, 17, 18	4 layers	Onyx	0.125	$(+45°,-45°)_2$	4L Onyx
5,6, 7, 8, 9 10, 11, 12, 13, 14	10 layers	Carbon Fiber	0.125	$(0°)_{*10}$	10L CF
1,2,3, 4	4 layers	Onyx	0.125	$(+45°,-45°)_{*2}$	4L Onyx

Modeling steps

Structures fabricated from composite material layer-by-layer method to create laminates are represented better by shell element in ANSYS software [44]. SHELL181 element 3D 4-node having 6 degrees of freedom (DOF) at each node was one of the elements suitable for modeling composite materials. Shell181 allows large strain and has capability to include up to 255 layers. SHELL181 was used in this study because of their efficiency to model and analyze thin to moderately thick structures containing a number of layers and it has full nonlinear capability including large strains [35]. SHELL181 element with 4-node uses 6 DOF at each node, 3 translation (x,y,z) and 3-rotations. when selecting appropriate the KEYOPT, for instance KEYOPT(8)= 1, the mid value is retrieved from the result file rather than calculated by averaging top and bottom. If KEYOPT(8) is set to 2 a parabolic variation of element solution can be obtained. KEYOPT(8) = 2 was used in this study so the results of the top, bottom , and middle layers of a specific layer number can be stored.

Shell elements offer computationally efficient solution for modeling shell structures compared to solid elements. 3D finite strain shell elements such as Shell181 and shell181 provide better nonlinear analysis, and important improvements in cross sectional data definition, analysis and visualization.

Basic modelling steps in Ansys Mechanical APDL
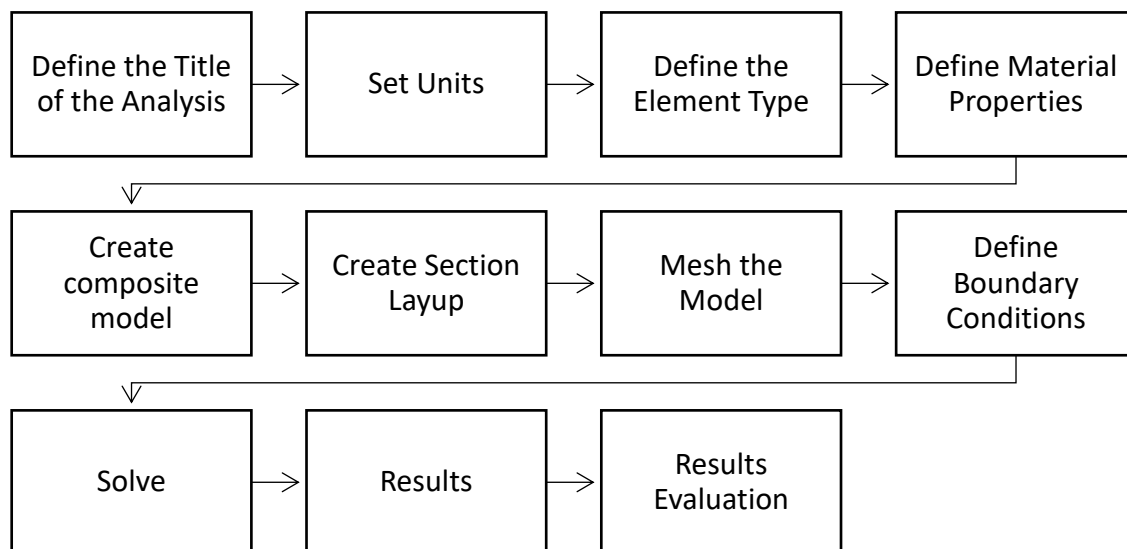
Figure 3-14. Modelling Steps in ANSYS Mechanical APDL.

Shell181 provides stress and strain output at the center of the layer and the edge and surface between the nodes stay straight. While shell281 provides at 4 in-plane integration points of the layer and it considers the curvature of the shell between nodes. Element loads are described in nodal loading and pressure can be input as surface loads on element surface. A positive pressure input acts into the element and the face number of the element should have to be defined.

Another thing to consider is, shell edge pressure are input as on a per-unit-length basis and they should have to be multiplied by the thickness [44].

Shell181 is used with several assumptions and restrictions in Ansys. The assumptions and restrictions are listed below [44].

- Zero-area elements and zero-thickness elements are not allowed, but zero-thickness layer are allowed.
- No slid is assumed between the element layers.
- The through -thickness stress (SZ) is always zero.
- This element works best with the full Newton-Raphson solution scheme
- If a shell section has only one layer and the number of section integration points is equal to 1 or keyopt(1)=1 then the shell has no bending stiffness.

In additions to the above restrictions and assumptions, there are considerations for using Pre-integrated shell sections also. These include among others, successive layers are free of voids, the shell thickness remains constant even in large strain analysis and stress results output are available as element table not as shell stress.

Two material groups with material ID #1 and #2 were created and their material properties were defined in the Material-model. Material ID #1 represent the Onyx which functioned as a matrix and material ID #2 was for the reinforcing carbon fiber. Carbon fiber has orthotropic material properties, while the orthotropic property of Onyx was neglected and assumed as isotropic in this study.

- ***Main Menu- Preprocessor- Material Props- Material Models- Structural- Linear - Elastic*** *– [isotropic for the matrix material (Onyx) and orthotropic for the CF from* Table 8*]*

The material properties presented on Table 8 were used when defining the material properties. Since the model was shell model with layer sections as shown in Figure 3-18, it requires to define the layer data, which contains individual layer thickness, material properties, orientation angle and number of integration points per layer as shown in Figure 3-18. The layer orientation angle is the angle between the layer-coordinate system and the x-axis of the element-coordinate system. These layer properties are inputted in the Sections part by defining layer-by-layer from bottom (layer 1) to the top in the direction of the element coordinate system (z-direction). Three integration points through the thickness of each layer were selected, where 2 points were located on the top and bottom surface respectively, while the remaining one point was located at the middle.

- ***Main Menu- Preprocessor-Sections -Shell- Layup- Add/Edit-*** *[32 layers for the bending model and 14 layers for the tensile model had been created]*
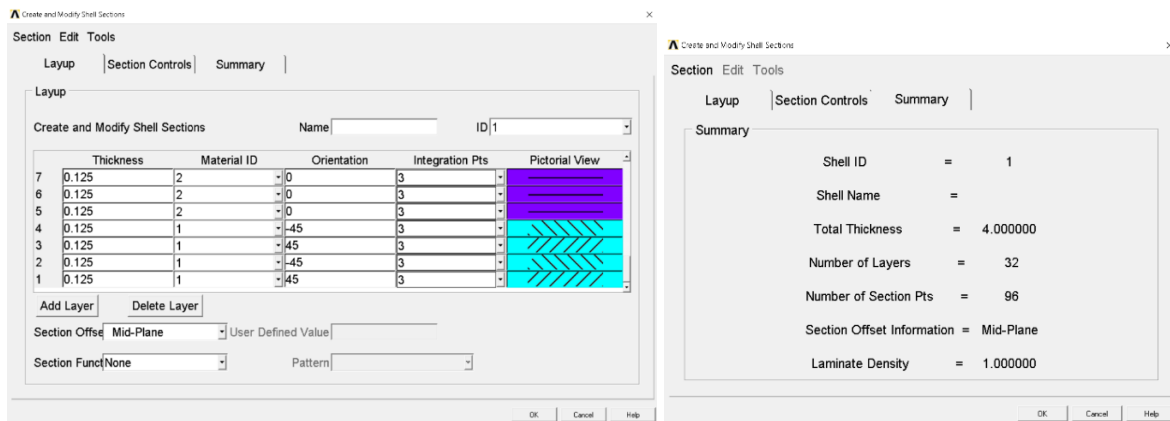
Figure 3-15. shell section layup for the flexural model, (should have to read in combination with Table 10.)
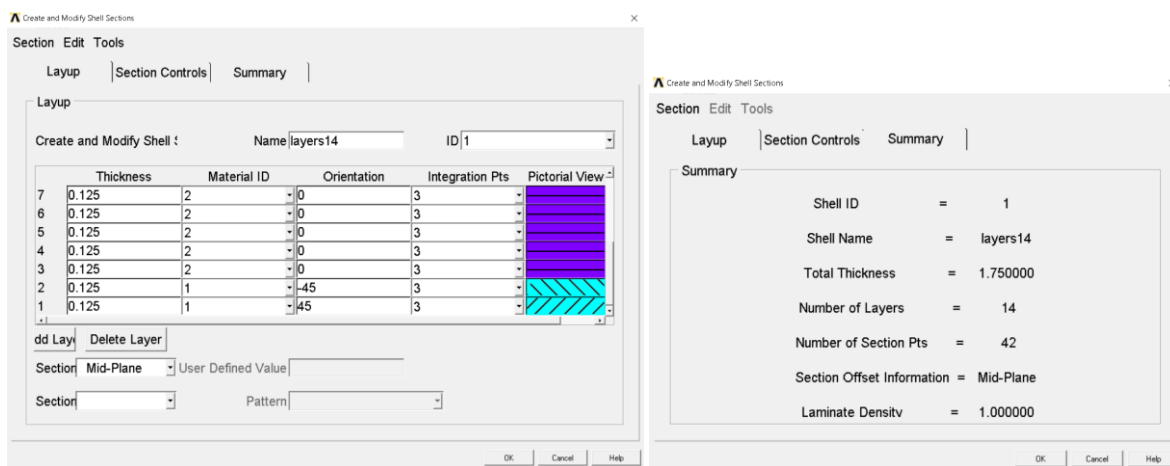
Figure 3-16. Shell section layup for the tensile model

After Sections had been defined the 3D model was modeled under the Modeling and when modeling a two-corner rectangular area was used.

- ***Main Menu- Preprocessor-Modeling- Create-Rectangle= By 2 Corners – [138x15 mm for tensile and 124 x13 mm for flexural]***

When modeling the test samples, it has been modeled only the part of the specimen with in the gage length for the tensile sample and only the span length for the flexural sample. Once the solid model was completed, a mesh using size control and mapped mesh option by corners was applied as in Figure 3-18. Total 10230 elements for the flexural model and 3680 elements for the tensile model were generated.

- ***Main Menu > Preprocessor > Meshing > Size Cntrls- ManualSize – Area- Picked Areas***, *was used to define the mesh size.*
- ***Main Menu > Preprocessor > Meshing > Mesh > Areas > Mapped > By Corners,*** *was used to map the mesh.*

The mesh density was achieved by using area mapped meshing . Mapped meshing was used due to its advantage on generating computationally well-behaving meshes [44]. However, the

solid model entities meshed with this option do not use quadrilateral (4-sided) elements since the element used was shell181 without thickness. The thickness of the model was provided by 14- and 32-layer sections of 0.125 mm thick for the tensile and the flexural model, respectively.

Furthermore, under the Solution a static type of analysis, boundary conditions, load and supports were defined. For the bending beam fixed supports at both ends and a bending force at the middle of the span was applied in z-direction. While for the tensile test one end was fixed and a load was applied on the other end in the positive x-direction. Moreover, static analysis was applied. Static analysis is valid for all DOF, but it ignores all inertial and damping effects [45].

- *Main Menu > Solution > Define Loads - Apply – Structural - Displacement- On Nodes- [both ends with All DOF = 0]*
- *Main Menu > Solution> Define Loads - Apply- Structural - Force/Moment- On Nodes- [Force applied at nodes at the mid-span of the beam in positive z-direction]*
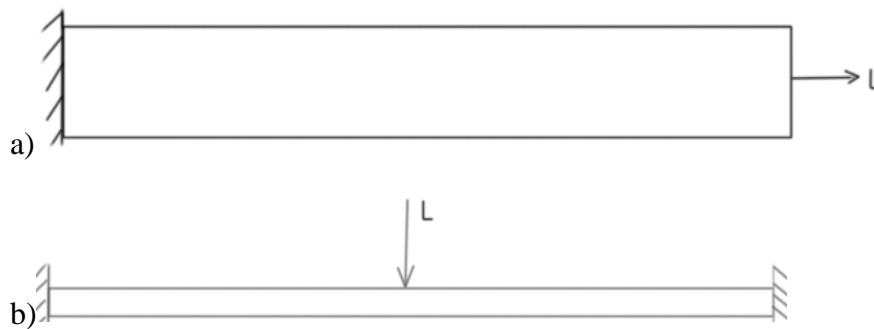
Figure 3-17. Illustration of BC, where L is pressure on a line

Then the equations are solved in the *Main Menu > Solution >* **Solve - Current LS.** Moreover the Solutions are post processed in the General Post-processer and all results can be, plotted, listed and analyzed [34].

- *Main Menu > General Postproc > Plot Results/List Results/Read Results*

Results can be extracted as a list/table for nodes or elements. It is also possible to create a path and define a table to provide results.
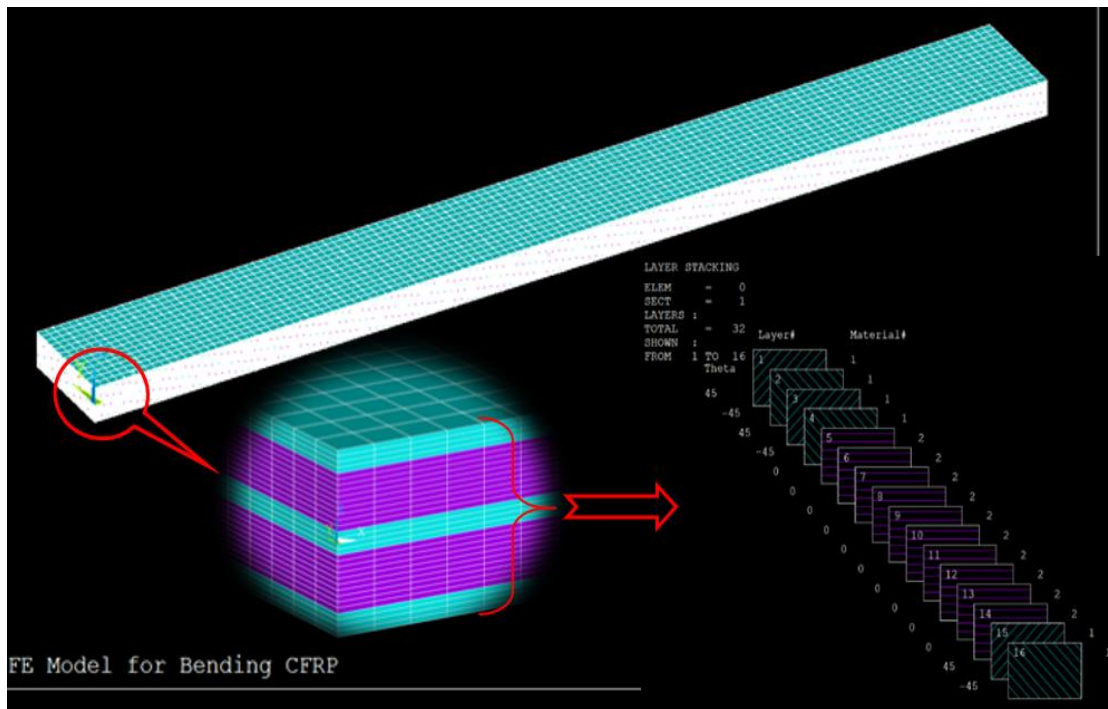
Figure 3-18. Layer Stack up for the flexural model

4 RESULTS

The results from the tensile and flexural experimental tests and FEA results are presented on the next sections. The experimental tests were performed according ASTM D-3039 and ASTM D-7079 standards for the tensile and flexural experiments, respectively. Stress-strain curve for both experiments tests and FEA results are also presented. Moreover, comparative diagram between experimental results and FEA results are presented. All testes were carried out at room temperature and normal humidity.

4.1 Experimental Test Results
The results obtained from the experimental tests are presented on this subsection.

Tensile test results
The tensile samples were tested in Instron-5000 testing machine at room temperature and normal humidity until complete failure occur. ASTM D-3039 standard was followed for this test. Carbon fiber reinforced samples of Onyx size 248.70 mm x 14.99 mm x 1.87 mm were fabricated by the Mark-Two 3D printer. A constant strain rate of 0.008 min^{-1} was used as the strain rate 2 min^{-1} recommended by the standard was fast and a fatigue failure occurred at the extra sample which were used to test the recommended strain rate . These samples consist of 10 layers of carbon fiber which makes a fiber volume of about 62%. The average maximum tensile strength obtained from the carbon fiber reinforced Onyx samples was 559.90 MPa with a standard deviation of 17.70 MPa and tensile elastic modulus of 25.04 GPa with 2.65 GPa standard deviation. The average yield strain was about 0.026 mm/mm.

Some tensile samples had poor surface finish due to the support provided by the 3D printer were attached with the lower surface of the sample. However, these samples were excluded from the results. The designed thickness of the samples was 1.75 mm, but because of the last layer of the support was not possible to remove it without damaging the sample layer it was left without removing. This increased the final thickness of the samples to an average of 1.87 mm.

Table 11. Results from tensile samples 3D printed from CF and Onyx.

Standard ASTM D 3039	Average Width [mm]	Average Thickness [mm]	Max. Load [kN]	Max Tensile Strength [MPa]	Tensile Modulus [GPa]	Tensile Strain [mm/mm]
S1	15.06	1.87	14.99	558.87	24.63	0.027
S2	14.98	1.86	15.07	537.75	20.59	0.032
S3	14.96	1.87	16.05	567.61	26.81	0.024
S4	14.98	1.88	15.40	550.37	26.27	0.025
S5	14.96	1.86	16.47	584.68	26.89	0.023
Mean	**14.99**	**1.87**	**15.60**	**559.86**	**25.04**	**0.026**
SD	0.04	0.01	0.64	17.72	2.65	0.004
CV [%]	0.3%	0.4%	4%	3%	11%	14%
SD - Standard Deviation and CV - Coefficient of variation						

A stress- strain curve was generated from the individual tensile test sample results and a combined stress-stain curve of the five samples is shown in Figure 4-1. All the samples started to fail with delamination of adjacent layers starting from the outer edge before they explode. The final failure occurred near the grip on samples S1, S2, S5 whereas S3 and S4 fail at the gauge length near the middle as shown in Figure 4-3(b). The failure occurred in all the samples in several locations due to delamination and some fiber strands were pulled out.
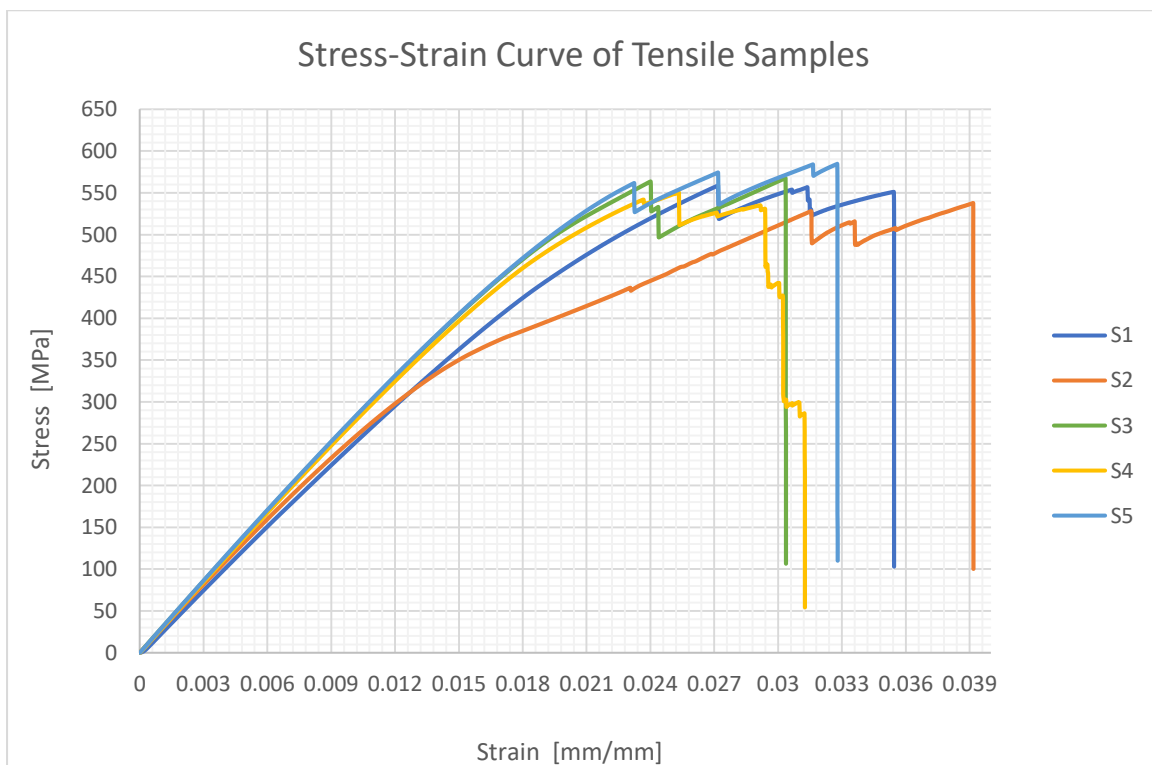
Figure 4-1. Stress-Strain curve of all five tensile specimens

Figure 4-2. (a).Tensile Testing Instron universal testing machine setup , (b) explosive failure of S3

Table 12. standard and final 3D printed average dimensions of test samples.

Samples		Length [mm]	Width [mm]	Thickness [mm]
Tensile	Standard 3D modeled	250	15	1.75
	3D Printed average	248.70	14.99	1.87
Flexural	Standard 3D modeled	154	13	4
	3D Printed average	153.86	12.98	4.03
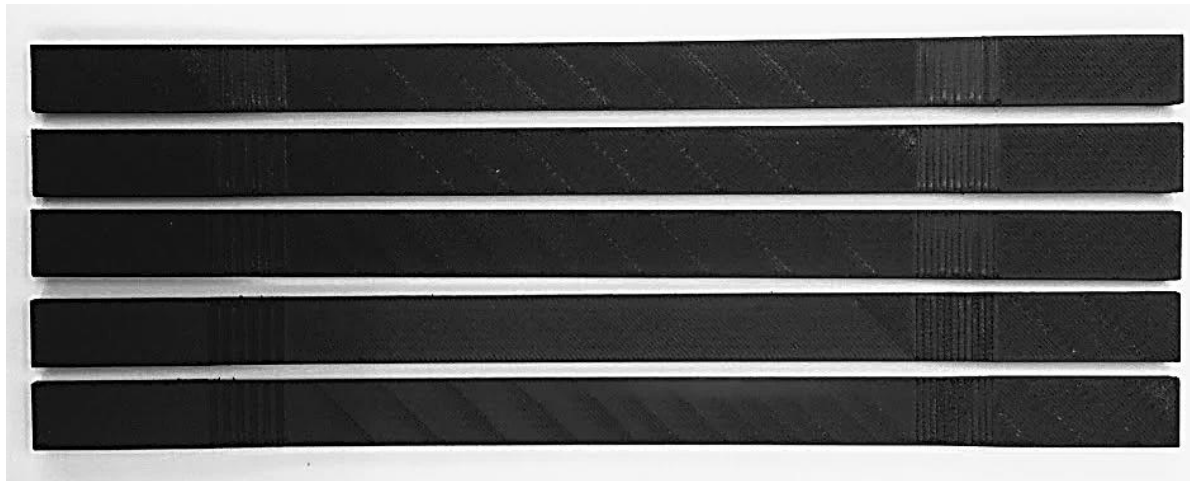
a)   Untested unidirectional tensile samples

b) Failed unidirectional tensile samples S1, S2, S3, S4, S5 from top to bottom.

Figure 4-3. Tested tensile samples

Flexural test results

Five test samples each with 20 layers of carbon fiber and 12 layers of Onyx were fabricated
by Mark-Two 3D printer. The samples hade fiber volume fraction of approximately 42%.
The general beam theory was considered during fiber reinforcing the specimens and the
volume fraction was estimated as discussed in section 3.3. The three-point bending test were
performed on Zwick/Z020 testing machine. The length to thickness ratio of 32:1 was used
and the span between the supports were 124 mm and the head speed of test were 1 mm/min at
room temperature and normal humidity. All tests were carried until failure. Results are shown

on Table 13. The dimensions of designed specimen and final tested specimens had some
differences due to the nature of the 3D print and formation of voids between layers and
among consecutive layers as shown in Figure 3-8. A delamination failure was occurred first
between the layers because of weak bonding due to the voids. The specimens had an average
12.98 +0.02 mm and 4.03 +0.01 mm width and thickness, respectively. The thickness of all
the printed specimens was larger than the dimensions provided in the 3D model by
approximately +0.03 mm, which was within the tolerance of the Mark-Two 3D printer +0.05
mm. Since all specimens had a thickness greater than 4mm, it appears to contain voids
between layers.

Table 13. Flexural 3-point test Experimental Results

Standard ASTM D7079	Average width [mm]	Average Thickness [mm]	Max. Load [N]	Flexural Strength [MPa]	Flexural Modulus [GPa]	Flexural Strain [%]
T1	12.98	4.01	328.27	293.55	15.53	2.30
T2	12.97	4.04	271.58	242.86	16.17	4.19
T3	13.01	4.03	339.05	303.19	16.73	2.28
T4	12.96	4.04	270.26	241.68	18.56	2.64
T5	12.98	4.03	304.47	272.27	15.11	2.63
Mean	**12.98**	**4.03**	**302.73**	**270.71**	**16.42**	**2.81**
SD	0.02	0.01	31.62	28.27	1.35	0.79
CV [%]	0.14%	0.30%	10%	10%	8%	28%
SD = Standard deviation and CV= coefficient of variance						
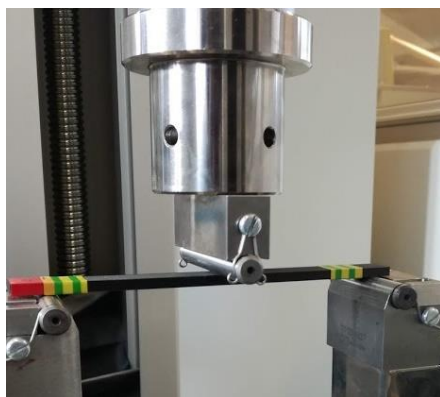
Figure 4-4. Three-point flexural test setup

Figure 4-5. Failed sample of flexural test
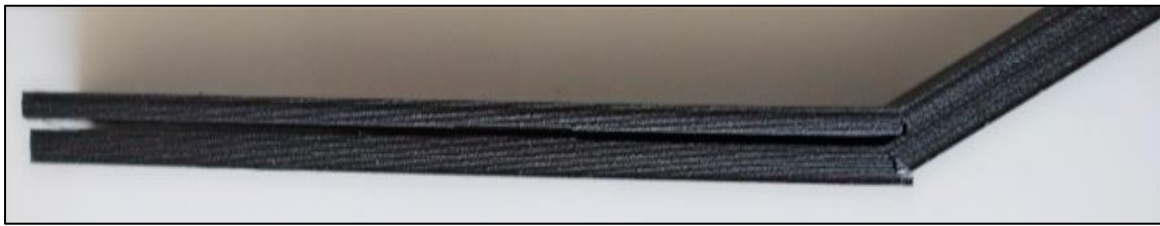
Figure 4-6.. Delamination failure between the matrix and reinforcing materials in three-point flexural sample
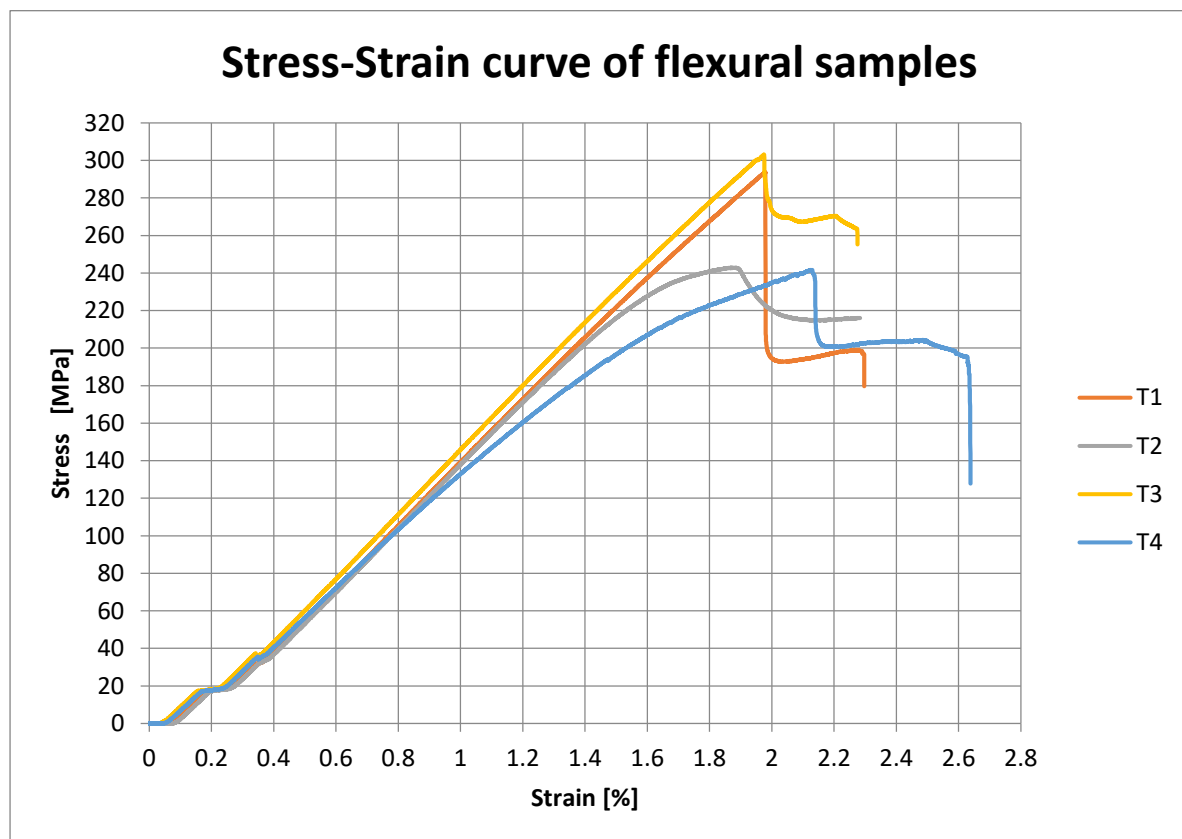
Figure 4-7. Stress-Strain Curves of all Five Flexural test Samples

Tensile test of pure Onyx:

In the tensile test of pure Onyx, five samples with 8 x 8 mm^2 cross-sectional area had been tested to estimate the Poisson's ratio of the new material (Onyx). The failure occurred at about +/- 45-degrees along the printing direction close to the grip section of the movable testing machine head. Once the failure starts, the crack followed the printing angle of the material. This was possibly due to the weak bonding between adjacent layers. Layers with same orientation have same position in the 3D cartesian coordinate. That means if we choose only +/-45° orientation, then the printer extrudes the material at the same position in xy-plane at every second layer Figure 4-8c.

Note; the tensile test of pure Onyx was meant only to estimate the Poisson's ratio of Onyx for use in the FEM only in this thesis. Therefore, it is important underline the exact Poisson's ratio of Onyx is not determined and this is left for future study.

(a) Failed Onyx at near the grip at +/- 45°

(b) Cross-sectional of failed pure Onyx sample tested in tensile.

(c) Cross-sectional illustration of +45° and -45° angle of print and alignment of layer bonding between successive layers.
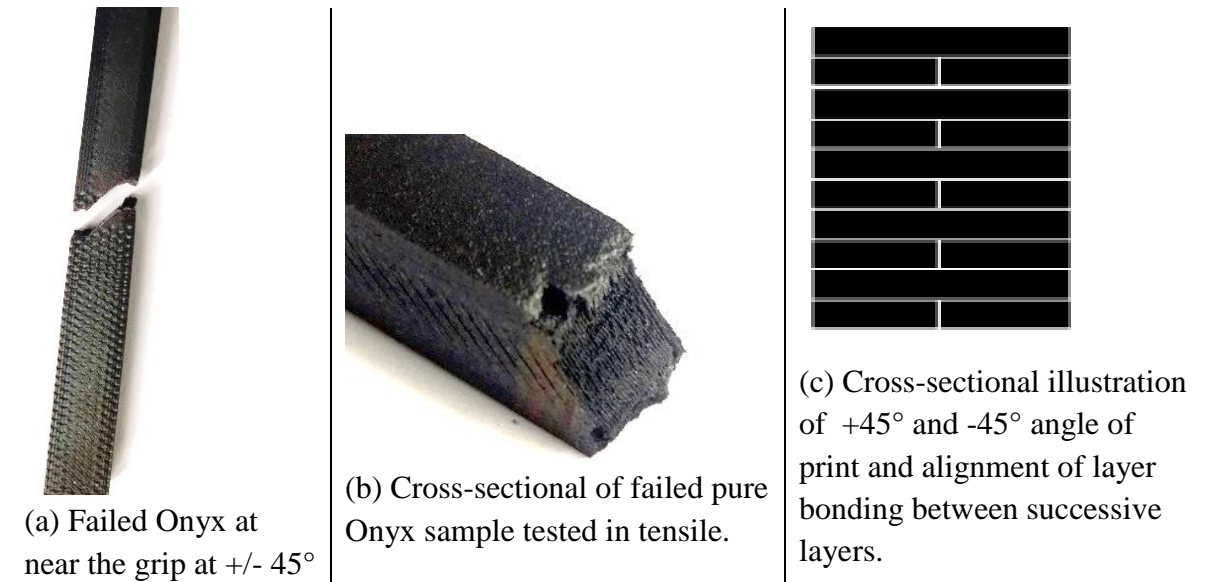
Figure 4-8 Failure type of 8x8mm pure Onyx

4.2   Finite Element Analysis Results from Ansys

FEM for the tensile and the flexural was developed and the results obtained from the simulation using ANSYS software are presented in this section. For simulation only the gauge section (uniform rectangular section of the tensile sample) and only the span between the supports of the three-point bending were modeled. Furthermore, a zero DOF in all possible movements on the fixed end and a pressure at a line on the free end was applied for the tensile model. Whereas both ends of the flexural model was fixed (zero all DOF) and a load was applied at the mid-span between the supports. After that solutions were post processed, nodal and element solutions such as stress, strain, and deformation analysis results were evaluated from the General-Postprocess.

4.2.1.1   FEA of the tensile model

A finite element model of 1.75 mm thick, 15 mm wide and 138 mm in length (represents only the gauge section) was modeled in ANSYS mechanical APDL 17.0. Shell181 element with 4-nodes were used and detailed modeling steps were discussed on section 3.5. The left end of the model had a fixed boundary condition with zero displacement in all possible movements, whereas negative 559.9 MPa uniformly distributed pressure was applied at a line at the right end of the model. Moreover, all the BC were applied on a line. The fixed end had a reaction force of 8398.5 N/mm. Furthermore, the model was meshed with an element size of 0.75 creating 3680 elements. Moreover, the model had one element throughout its thickness. A nodal displacement of 1.13 mm and a maximum tensile stress of 470.50 MPa along the fiber direction was obtained from the simulation. The model had its max. stress at the edges of the fixed side due to contraction of the width, and the stress gradually decreasing until about 20

mm from the fixed end (Figure 4-13), while it had a uniformly distributed average stress of 442.60 MPa at the rest of the model.

Table 14. FEM results of tensile model

Description	Nodal solution	Units
Displacement UX	1.13	mm
Max. stress Sx	470.50	MPa
Von mises SEQV	469.30	MPa
Max strain EPELX	0.009	mm/mm
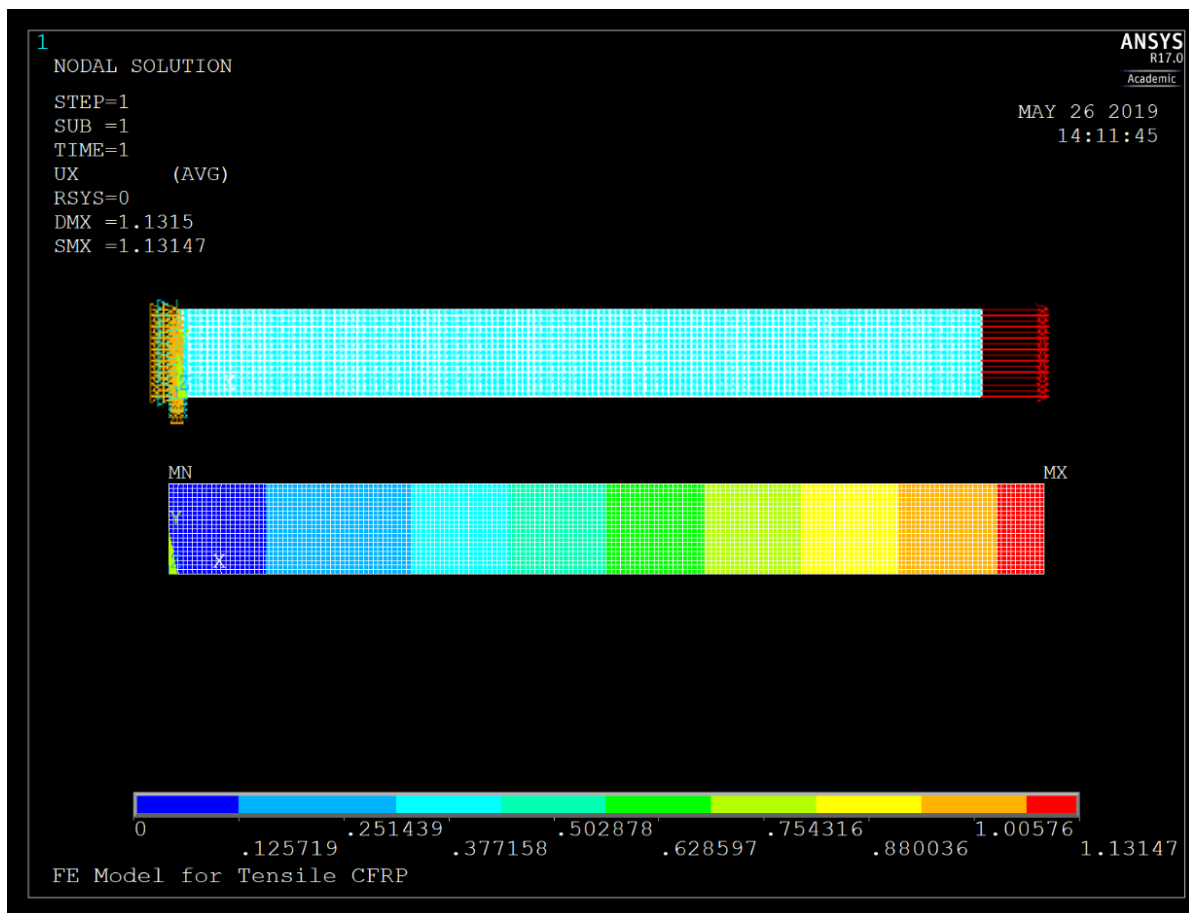
Figure 4-9. FEM displacement of the tensile model from Nodal solution
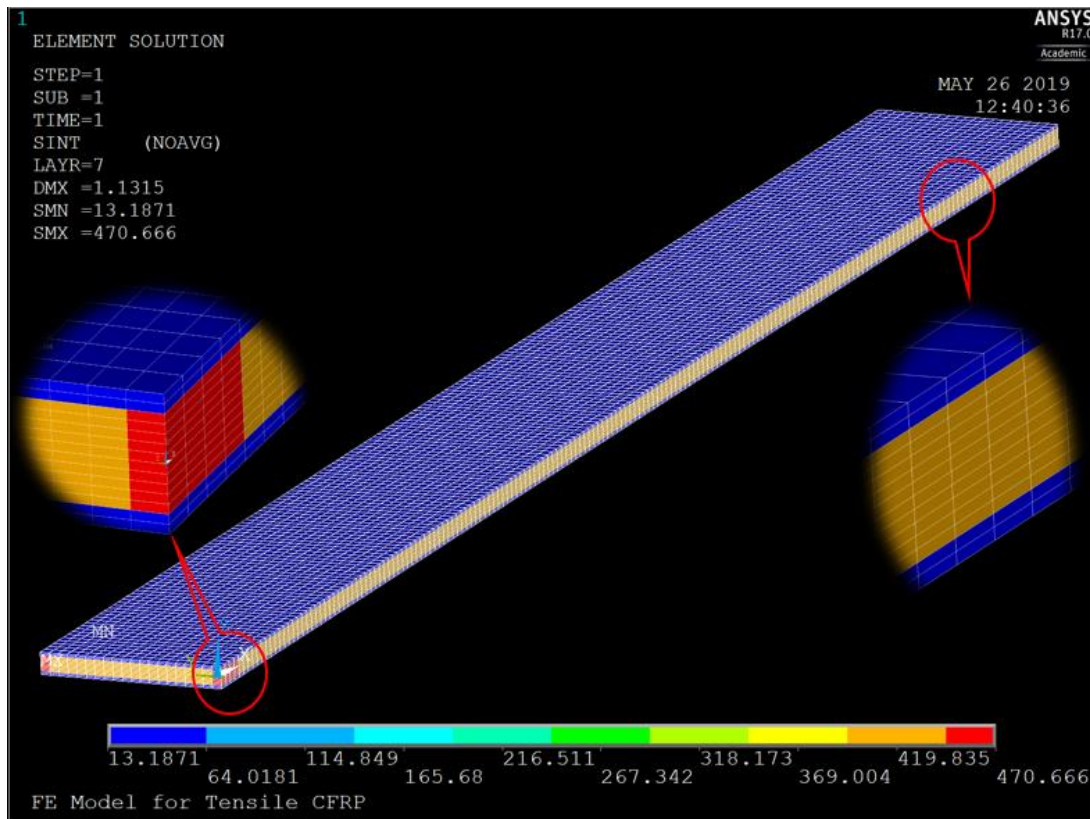
Figure 4-10. FEM for tensile. element solution

From results in Figure 4-10, the model failed at the two edges where the zero DOF was applied. These ends had the maximum stress value of 470.67 MPa, while the rest of the sample had a uniform stress of 442.6 MPa and 13.30 MPa for the CF and Onyx layers, respectively.
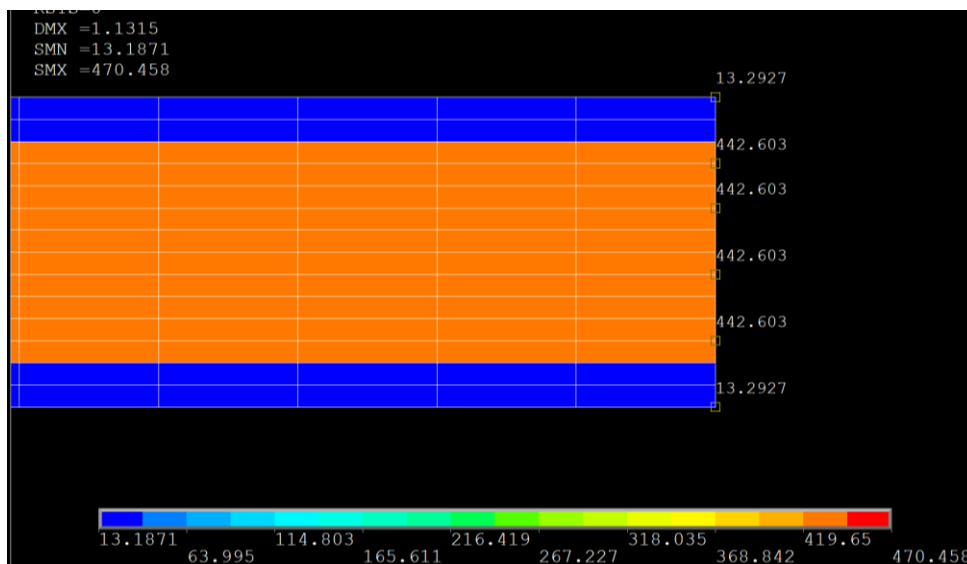
Figure 4-11. Stress in the tensile model for Onyx(blue) and CF (orange) along the depth of the sample

From results in Figure 4-11 the stress distribution along the width of the model was investigated. Except the stress differences between the matrix and fiber materials due to their

strain difference, it had not been observed any difference between identical layers and materials. These indicates that the model was symmetrically reinforced.

b) Stress- elastic strain (direct data from defined path exported to excel).

a) Stress distribution along model length Ansys when high stress at the fixed edge included.

d) Calculated Force -Extension including the high edge stress.

c) Stress distribution along the model length from Ansys, excluding the high stress at the edge.

Figure 4-12. Stress distribution of a Path defined at middle layer along the length of the tensile model

In Figure 4-12(a) the stress distribution along the length of the tensile model was presented from a path defined at one edge of the model that includes the maximum stressed edge. It had been defined several pathes at top, bottom, middle along the length of the model to analyze the presence of stress difference. All the pathes except these defined at the edges provide results presented on Figure 4-12(c). Furthermore, strain, extension and stress from the defined path nodes had been exported to excell. Moreover, force per length (thickness) was calculated from the exported results in excell and are presented on Figure 4-12(b and d).
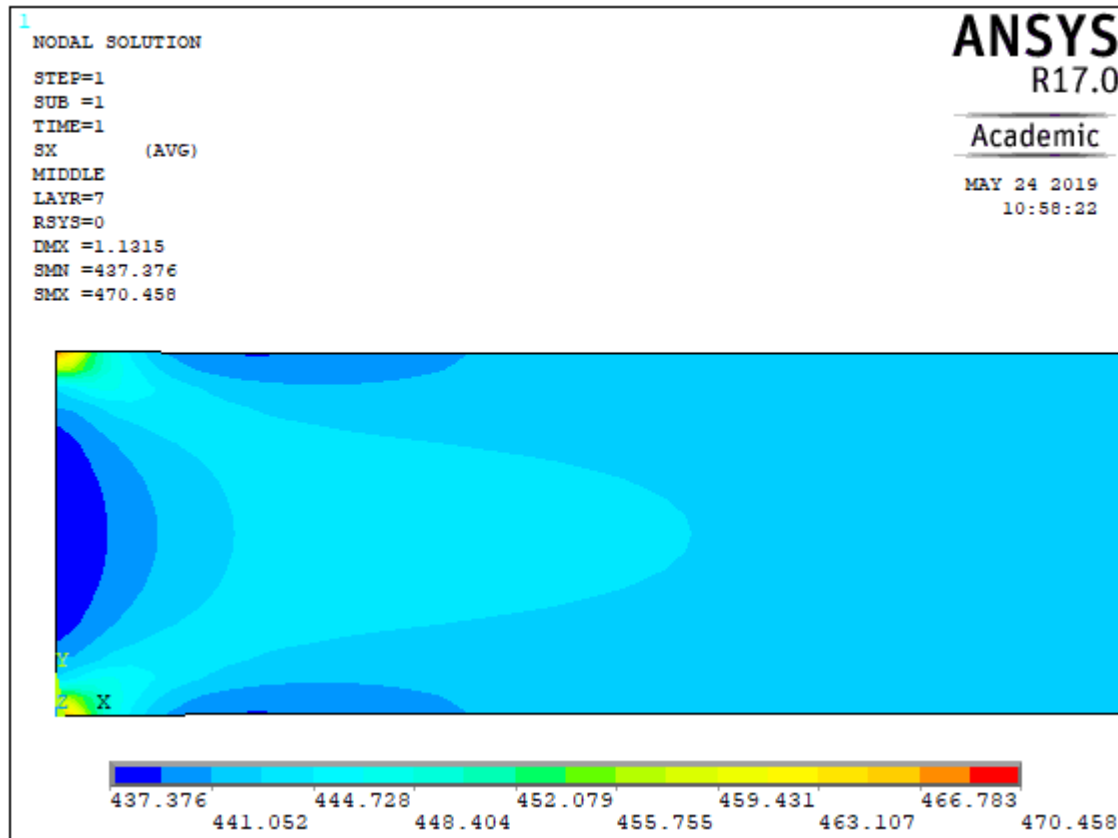
Figure 4-13. Close investigation of layer7 in the tensile mode at the fixed end.

The finite element model had been stressed maximum at the fixed edge, while the test of the sample part was uniformly stressed. The same amount of load was applied to both materials. However, the Onyx material was less stressed while the carbon fiber was fully stressed. This was due to the strain difference of the two materials. Referring to the material properties provided by Markforged®, Onyx and carbon fiber have 58% and 1.5% tensile strain at break, respectively. The results from the model shows that the largest part of the CF in the model was stressed to about 442.6 MPa. There was no stress difference in through the thickness of the sample between carbon fiber layers. The two layers of Onyx at each side of the sample had also a stress of 13.19 MPa.

4.2.1.2   FEA of flexural model

A finite element model of 4 mm thick, 13 mm wide and 124 mm in length (represents only the span length) was modeled in ANSYS. The FEM for flexural analysis had a fixed support with zero degrees of freedom (DOF) at both ends and a total force of 302.70 N was applied at two 'Keypoints'. The two keypoints were located at the mid-span of the beam one at each edge Figure 4-14. The area was meshed with an element size of 0.40 and the free quadrilateral dominant meshing method was used. The mesh produced 10230 elements and the model had one element through the model thickness. A maximum flexural stress of 254.10 MPa and maximum deflection of 9.14 mm in positive z-direction was obtained. In the flexural model analysis the keyopt(3)=2 was activated to obtain bending results from the shell181. This option is recommended to be used with layered applications that have only one element through thickness [35].

Maximum compression and tensile stress were observed at the fixed edges of the beam between CF and Onyx layers. The next higher compression and tension stresses also presented at the mid-span of the beam. Furthermore, if the maximum stress at the fixed ends of the beam is excluded, then the failure would occur at the mid-span of the beam in both the compression and tension regions. Moreover, failure at the bottom of the beam occurred specifically between layer number 4 and 5. The 4th layer was modeled to have only Onyx material whereas the 5th layer was of carbon fiber. The shear failure between the layers indicates the materials have large strain difference and this leads to high stress on the layer bonding between the materials. Generally, the CF was largely stressed while the Onyx was still relaxed. This occurred, because carbon fiber is brittle and have low strain compared to the Onyx material.

Table 15. Results from the flexural FEM

	Units	Nodal solution	Element solutions at Mid-span
Displacement UZ	mm	9.14	
Max stress SX	MPa	254.10	166.75
Von mises SEQV	MPa	312.50	277.58
Max strain EPELX	mm/mm	0.049	
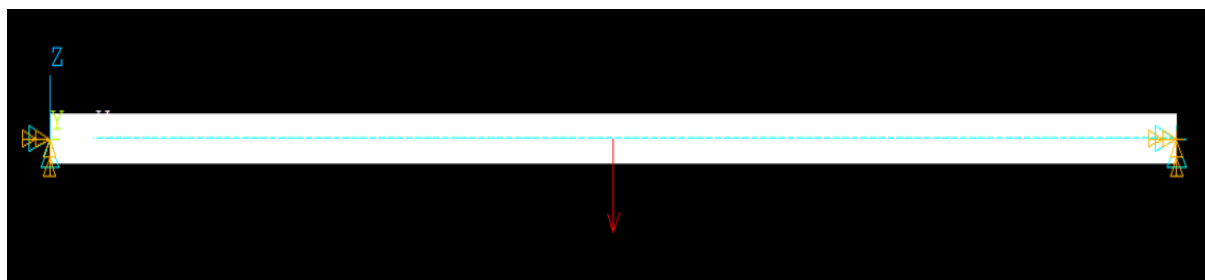
Figure 4-14. Boundary conditions of the flexural model
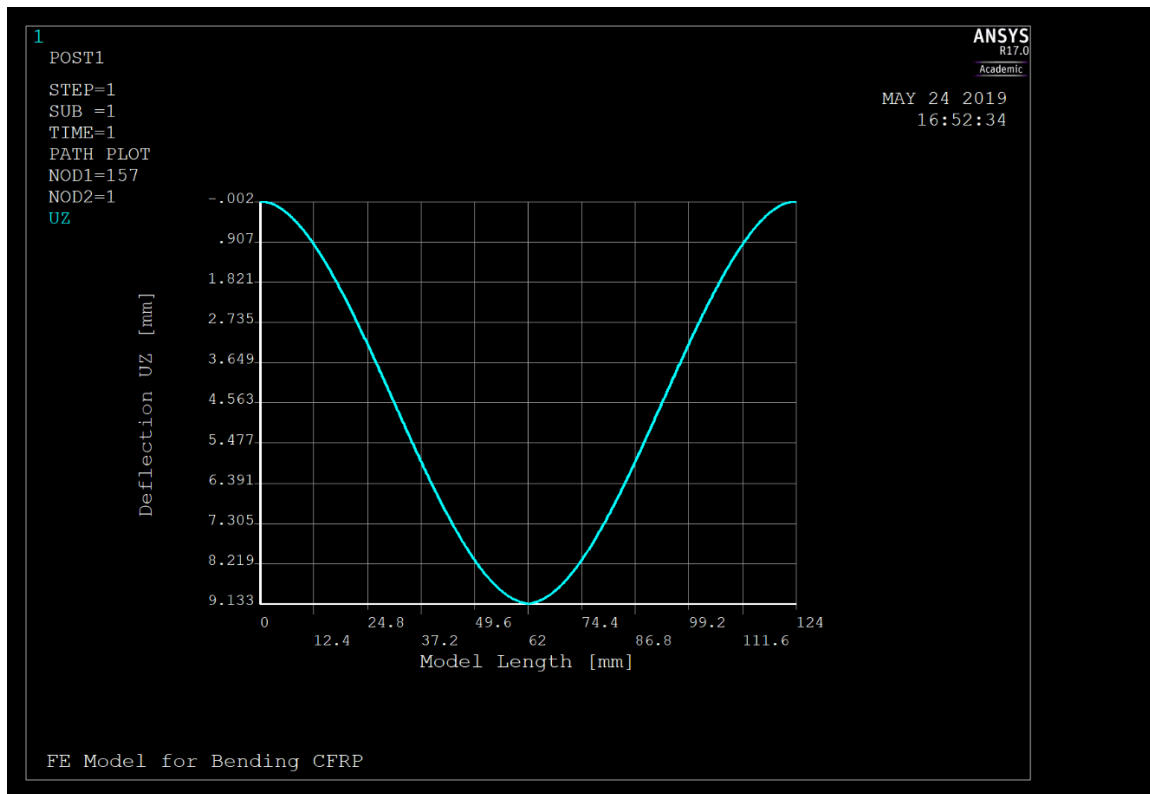
a) Beam deflection along defined path
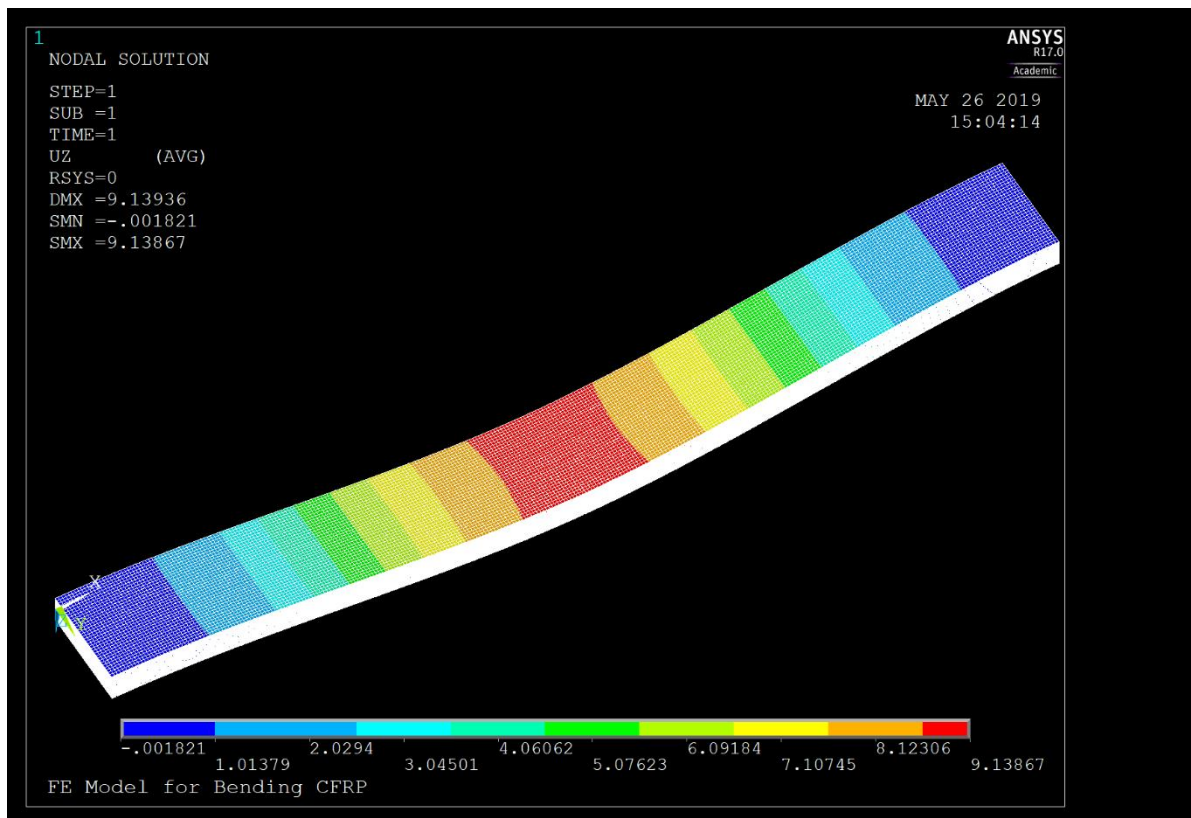
b) Deflection of beam from Nodal Solution

Figure 4-15. Deflection of the flexural beam in z-direction

Figure 4-15 a and b presents , the results of the flexural beam deflection of the model along a
defined path and a counter plot of deflection from nodal solution in millimeters, respectively.
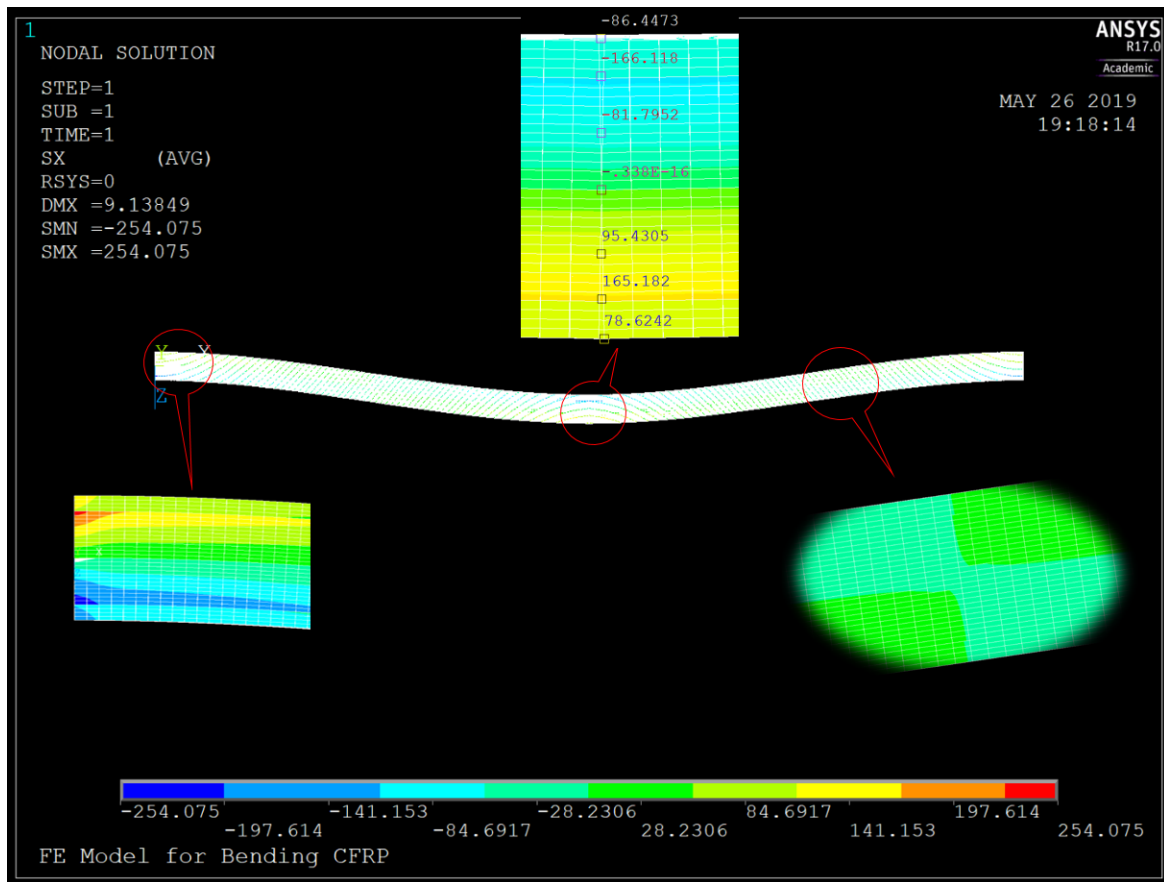
Figure 4-16. Max Stress from the flexural Model

From the Figure 4-16 nodal solution results, the model faced a maximum absolute stress of
254.10 MPa in x-direction and a von Mises (SEQV) stress of 312.5 MPa. Closer investigation
showed that the maximum stress was located at the edges of the fixed beam ends, between the
CF and Onyx layers. However, the middle bottom and top of the model had an absolute
maximum stress of about 166 MPa. Furthermore, at about one quarter of the span length from
both ends, top to bottom transition of region from tensile to compression and vice versa were
observed Figure 4-16. Moreover, the beam deflects 9.14 mm in positive z-direction and
produced an elastic strain of 0.044 mm/mm perpendicular to the cross section of the beam.
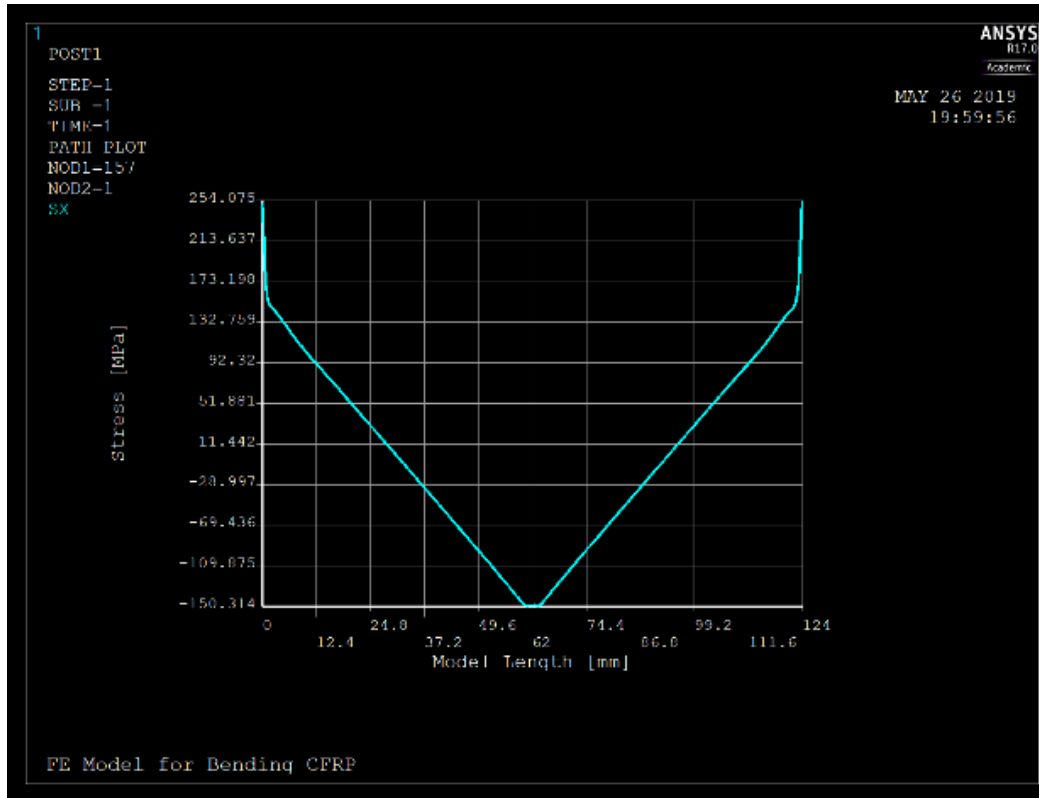
a) Stress at the top face
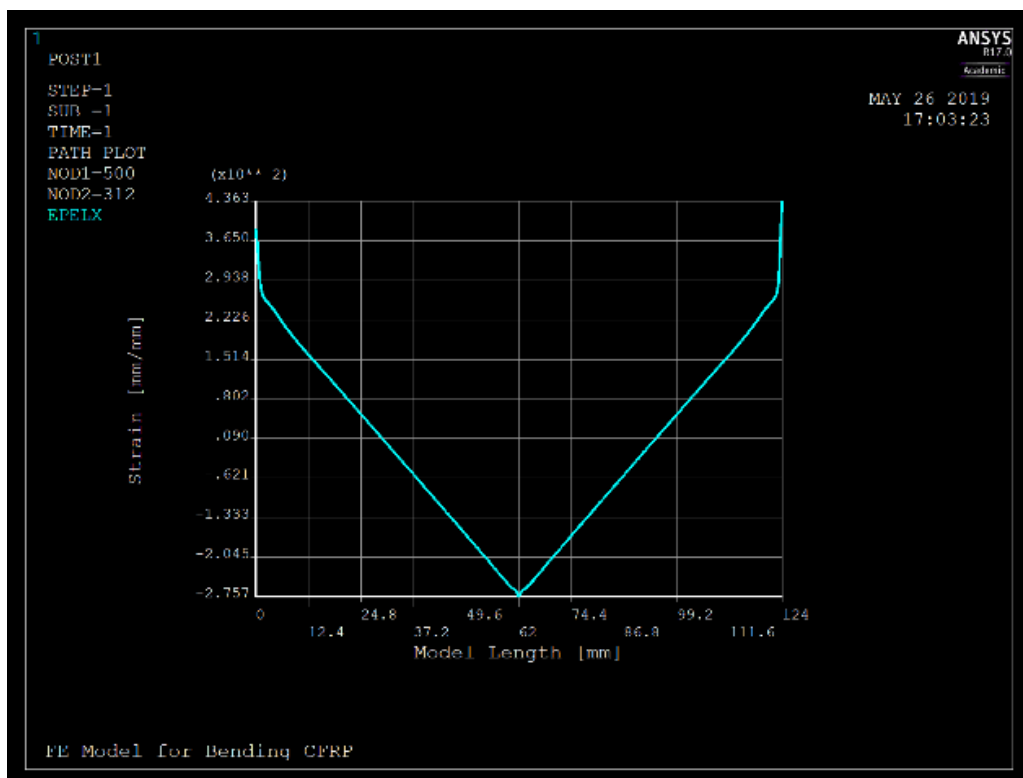
b) Strain in x-direction at top face

Figure 4-17. Stress along Model Length of flexural model at top face

A path was defined along the flexural model length at nodes located at the edges of the beam. This location was selected due to the presence of the maximum stress at the edges of the beam. The results for the top and bottom sections of the beam was obtained by selecting the layer number from the "Options for Output". Since the load applied and the layup of layers was in positive z-direction the first 16 layers experienced a compression stress.
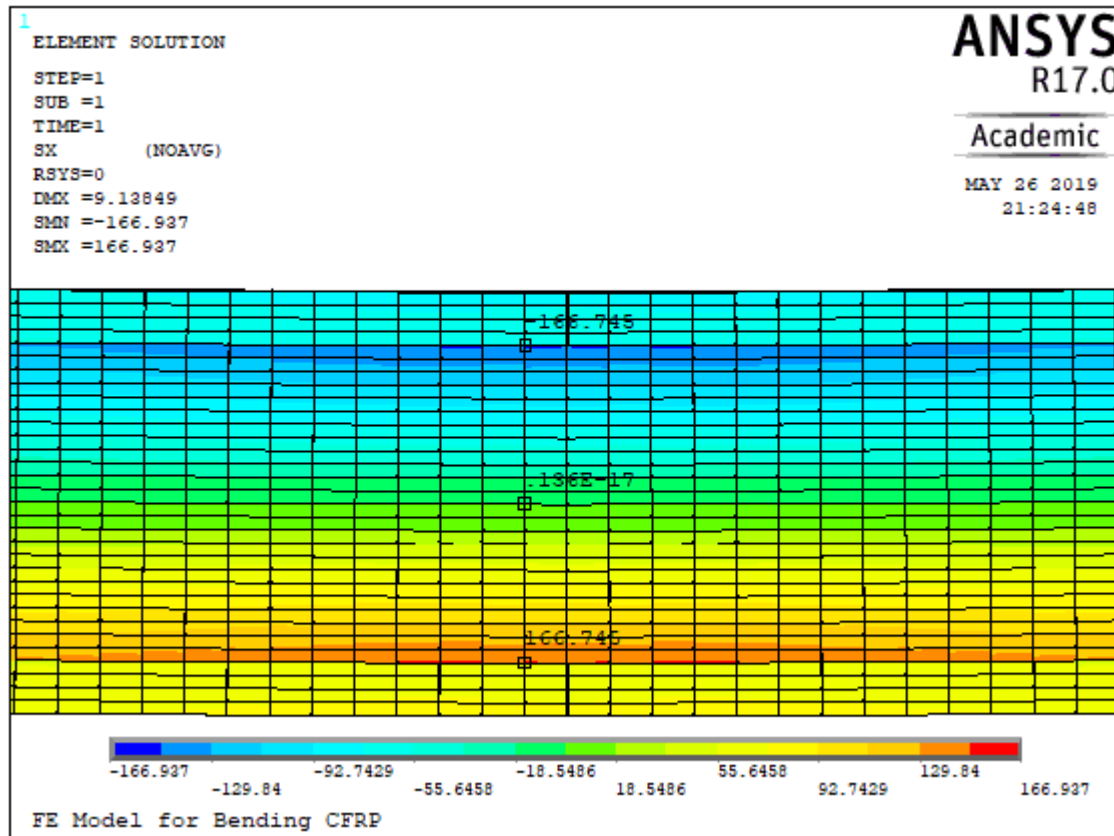
Figure 4-18. Stress distribution on the depth of the flexural model, layer 1 at bottom

The layer-by-layer stress distribution from the Element Solution at the mid-span of the beam is presented on Figure 4-18. The value of neutral nodes, maximum values for compression and tension are marked on the figure. Due to the uncertainty in the material properties used in Ansys, only results along the direction of the fiber were considered. For comparison reasons, the maximum von Mises stress and the principal stress in x-direction was 312.50 MPa and 254.10 MPa, respectively. Since the task of the flexural simulation was to estimate the principal bending stress, the principal stress in x-direction (SX) is reported as a result in this study.
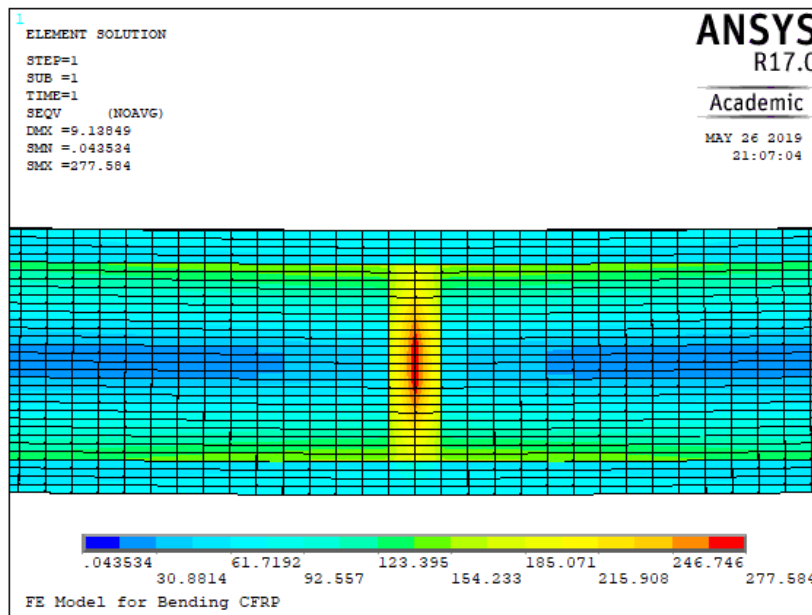
Figure 4-19. Von Mises Stress at the mid-span of the shell beam model

4.3   Validating Results

The results from ROM, experiment and FEA are presented for both tensile and flexural samples in Table 16. When comparing max. stress form FEA and experimental results, the max. stress from FEM had 16% and 6% lower results in tensile and flexural, respectively. While the max. stress obtained from ROM are 19% and 10% lower than the corresponding tensile and flexural experimental results. Moreover, the strength of the composite samples and composite materials are illustrated on Figure 4-21. The illustration show the tensile and flexural properties of the composite samples have strength   in between the minimum and maximum strength of the individual materials.

Table 16 Comparative results from ROM, Experiment, FEA

CF/Onyx matrix (UD reinforced composite)						
Sample type	Type of result	Fiber volume fraction, V_f	Max. stress [MPa]	Stress mismatch w.r.t Experimental	Strain at break [mm/mm]	Elastic Modulus E_{11} [GPa]
Tensile	Experimental	62%	559.9	-	0.026	25
	FEA		470.5	16%	0.01	-
	ROM		453.4	19%	0.10	34.50
Flexural	Experimental	42%	270.7	-	0.028	16.40
	FEA		254.1	6%	0.05	-
	ROM		244.4	10%	0.021	23.10

Author: Fithawi Ghebretinsae
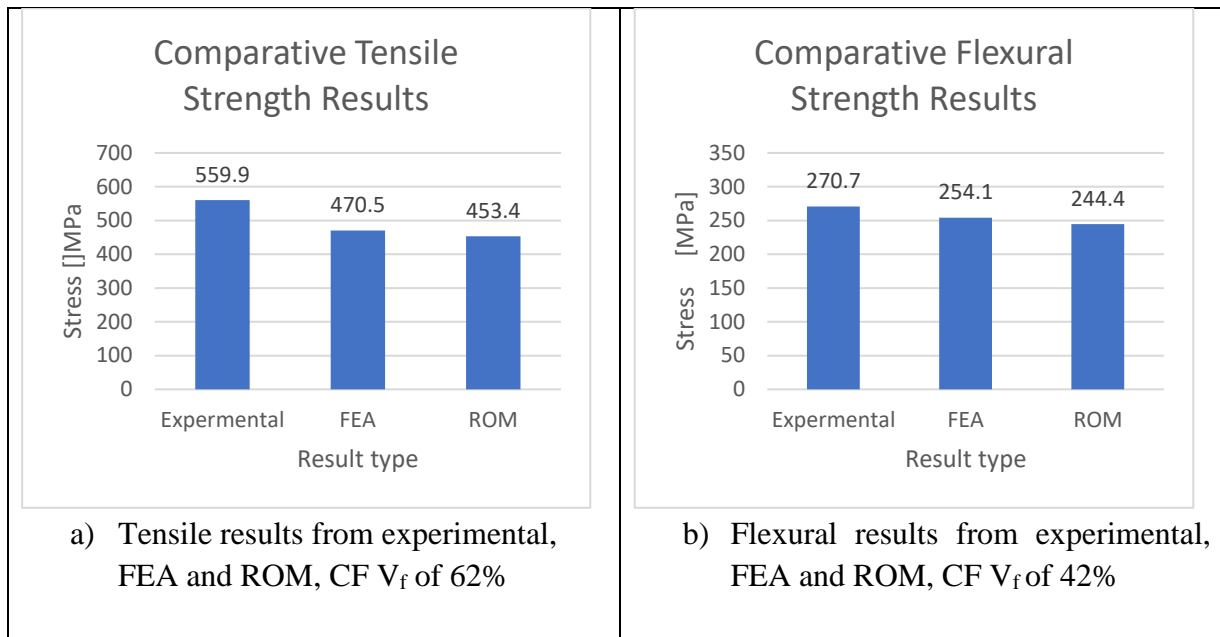
Figure 4-20 Comparative strength of composite samples obtained from experiment, FEA and ROM

Results from Figure 4-20 illustrates the experimentally obtained max. stress are higher than the analytical results . This can be due to the several assumptions taken during analyzing and estimation of the fiber volume fraction. Beside all the assumptions of the material property of both CF and Onyx, and the fiber volume fraction estimations, the results difference is reasonable.
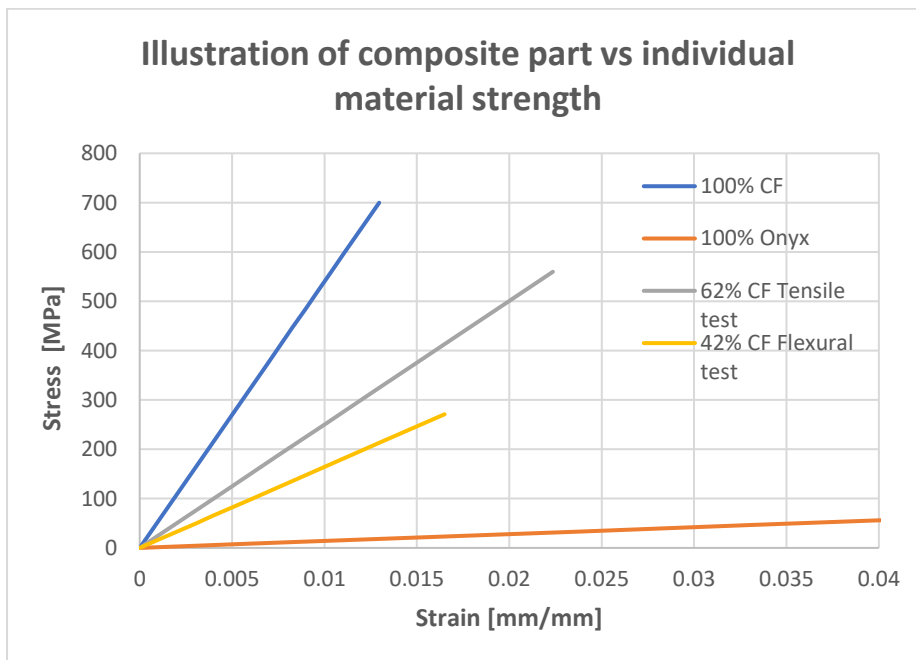
Figure 4-21. Illustration of composite sample and individual material strength

5 DISCUSSION

In this study, fabrication processes of samples from carbon fiber and Onyx using Mark Two 3D Printer was studied. Tensile and flexural tests was performed to understand the material properties of the 3D printed composite materials and the performance of the CFF 3D Printing technology. Furthermore, a Finite Element Model was developed in ANSYS Mechanical APDL 17.0, and the results obtained from the simulation were validated with the experimental results.

The 3D printer and the slicing software had been studied before the fabrication of the samples. This was an important issue due to the printing parameters have a big impact on the strength of components. In the experiment, delamination or interlaminar failure had been observed in both the flexural and tensile test samples. The delamination in both samples were between the matrix and fiber layers. Significant difference in the mechanical properties of the individual composite materials, such as strain property, lead to high shear stress between the matrix and the fiber. In addition, it had been observed formation of voids between layers of both matrix- and fiber- materials during the fabrication of samples. This results to the weak bonding and increase the thickness of the samples on both experiments. From dimensional point of view, the thickness of the samples increased by average 0.03 mm and 0.12 mm for the flexural and tensile samples, respectively. This was due to formation of voids between successive layers which were also noticed during fabrication of the samples. From the dimensions of 3D fabricated samples and the standard dimensions on Table 12, dimensional shrinkage in the xy-plane was observed, while dimension increased in the z-direction. The shrinkage might be caused by the contraction of the hot extruded material.

The carbon fiber failed first due to its low strain property, while the Onyx material had much larger strain capability. This was clearly visible in the FE models, where the fiber failure was the main cause of failure. Furthermore, since the materials used in 3D Print are different from the materials used in the traditional manufacturing processes and are patented, thus all the orthotropic material properties of both CF and Onyx was not available. Therefore, there had been taken several assumptions when defining material properties in the FEA. Moreover, five samples were fabricated with solid 100% infill of pure Onyx and a tensile test had been performed to assume its Poisson's ratio. Since Onyx is new material the Poisson's ration used was pure assumption.

Normally, results from the finite element are approximated results and the accuracy of the FEA solution depends on the choice of the elements and mesh density. The flexural and tensile models had 3680 elements of size 0.75 and 10230 elements of size 0.4, respectively. Shell elements have several layers and it was important to select the layer of interest during post-processing the results. In the tensile model, the layers of identical materials were stressed

uniformly. Whereas in the flexural model, the 5th and the 28th layer experienced the highest stress.

Table 17. Comparison between experimental and FEA results for bending and tensile

Type of test	Max. Load [N]	Experimental			ANSYS APDL		Mismatch in Stress [%]
		Max. Extension [mm]	E-modulus [GPa]	Max. Stress [MPa]	Stress [MPa]	Extension [mm]	
Tensile	14700	5.50	25.04	559.86 ± 17.72	470.5	1.13	16%
Flexural	300	13	16.42	270.71 ± 28.27	254.1	9.14	6%

When observing the failure of the flexural specimens, the failure occurs at the region exposed to tension. A delamination between layers had been observed at two samples and closer investigation clearly showed separation between layers of Onyx and carbon fiber. Shear failure between the interface of the carbon fibers and the Onyx layers located at the center of the beam occurred on both the delaminated samples. The delamination was probably due to the nature of AM , specifically weak bonding between successive layers and no fusing between the Onyx and the carbon fiber materials. Furthermore, the Onyx material was easy to peel off from the CF and this reduces the stress transformation ability of the Onyx.

From flexural test results, a maximum flexural stress of 270.71 MPa and flexural modulus of 16.42 GPa was obtained. The average results had a standard deviation of 28.27 MPa and 1.35 GPa for the maximum stress and modulus, respectively. Furthermore, about 2.80% of flexural strain at break was obtained.

Referring to the Tensile test, all the tensile specimens fail within the gauge length near the grip section as in Figure 4-3(b). The failure started at the gauge section first by delamination at the edges and followed by an explosion which lead to multi area failure mode within the gauge length. Samples S1 and S5, first delaminated and then exploded at the top and bottom regions near the grip within the gauge length. In addition, a fiber pullout has been observed near top grip in sample S2. This was probably due to shear deformation of the tab where minor sliding appeared during testing . samples S3 and S4 were the samples which experienced a multi area explosion.

Results from this study show that tensile composites, with fiber volume fraction about 62% provided 559.90 MPa and 25 GPa in tensile strength and E-modulus, respectively. The max. tensile stress and elastic modulus had a standard deviation of 17.72 MPa and 2.65 GPa, respectively.

In the Finite Element modeling using Ansys mechanical APDL 17.0, it was challenging to provide the correct material properties of the both materials. The materials are patented, and all the orthotropic mechanical properties required for analyzing a composite material was not provided on the material data sheet prepared by Markforged®. Therefore, several assumptions had been taken. For instance, the orthotropic material properties that was not presented by the producer was estimated by taking 34.5% the AS4 carbon yarn properties.

Furthermore, Ansys uses higher fiber volume ratio in the ROM due to the layers were modeled without including the wall width that covers the CF layers in the test samples. Moreover, 470.50 and 254.10 MPa in tensile and flexural strength were obtained from the FEM. The models had a tensile displacement of 1.13 mm and a flexural deflection of 9.14 mm.

At last, the slicing software, Eiger®, should have more options such as dimension measurement and editing options. When preparing complex component that will fit to each other, it is necessary to check dimensions for required tolerance. The size of a part can be scaled when the model is uploaded to Eiger. However, the dimensions in Eiger shows only the building volume occupied by the whole component. This is essential to keep the maximum volume of a component within the capability of the 3D printer. Therefore, if the 3D printer is to be used to fabricate real engineering applicable components, it requires a dimension measurement tool. This is important to ensure the final printable part is as designed in 3D CAD model before executing the print command.

6 CONCLUSION

A delamination failure was the common cause of failure mainly in the tensile test. Bonding between successive non-identical material layers and adjacent layers of CF was weak. Specifically, the matrix-fiber interface bonding was the weakest part of the composite samples. It had been observed weak fusion between adjacent printed carbon fiber yarns which make the composite to significantly weaken in shear stress. This might be improved in the future by changing the adhesive constituents, usually added to hold carbon fiber yarns together during production, by polymers that have higher fusion properties with CF.

In contrast to all, the composite material provided a promising property with about 560 MPa max. tensile and about 271 MPa bending strength, respectively. Furthermore, the UD composite material achieved an elastic modulus of 25 GPa and 16 GPa for the tensile and bending (flexural), respectively. Moreover, max. tensile stress of 471 MPa and flexural stress of 254 MPa the were obtained from the FE simulation. This is 16% and 6% lower than the experimental results. However, the result was satisfactory remembering the several assumptions taken during simulation.

For comparison reasons, ultimate tensile strength of 6061-T6 Aluminum commonly used for bike frames is 310 MPa [46], while the obtained results from the tensile samples fabricated with about 62% CF was around 560. The tested samples had high fiber volume fraction and their strength was about 81% higher than Al6061-T6.

Unlike traditional manufacturing of composites, it is not possible to partially reinforce a single layer. In addition, Mark- two 3D printer is intended to use only nylon/Onyx materials provided by the producer of the machine and several settings are pre-defined by the manufacturer. This restricts the freedom of material selection and reinforcing a composite part only at desired location that can reduce the cost significantly. Furthermore, the slicing software locks the most valuable tool for engineers, namely the measurement tool. Therefore, it is recommended to add measurement tool features in cloud based slicing software. Furthermore, the predefined layer thickness, raiser layers and matrix orientation are some of the drawbacks and are recommended to develop more flexible options in the future. An option which allows printing the plastic and fiber layers in different individual layer-thickness can save printing time and cost while maintaining the strength of the composite parts.

7   REFERENCES

1.   Van Der Klift, F., et al., *3D printing of continuous carbon fibre reinforced thermo-plastic (CFRTP) tensile test specimens.* 2016. **6**(1): p. 18-27.

2.   Hull, D. and T.W. Clyne, *An introduction to composite materials*. 1996: Cambridge university press.

3.   Ning, F., et al., *Additive manufacturing of carbon fiber reinforced thermoplastic composites using fused deposition modeling.* 2015. **80**: p. 369-378.

4.   Jiang, D. and D.E.J.A.M. Smith, *Anisotropic mechanical properties of oriented carbon fiber filled polymer composites produced with fused filament fabrication.* 2017. **18**: p. 84-94.

5.   Hart, R.J., E.G. Patton, and O. Sapunkov, *Characterization of Continuous Fiber-Reinforced Composite Materials Manufactured Via Fused Filament Fabrication*. 2018, ARMY TANK AUTOMOTIVE RESEARCH DEVELOPMENT AND ENGINEERING CENTER WARREN MI ….

6.   Caminero, M., et al., *Interlaminar bonding performance of 3D printed continuous fibre reinforced thermoplastic composites using fused deposition modelling.* 2018. **68**: p. 415-423.

7.   Miracle, D.B., et al., *ASM handbook, Composites*. Vol. 21. 2001: ASM international Materials Park, OH, USA.

8.   Lozada, J.N., et al., *Tensile properties and failure behavior of chopped and continuous carbon fiber composites produced by Additive Manufacturing.* 2019.

9.   Sauer, M.J., *Evaluation of the Mechanical Properties of 3D Printed Carbon Fiber Composites.* 2018.

10.   Strong, A.B., *Fundamentals of composites manufacturing: materials, methods and applications*. 2008: Society of Manufacturing Engineers.

11.   Melenka, G.W., et al., *Evaluation and prediction of the tensile properties of continuous fiber-reinforced 3D printed structures.* Composite Structures, 2016. **153**: p. 866-875.

12.   Schwartz, M.M., *Composite materials handbook*. 1984: McGraw-Hill.

13.   Campbell, F.C., *Structural composite materials*. 2010: ASM international.

14.   Tuttle, M.E., *Structural analysis of polymeric composite materials*. 2003: Crc Press.

15.   Gay, D. and S.V. Hoa, *Composite materials: design and applications*. 2007: CRC press.

16.   Nicolais, L., M. Meo, and E. Milella, *Composite materials: a vision for the future*. 2011: Springer Science & Business Media.

17.   Jones, R.M., *Mechanics of composite materials*. 2014: CRC press.

18.   Callister, W.D. and D.G. Rethwisch, *Materials science and engineering: an introduction*. Vol. 9. 2014: John wiley & sons New York.

19.   Hodgkinson, J.M., *Mechanical testing of advanced fibre composites*. 2000: Elsevier.

20.   MBI, *<History of composite >.*

21.   Dickson, A.N., et al., *Fabrication of continuous carbon, glass and Kevlar fibre reinforced polymer composites using additive manufacturing.* 2017. **16**: p. 146-152.

22.   Mohammadizadeh, M., et al., *Creep behavior analysis of additively manufactured fiber-reinforced components.* 2018. **99**(5-8): p. 1225-1234.

23.   Nik, M.A., et al., *Optimization of variable stiffness composites with embedded defects induced by automated fiber placement.* Composite Structures, 2014. **107**: p. 160-166.

24.   Bandyopadhyay, A. and S. Bose, *Additive manufacturing*. 2015: CRC Press.

25.   Gornet, T.W.a.T., *<History of Additive Manufacturing.pdf>.* 2014.

26.   Hull, C.W., *Method for production of three-dimensional objects by stereolithography*. 1990, Google Patents.

27.   Sossou, G., et al., *An additive manufacturing oriented design approach to mechanical assemblies.* 2018. **5**(1): p. 3-18.

28.   Markforged, *<CompositesDesignGuide_V1-1.pdf>.* 2019, retrieved.

29.   Ahn, S.-H., et al., *Anisotropic material properties of fused deposition modeling ABS.* 2002. **8**(4): p. 248-257.

30.   Lee, C., et al., *Measurement of anisotropic compressive strength of rapid prototyping parts.* 2007. **187**: p. 627-630.

31.   Markforged, *<Mark Two product specification.pdf>.* 2016.

32.   Markforged-3D, *<Markforged-Products-and-Applications.pdf>.* 2016.

33.   Crease-Markforged, A., *Part One of a series on efficient fiber routing techniques using the Markforged 3D printer.* 2016,des.

34.   Barbero, E.J., *Finite element analysis of composite materials using ANSYS®*. 2013: CRC press.

35.   ANSYS, A., *ANSYS Mechanical APDL Structural Analysis Guide Release 15.* ANSYS, Inc., 2013.

36.   Matthews, F.L., et al., *Finite element modelling of composite materials and structures*. 2000: Elsevier.

37.   Mac Donald, B.J., *Practical stress analysis with finite elements*. 2007: Glasnevin publishing.

38.   Tesinova, P., *Advances in Composite Materials: Analysis of Natural and Man-Made Materials*. 2011: BoD–Books on Demand.

39.   Markforged, *Onyx, material specification.* 2019, retrived.

40.   Markforged, *<composites-data-sheet.pdf>.* 2018/6/15.

41.   Standard, A.J.A.D.D.M., *ASTM D3039-Standard test method for tensile properties of polymer matrix composite materials.* 2008. **3039**: p. 13.

42.   Standard, A.J.A.S.f.T. and P. Materials: Philadelphia, USA, *D7264 Standard test method for flexural properties of polymer composite materials.* 2007. **D 7264/D 7264M-07**: p. 11.

43.   Meddad, A., et al., *Micromechanical modeling of tensile behavior of short fiber composites.* Journal of composite materials, 2002. **36**(4): p. 423-441.

44.   ANSYS, A., *Mechanical APDL Structural Analysis Guide.* ANSYS, Inc., 2012.

45.   Kohnke, P., *ANSYS Theory Reference Release 5.6.* 1998.

46.   www.glemco.com, *<Alumina 6061-T6.pdf>.* p. 1.

8   Appendix:

8.1   Appendix A1

Tensile test stress-strain curve of each tensile specimen is shown below.

Stress-Strain Curve of Tensile Sample S2

Stress-Strain Curve of Tensile Sample S3

Stress-Strain Curve of Tensile Sample S4

Stress-Strain Curve of Tensile Sample S5
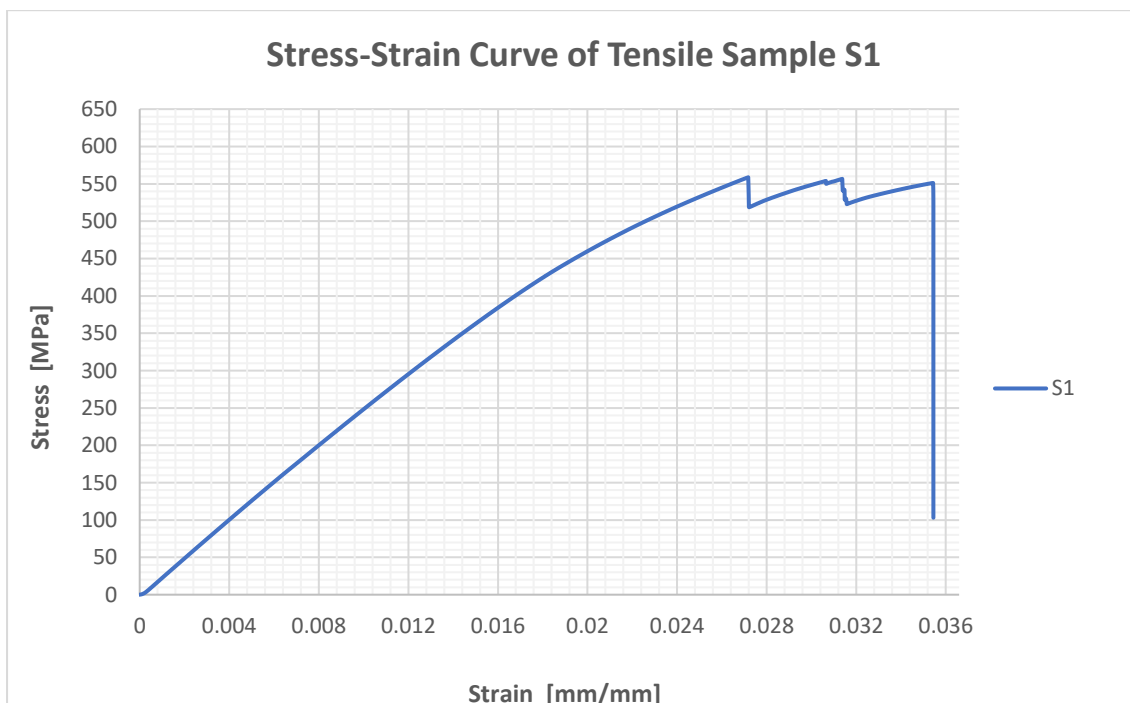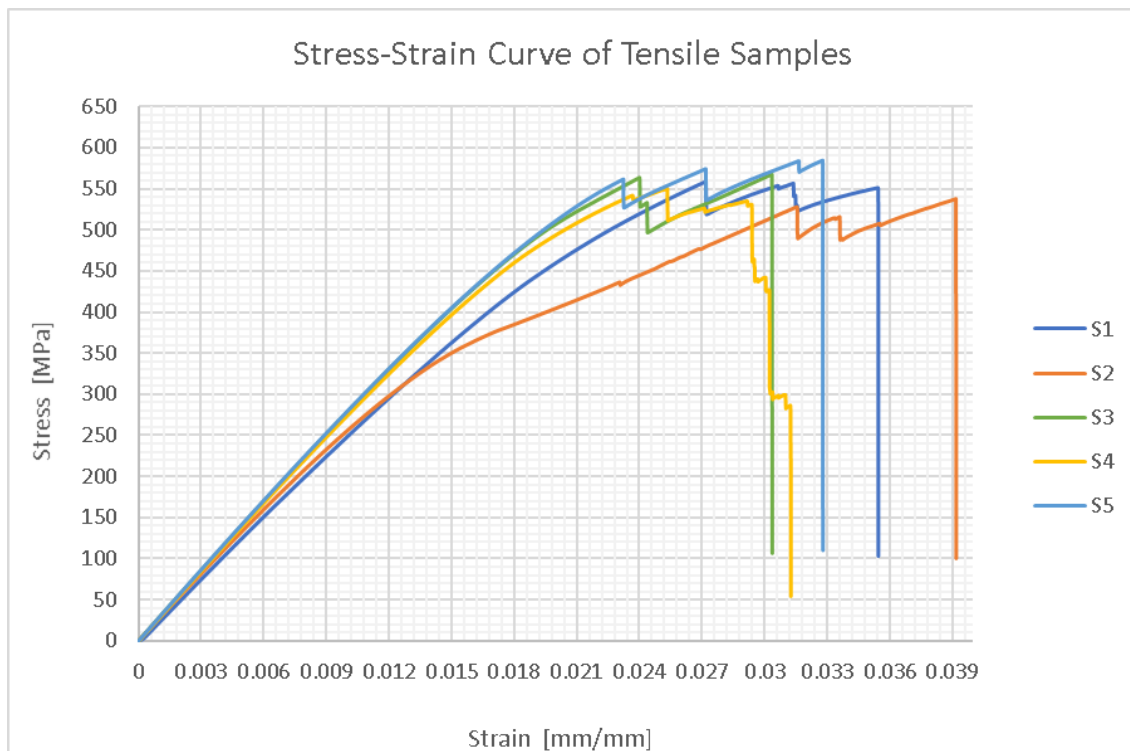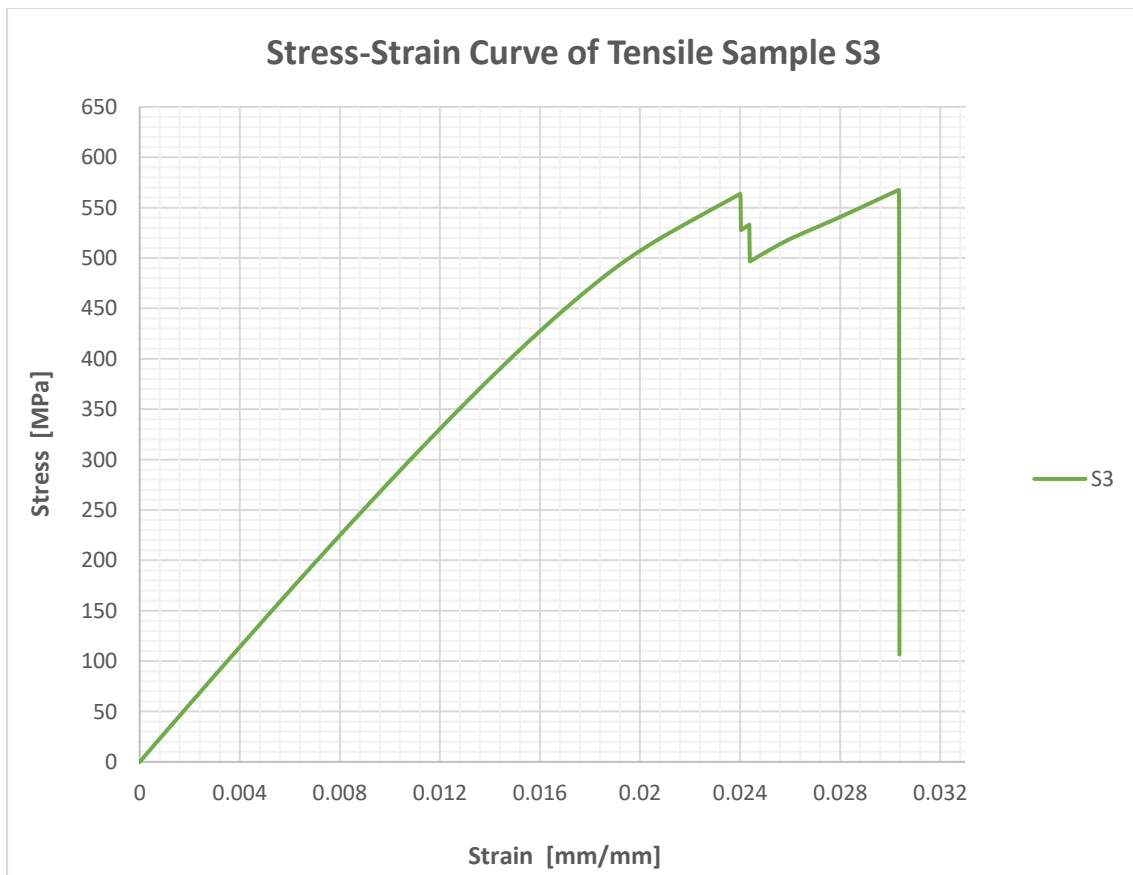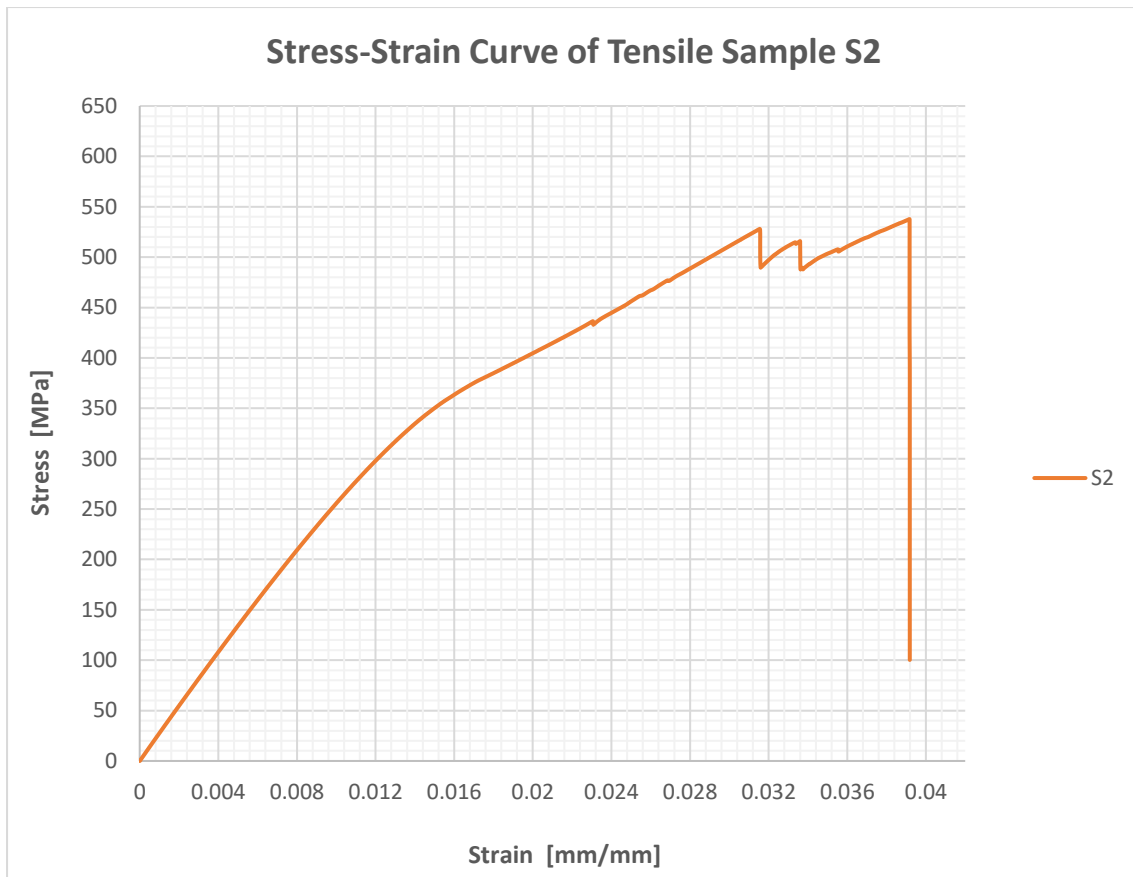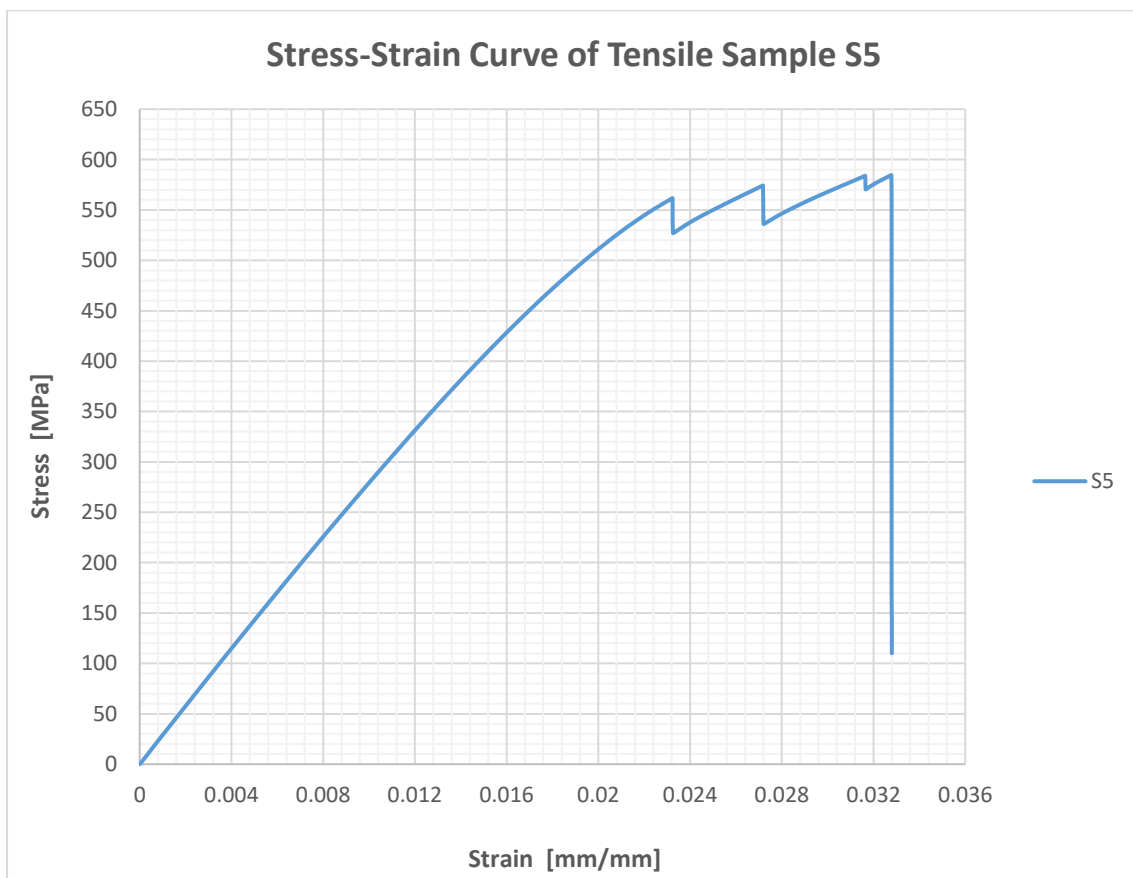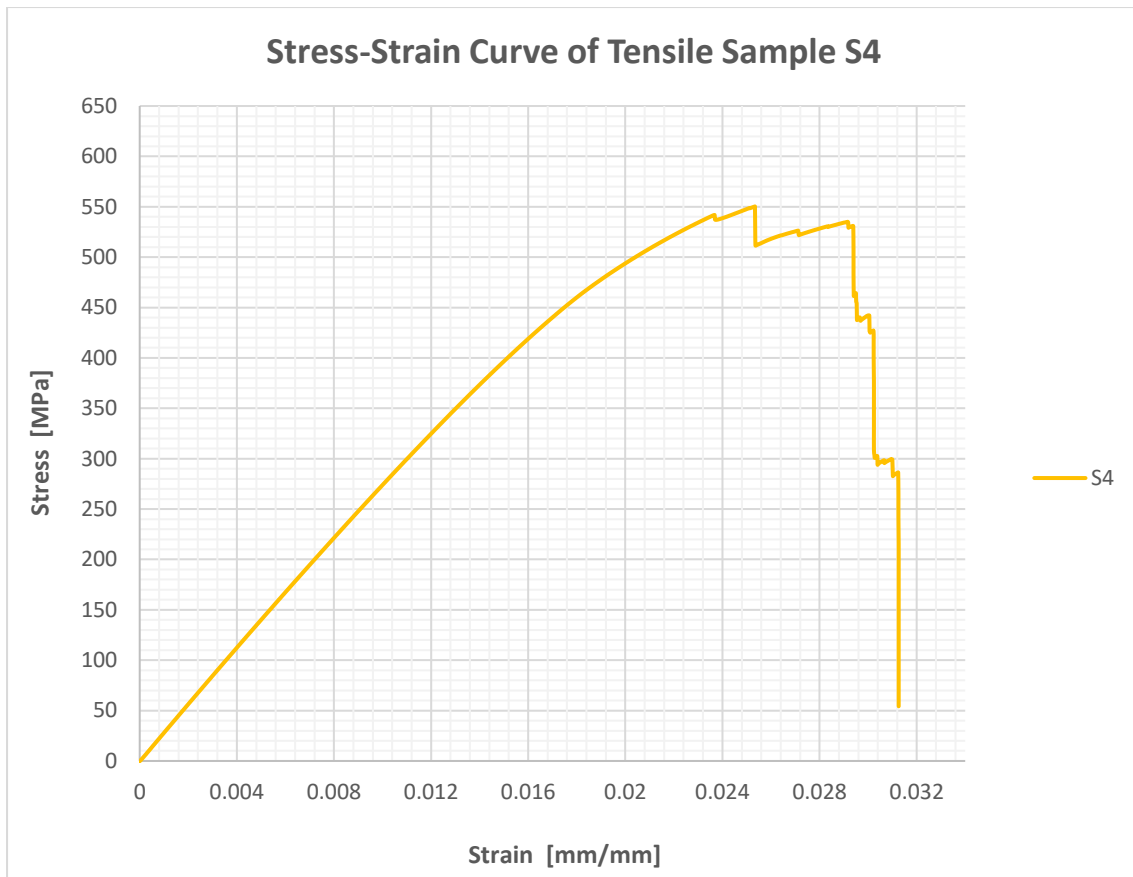
8.2   Appendix A2

The force-displacement curves of each tensile specimen are shown below

Force- Extension curve of sample

Force- Extension curve of sample 1

Force- Extension curve of sample 2

Force- Extension curve of sample 3

Force- Extension curve of sample 4

Force- Extension curve of sample 5
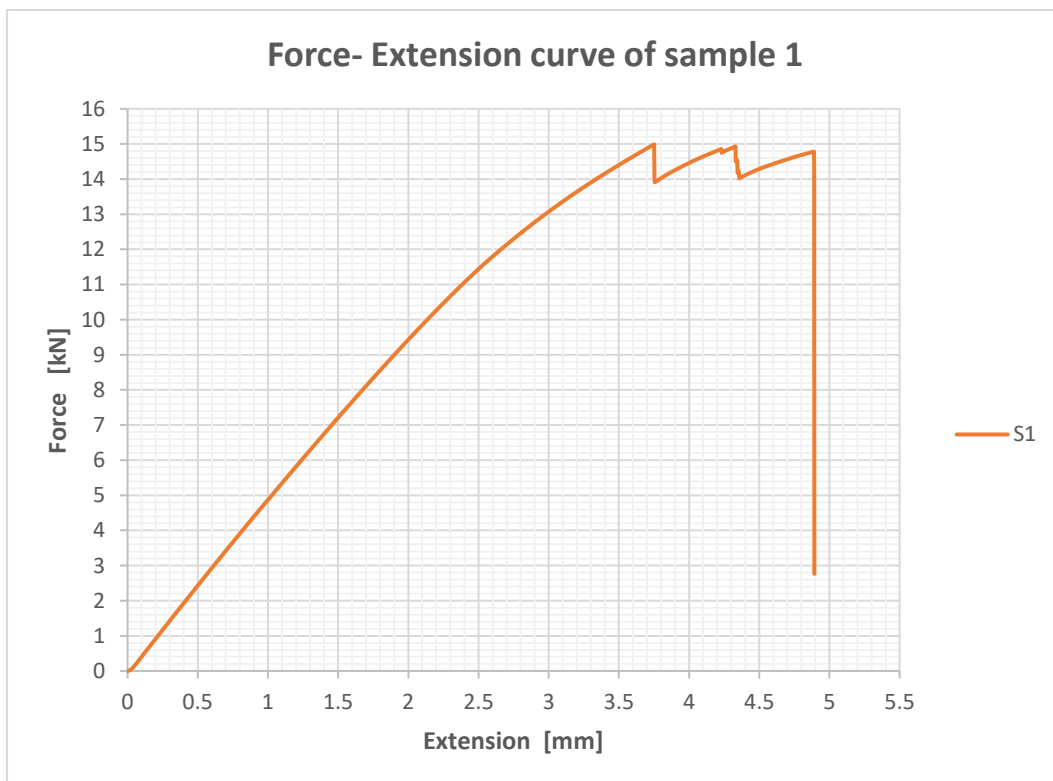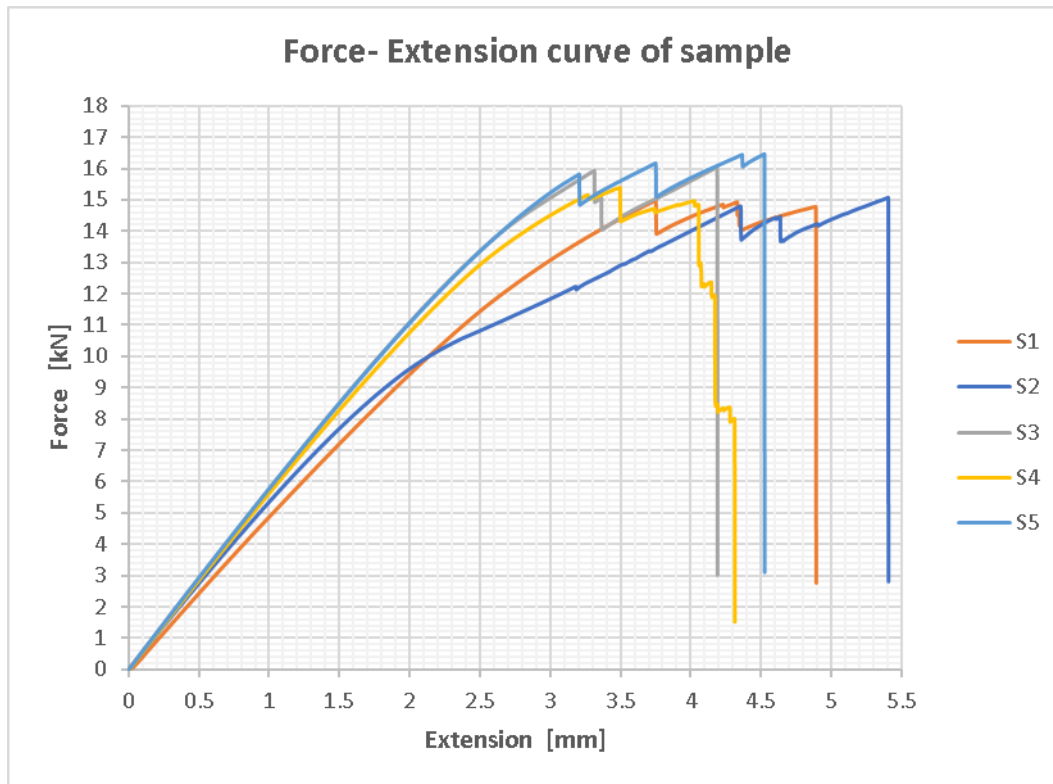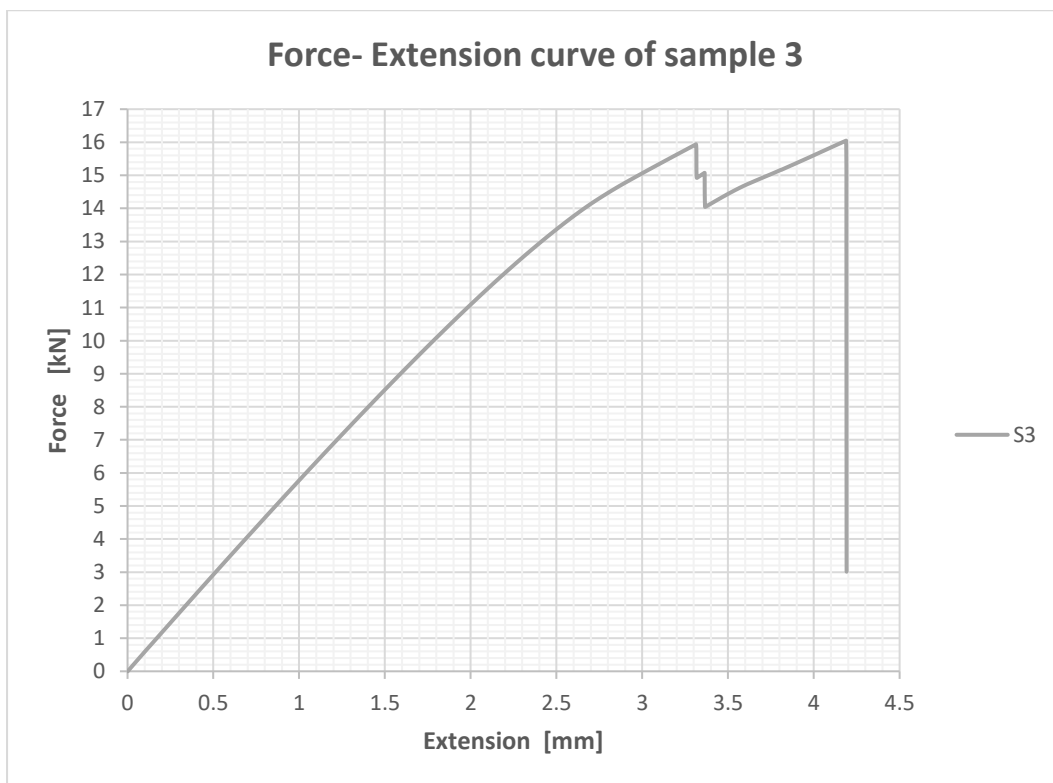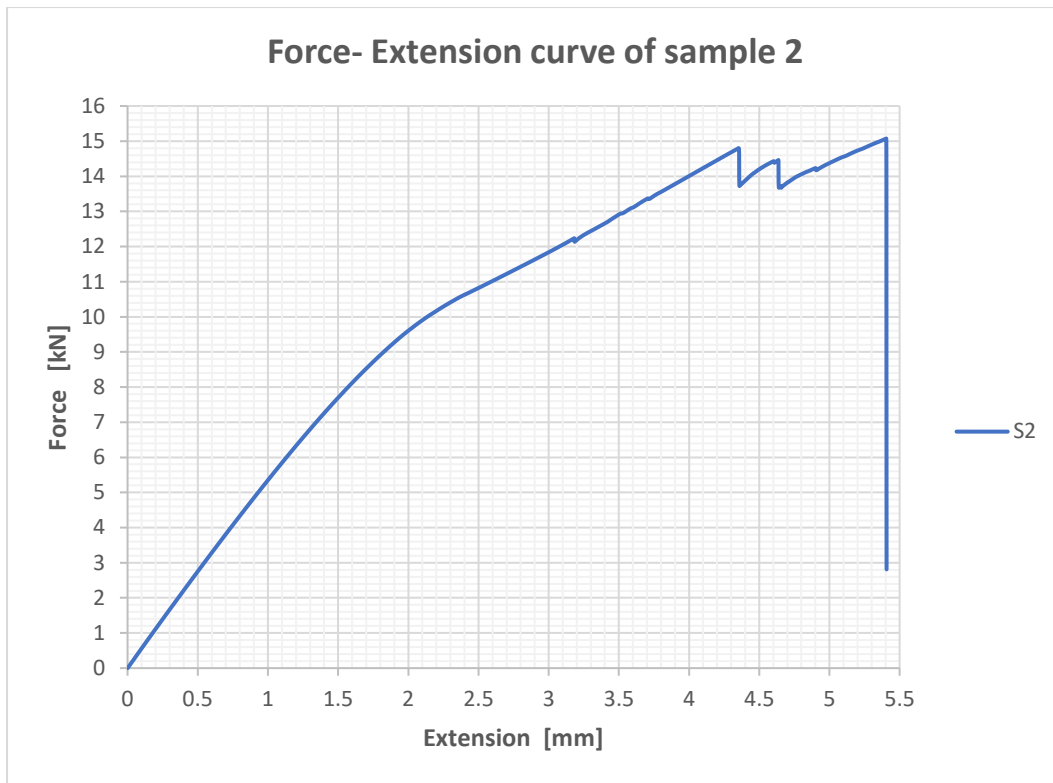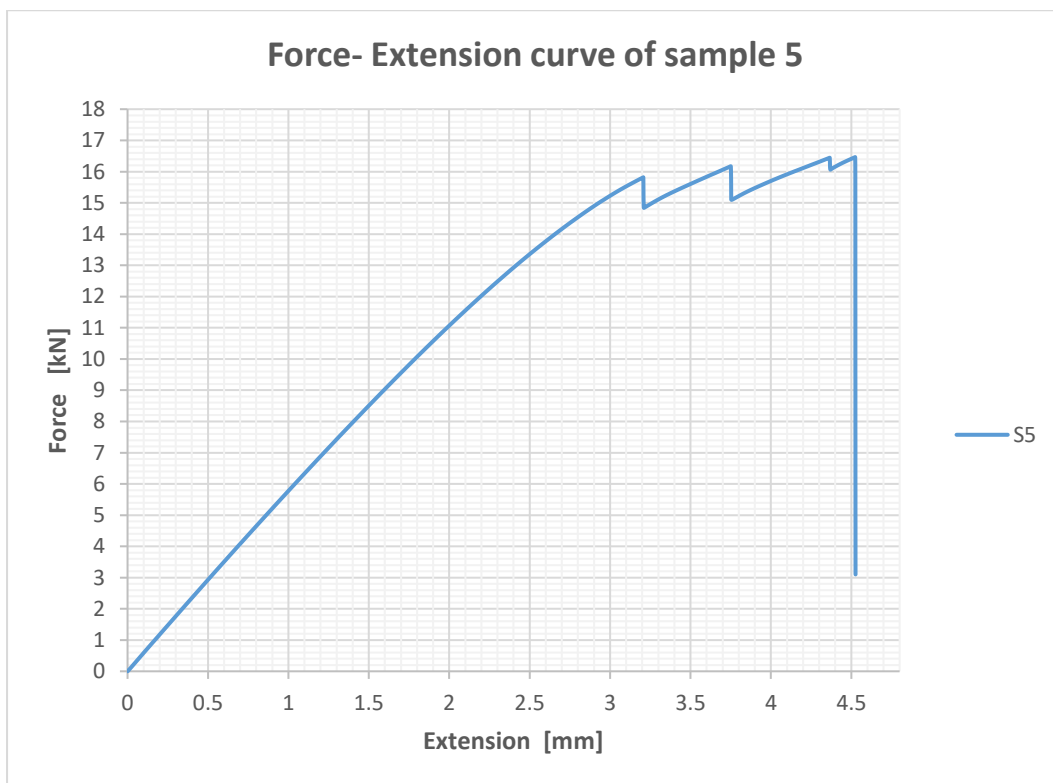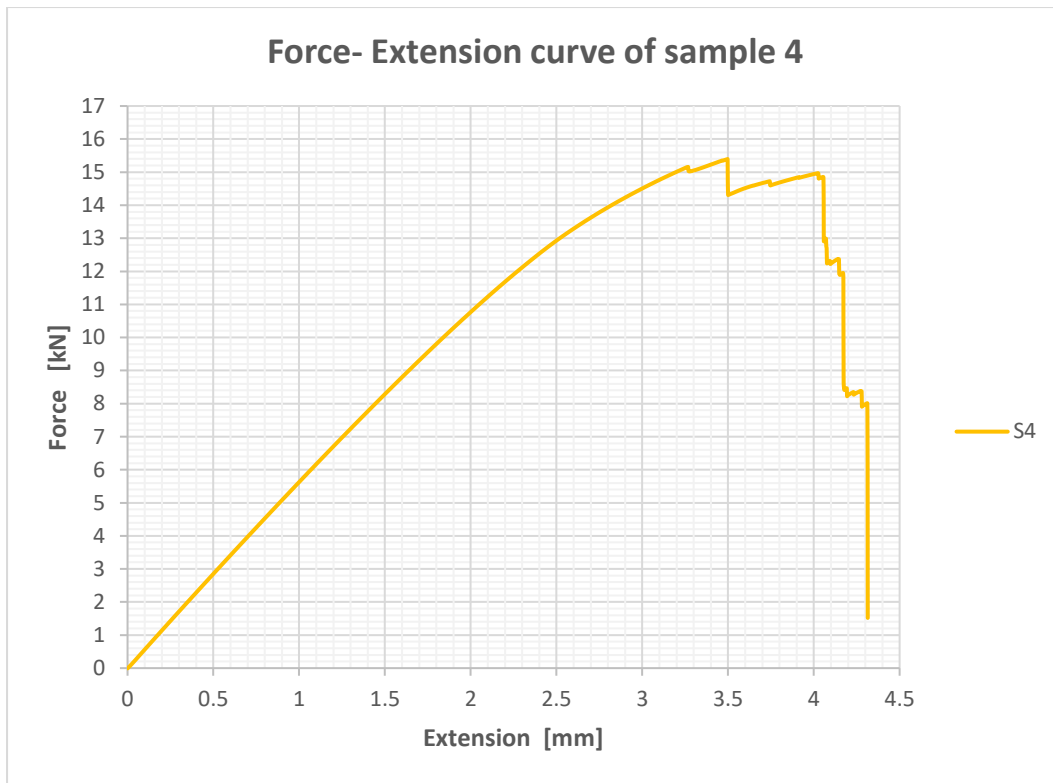
8.3   Appendix B1

The Stress-Strain curve of the 3-point flexural test for each sample is provided below.

Stress-Strain curve of flexural samples

Stress-Strain curve of T1

Stress-Strain curve of T4

Stress-Strain curve of T5
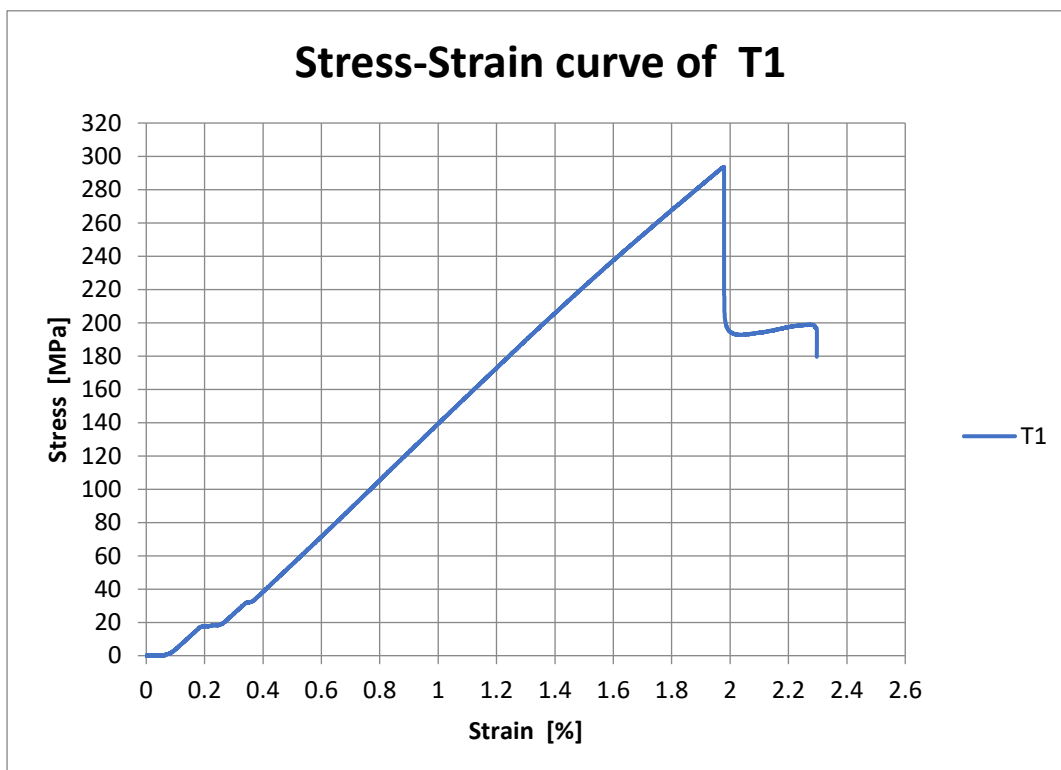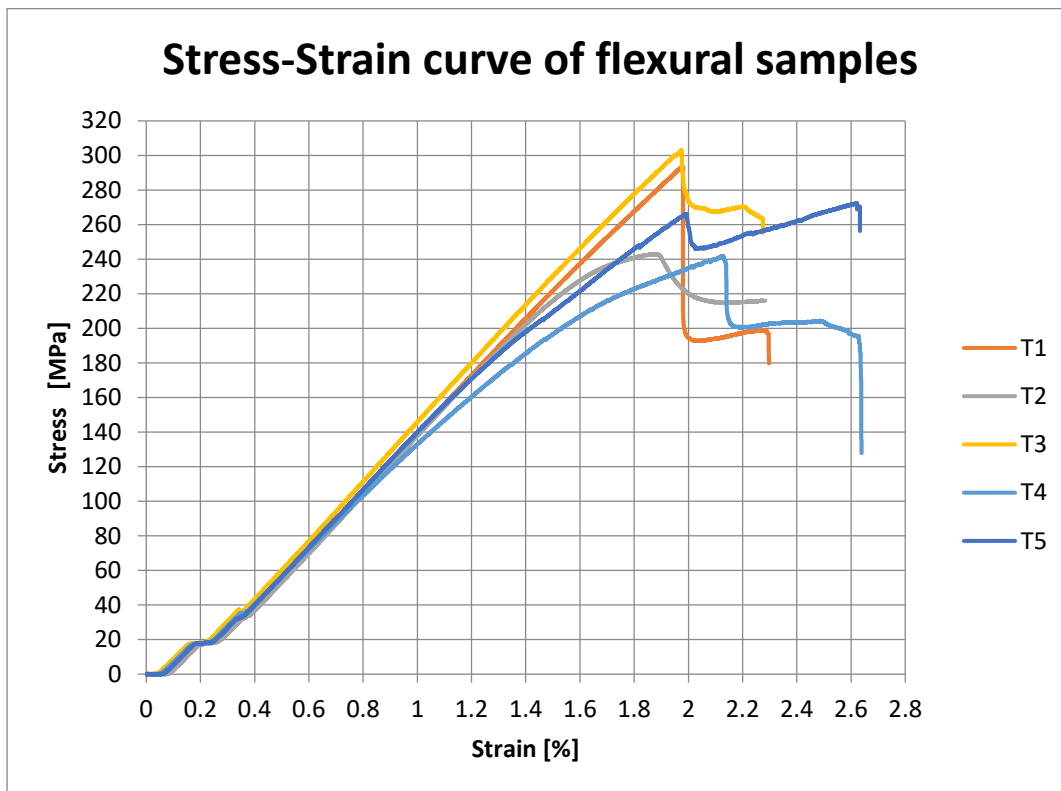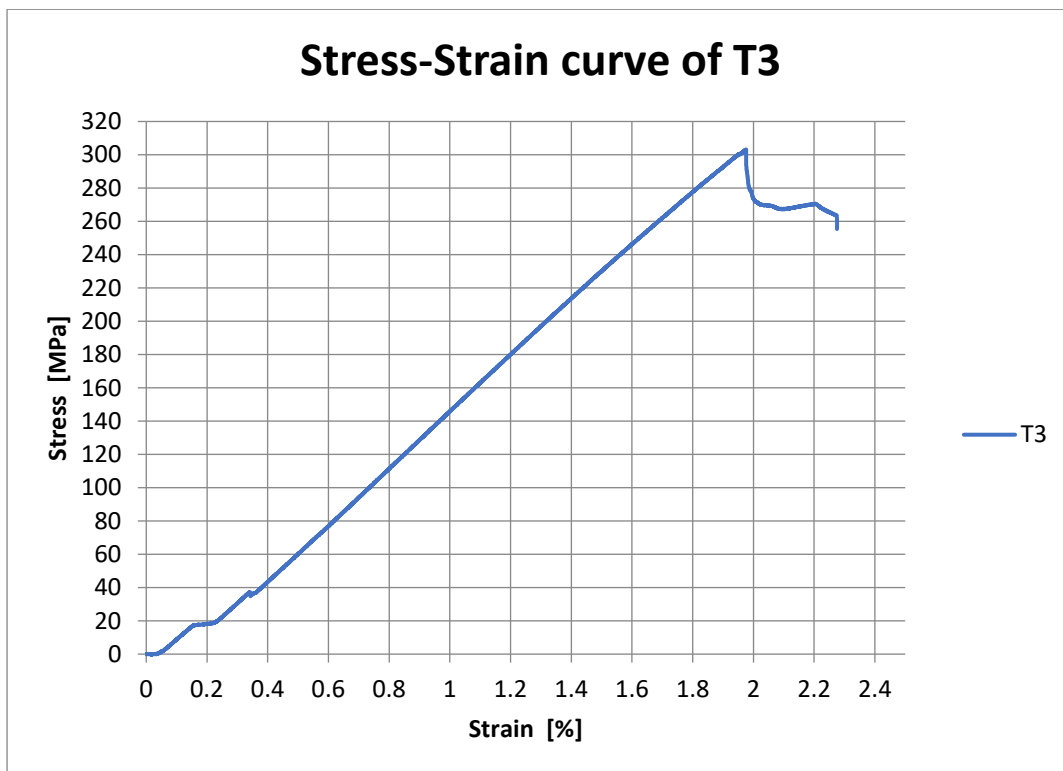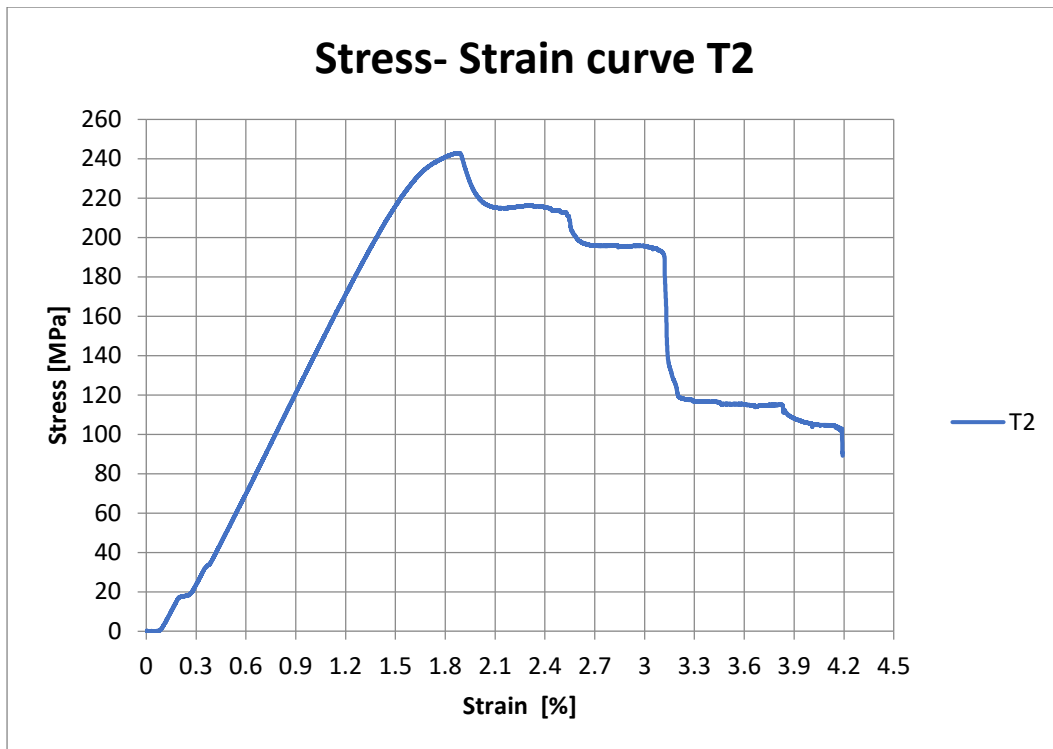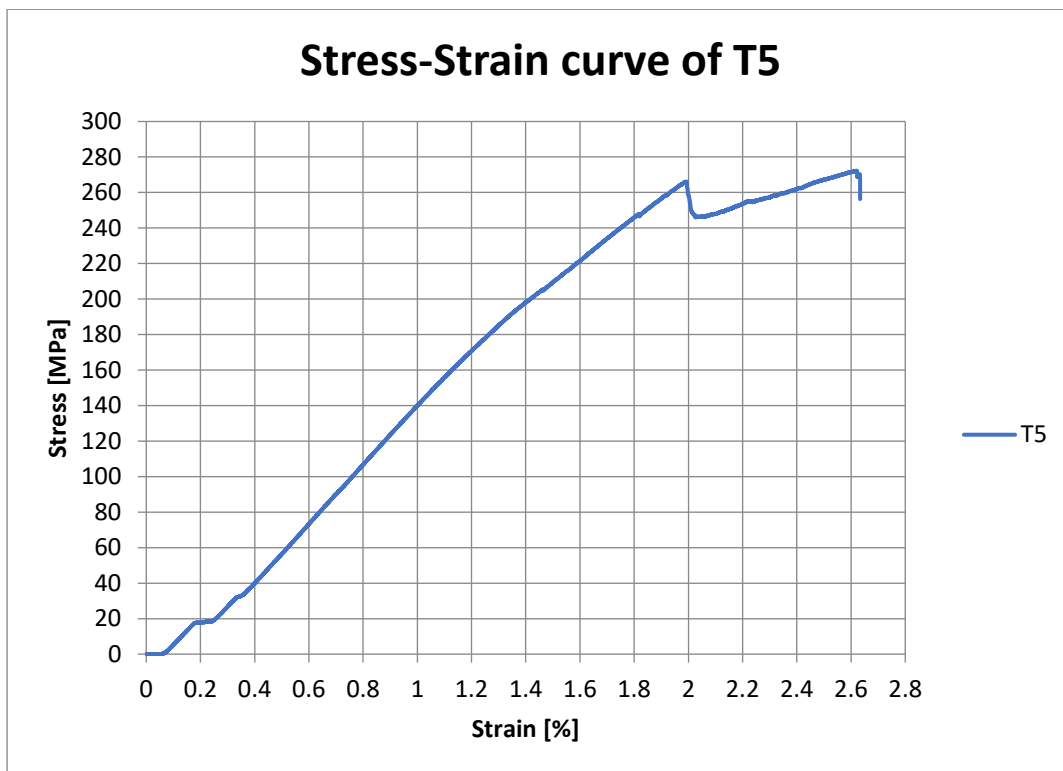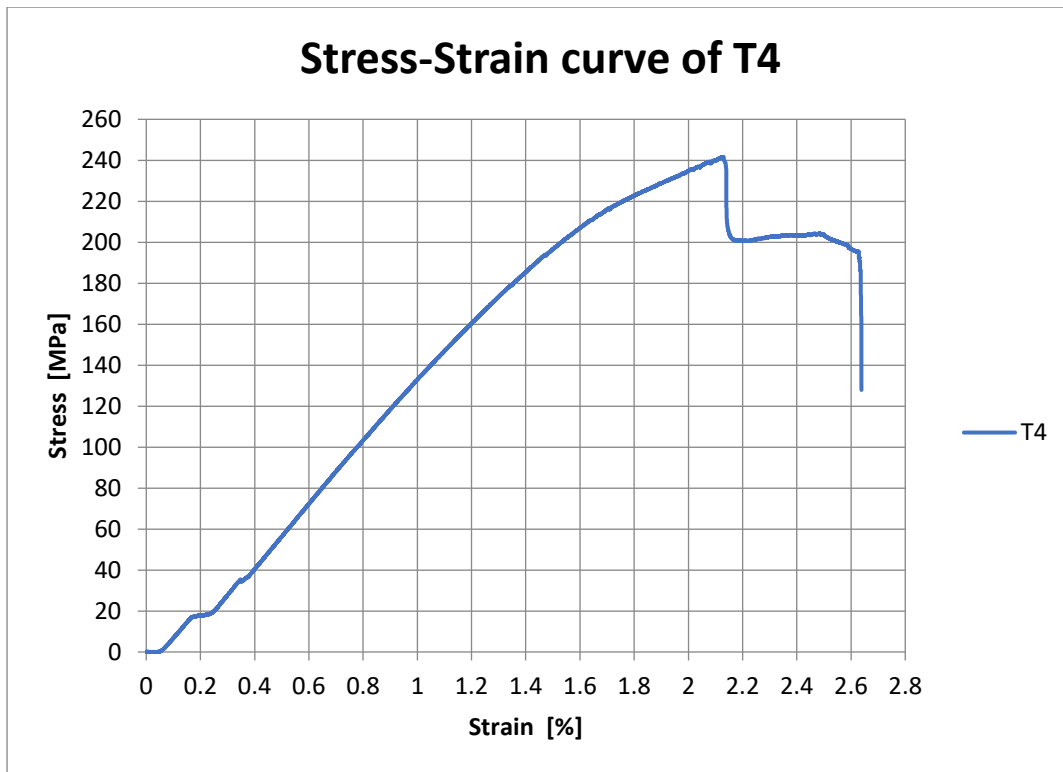
8.4   Appendix B2

The Force- Deflection curves of each flexural sample are presented below

Force- Extension curve of T2

Force- Extensiom curve of T3

Force- Extension curve of T4

Force- Extension curve of T5
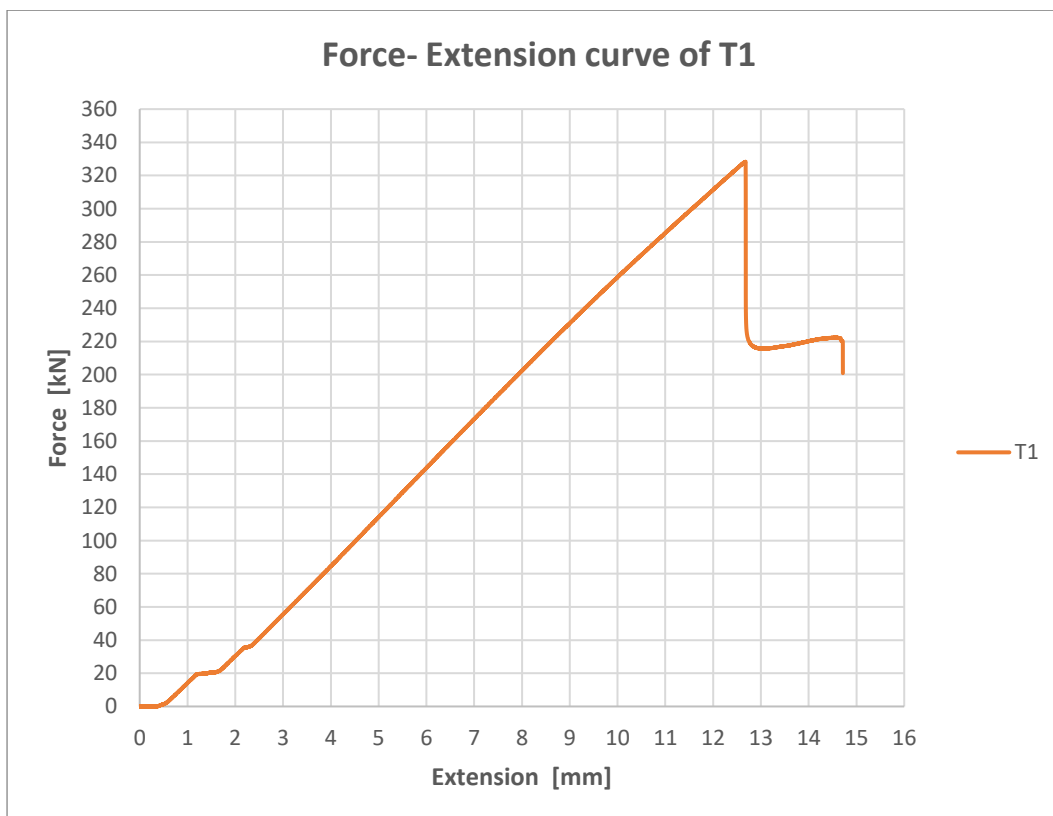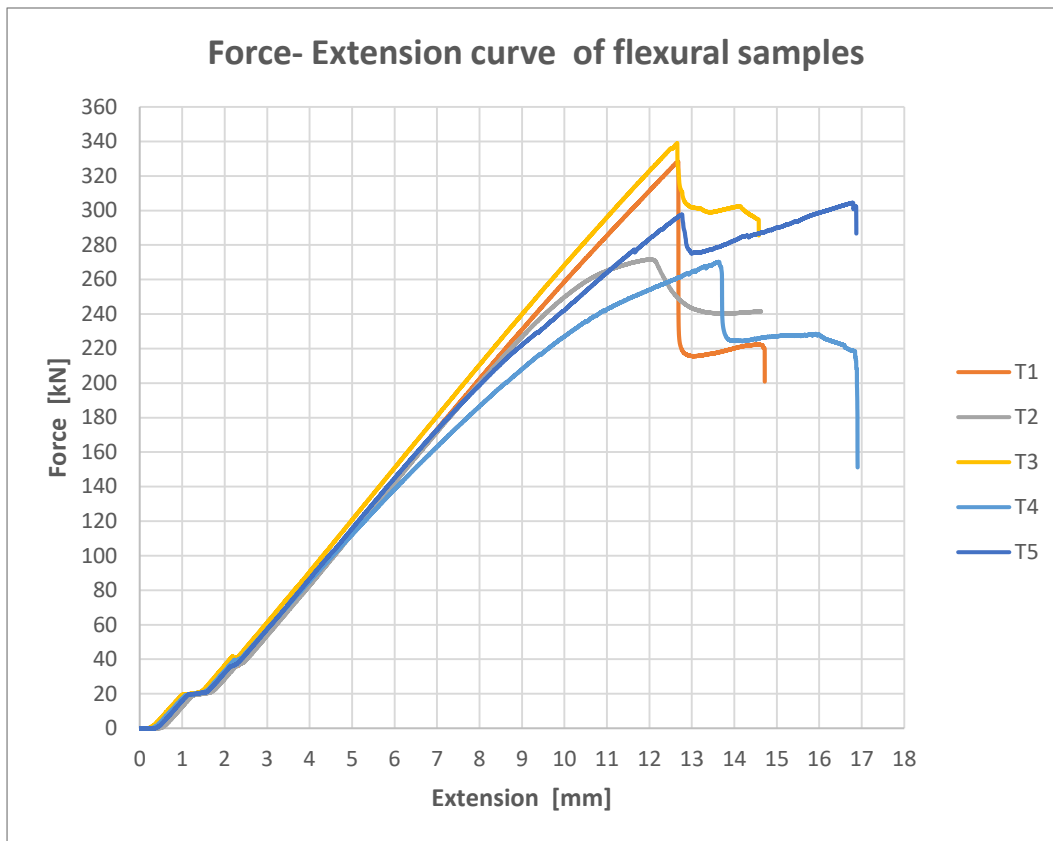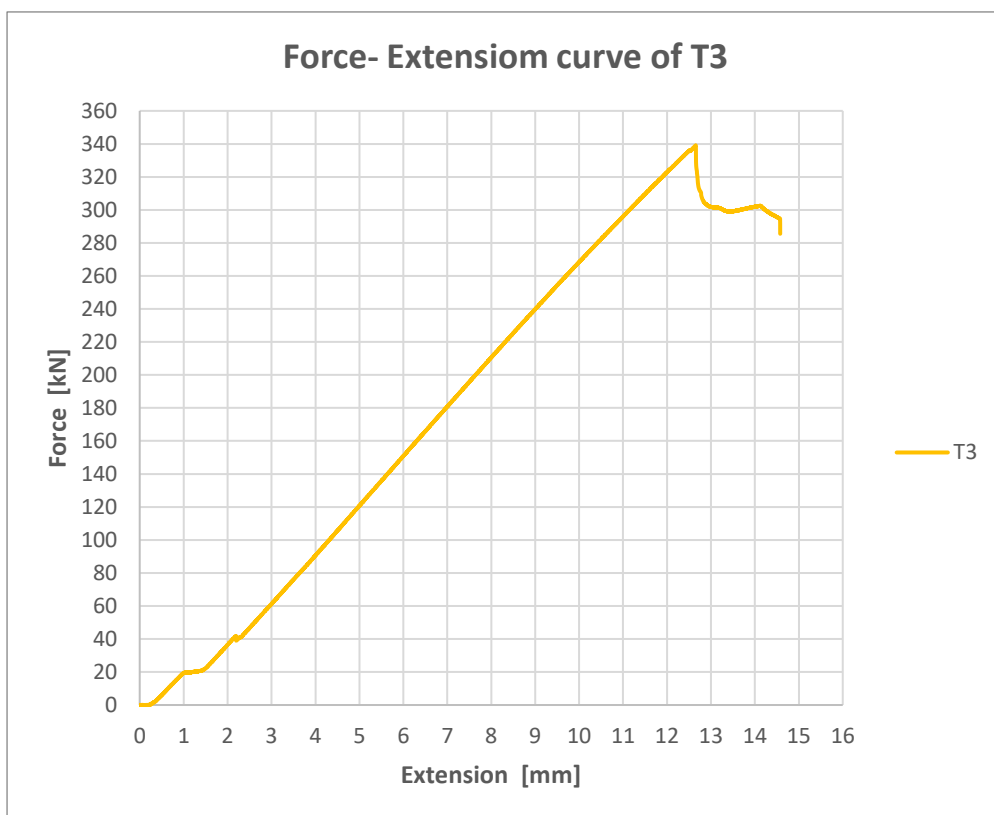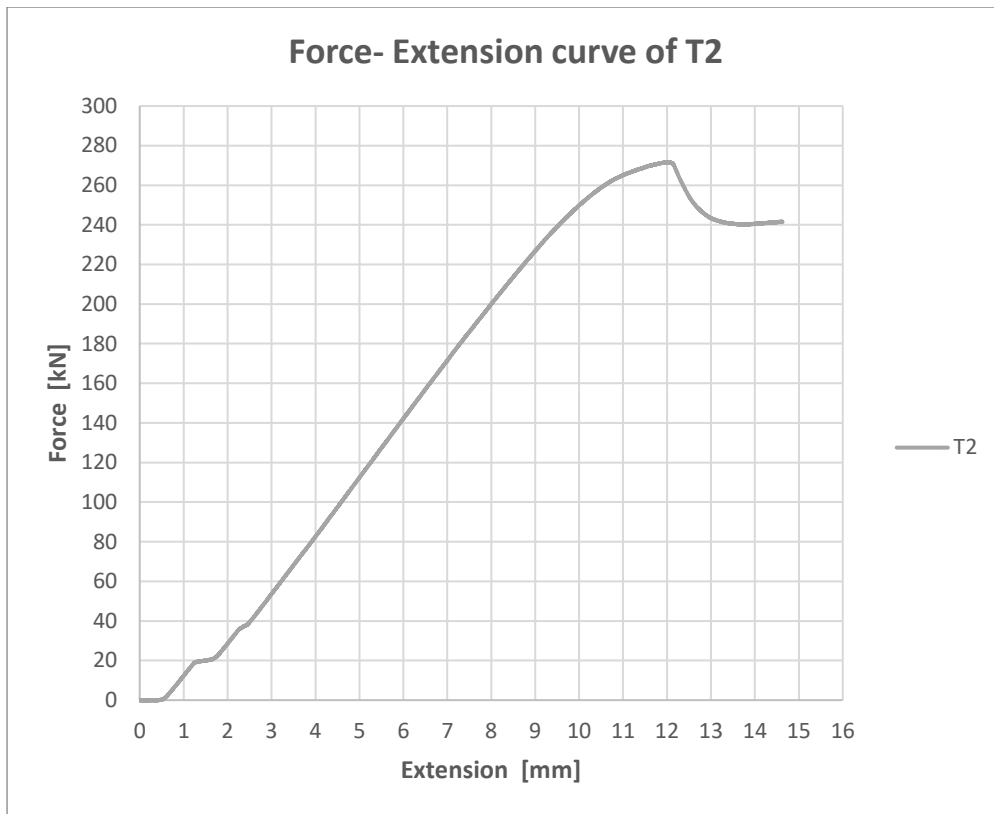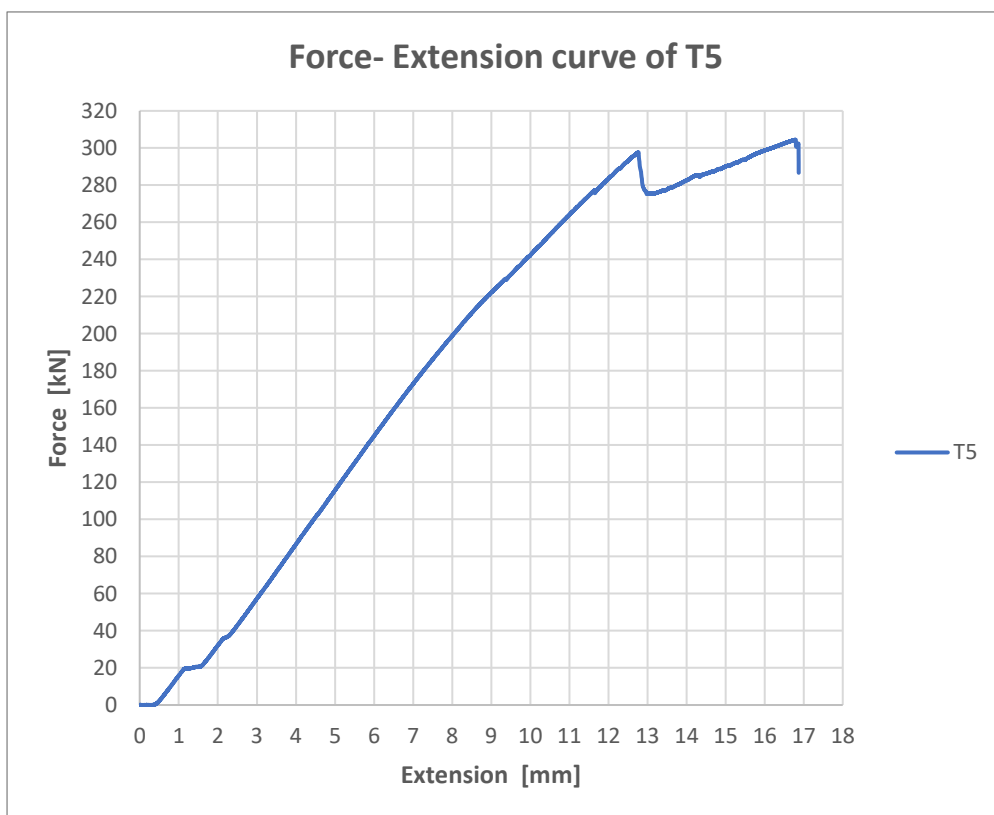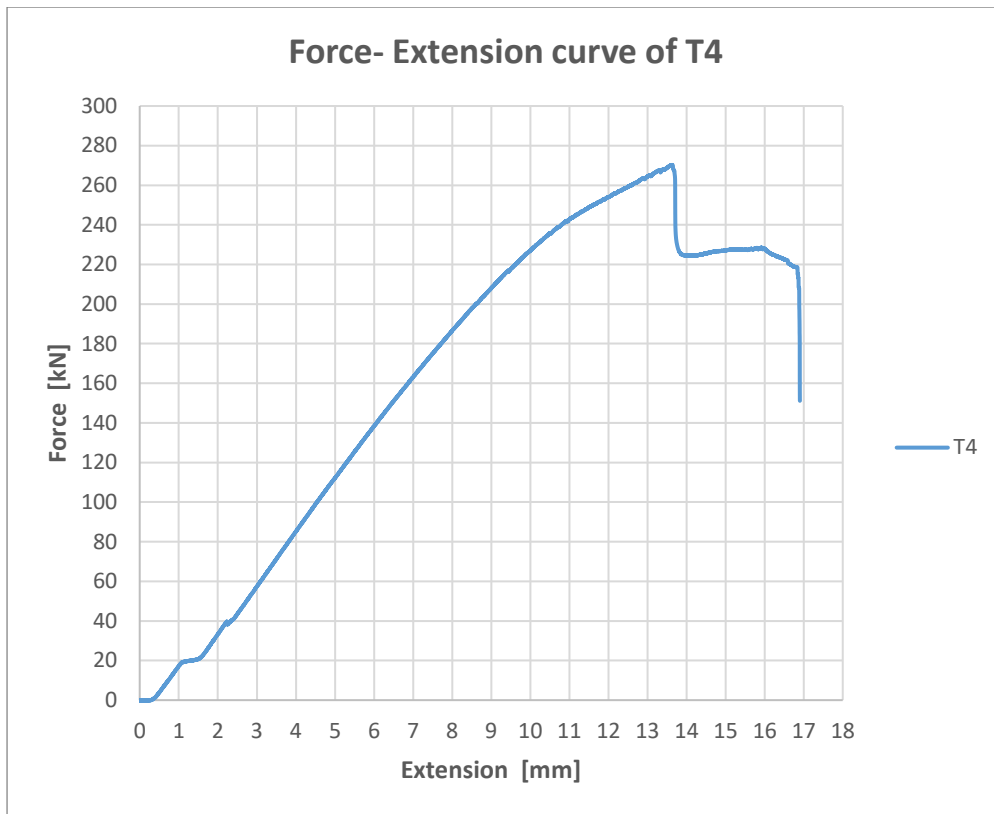
8.5   Appendix C1

More images of the tensile FE model
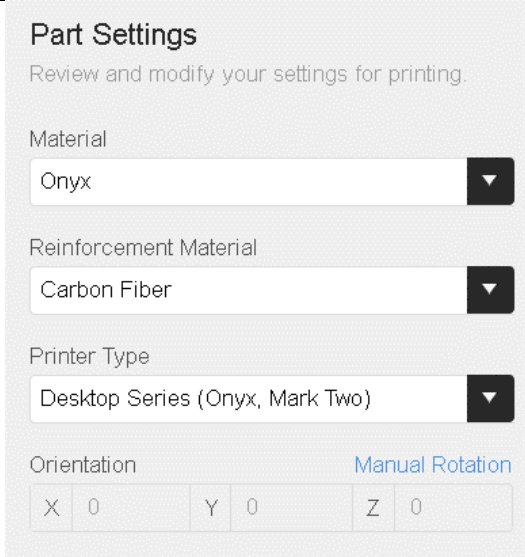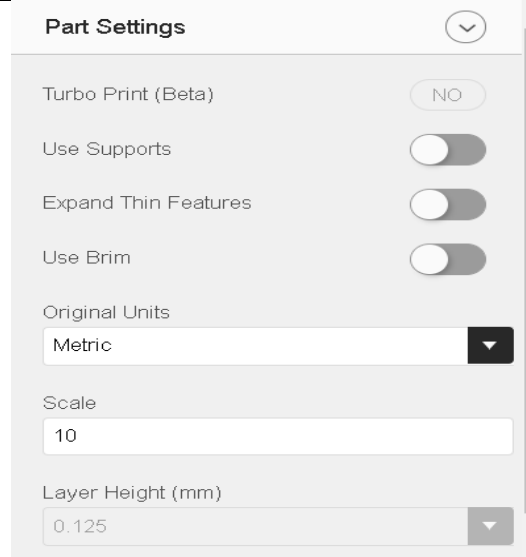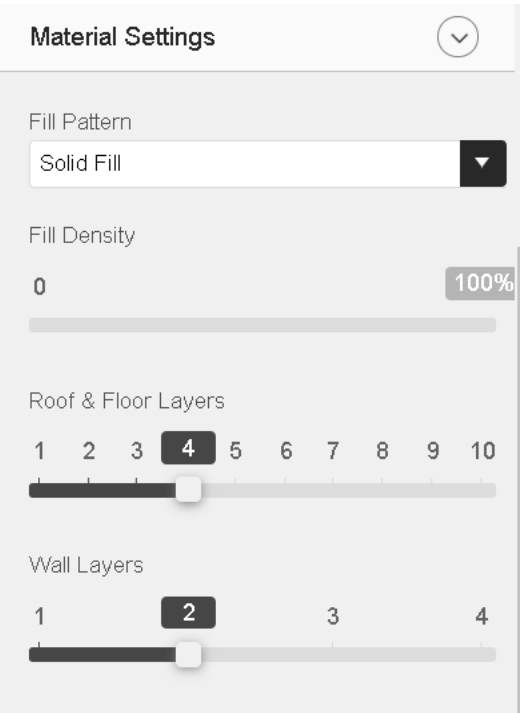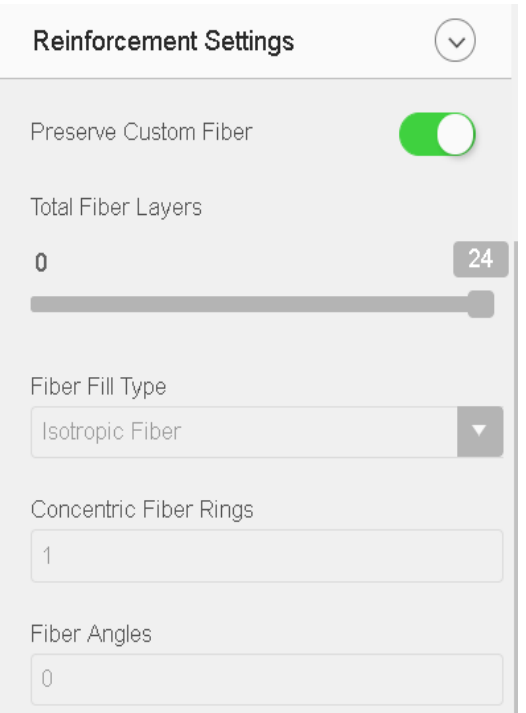
a) Boundary conditions of the tensile model

FE Model for Tensile CFRP
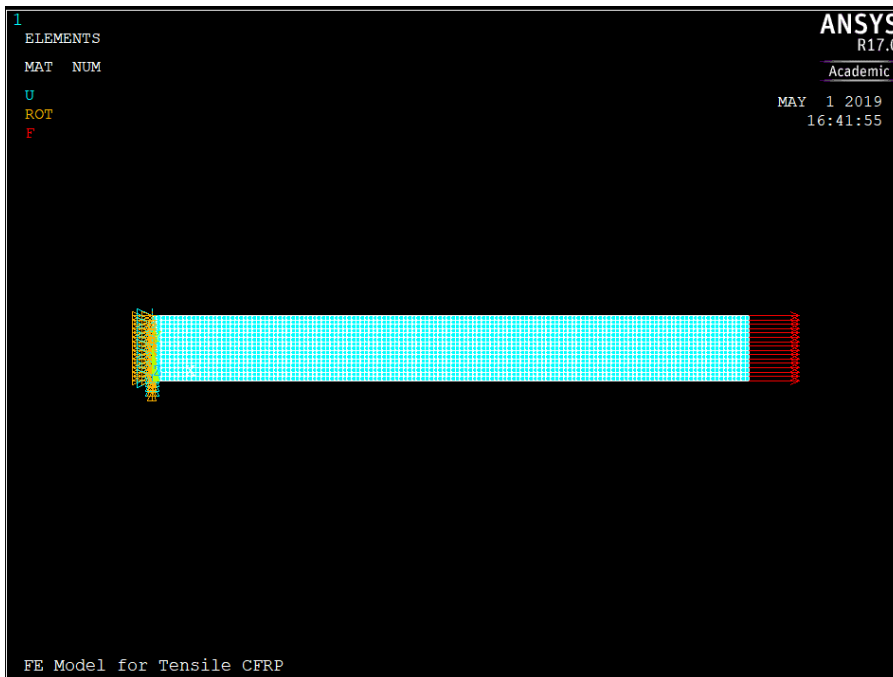
b) Layer stacking of the tensile model in ansys

FE Model for Tensile CFRP
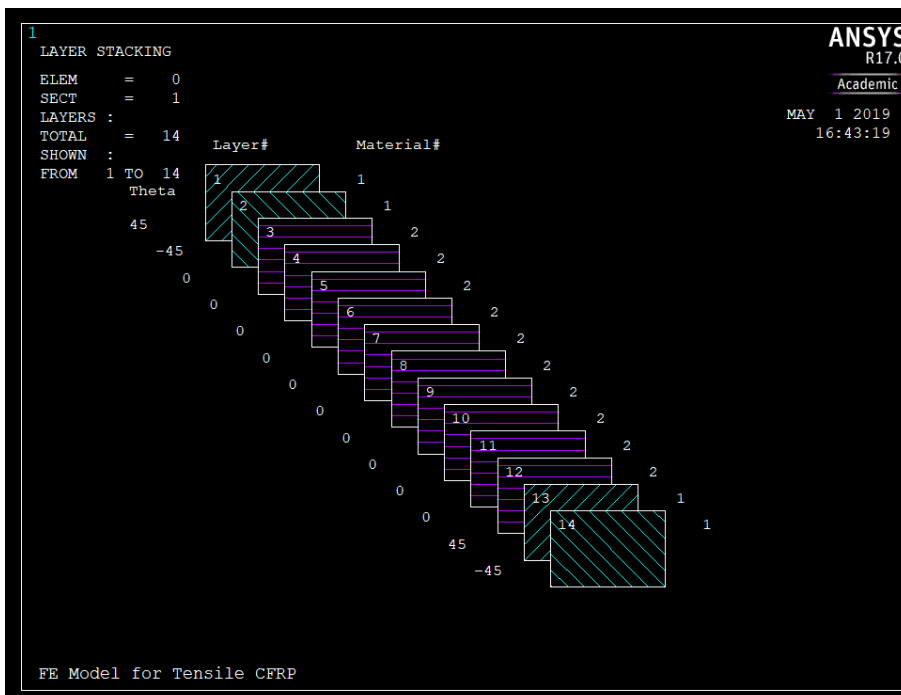
c) Eiger slicing software settings

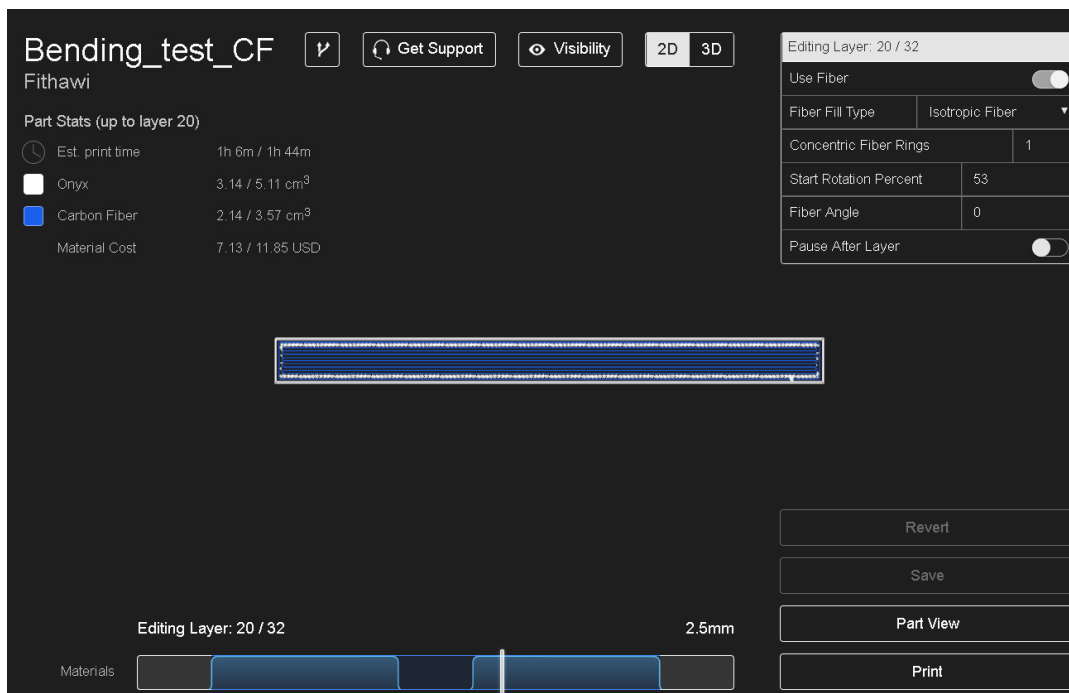|	
 Materials and Printer setting	 Size and Support settings
 Matrix material setting,	 Reinforcing material setting

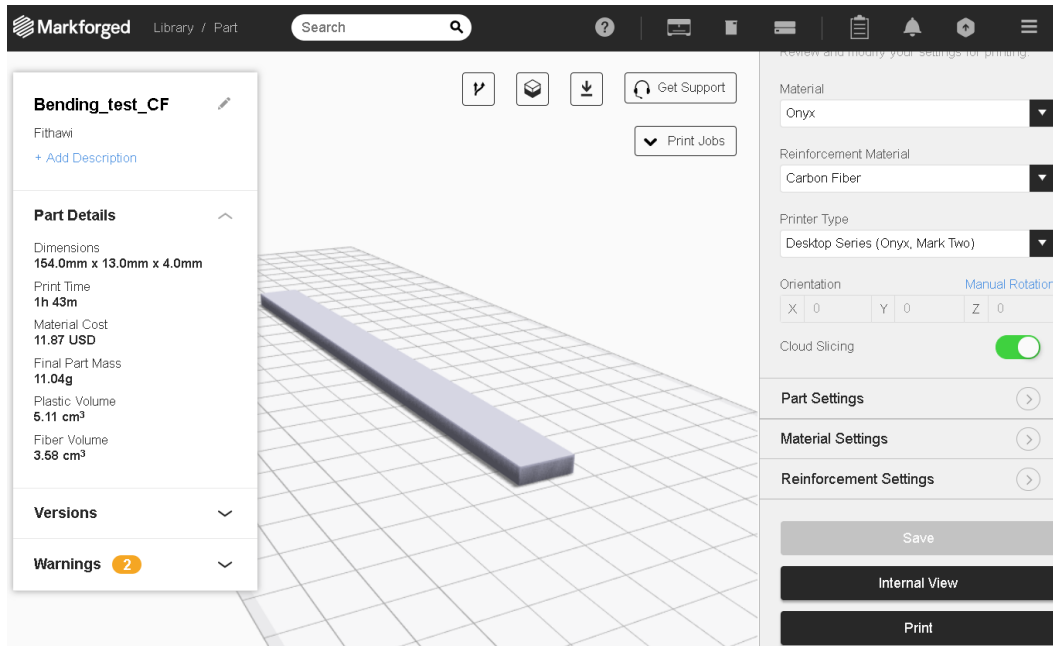d) Internal view setting of the detailed layers of both materials for tensile samples
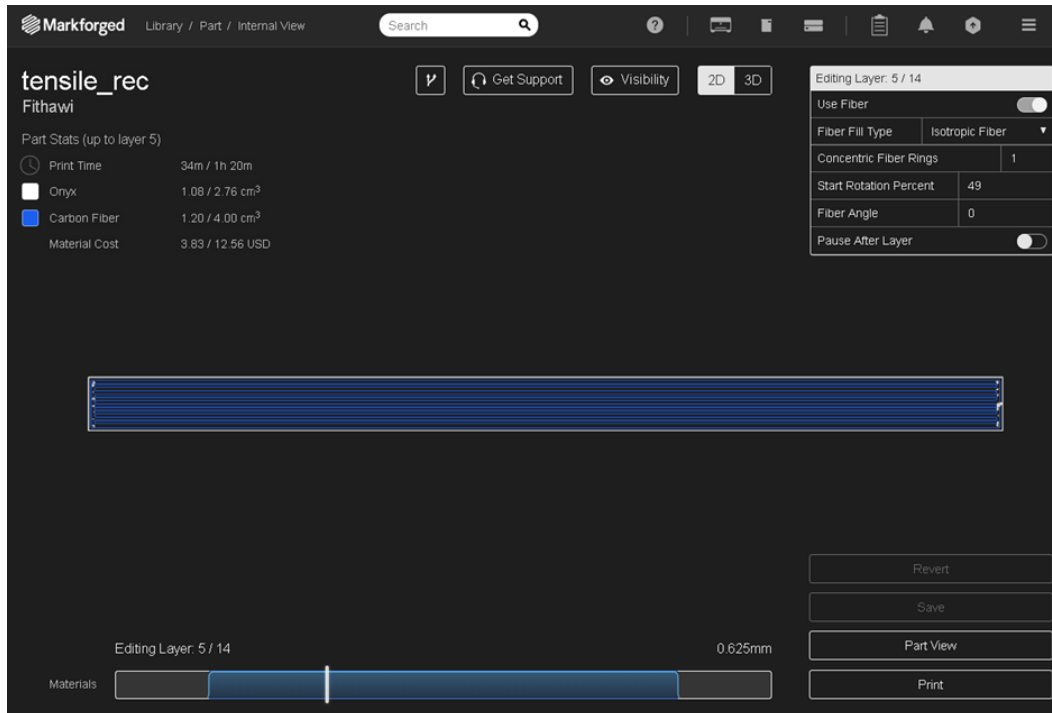
8.6   Appendix C2

Additional images of bending model are presented here

a) Internal view of the flexural model in Eiger

b) Eiger software windows overview and Part details and print settings

c) BC of the flexural model in ansys